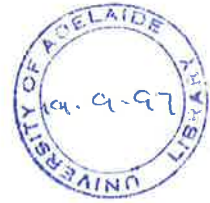# THE UNIVERSITY OF ADELAIDE

CORRELATION OF MAGNETIC RESONANCE IMAGES OF THE HUMAN TEMPOROMANDIBULAR JOINT WITH GROSS AND MICROSCOPIC ANATOMY

CAROLINE MARY HELEN CROWLEY, B.D.S.

Thesis submitted in partial fulfilment of the requirements for the Degree of Master of Dental Surgery, The University of Adelaide.

ORAL PATHOLOGY, FACULTY OF DENTISTRY, THE UNIVERSITY OF ADELAIDE, ADELAIDE, SOUTH AUSTRALIA

1997

TABLE OF CONTENTS

ERRATA

Page 32, line 15 dentitions
Page 38, line 21 Stegegna
Page 60, line 11 derangements
Page 62, line 15 arthrotomographic
Page 69, line 10 receivers
Page 71, line 4 receivers
Page 91, line 11 TMJs
Page 112, line 5 (C) should be after condyle
Page 143, Fig. 11f., page 151, Fig. 12f., page 159, Fig. 13f., page 167, Fig. 14f., page 175, Fig. 15f. Should all be T2 weighted turbo spin echo MR images.
Page 159, line 24 (C)
Page 159, line 27 (C)
Page 159, line 14 low
Page 182, line 12 nevertheless
Page 192, line 17 nevertheless
Page 201, line 8 receivers

A copy of the original MRIs for figures 8c, 9c, 10e, 10f, 10i, 10j, 11i, 11j, 12i, 12j, 13e, 13j, 14e, 14i and 14j are included in pockets in the back of the thesis for examination.

This thesis is dedicated to my mother, Mary, my husband, Nicholas and our daughter Georgina. To Mary in recognition of the encouragement, support and incentive to study that she always gave to me. To Nicholas for his constant love and support and to Georgina, who brings so much joy into my life.

PRECIS

Magnetic resonance imaging is a non-invasive, non-irradiating diagnostic procedure that has the potential to produce high quality tomographic images in any plane with excellent soft tissue resolution. Contrast between tissues in MR images is not dependent on tissue density but reflects variations in molecular structure and tissue characteristics allowing discrimination between osseous, muscular, fibrous, adipose and vascular tissue.

The objectives of the present investigation were:

1. To illustrate the accuracy of midsagittal and central coronal T1 Weighted MR images when compared to their corresponding anatomic and histologic sections.

2. To provide a comparative analysis of TMJ's based on macroscopic assessment of joint dissections and diagnosis by T1 Weighted MR images.

3. To compare T1SE, T1GE, T2SE and T2TSE MR images with corresponding anatomic slices and histologic sections.

This study was based on analysis of human cadaver material which was subjected to the following:

1. The TMJ's of whole human heads were imaged in both the sagittal and coronal planes using magnetic resonance imaging (MRI).

2. The TMJ's were then dissected from the cadaver heads, decalcified and sliced in either the sagittal or the coronal plane to produce blocks of tissue that matched the MR images.

3. The TMJ blocks were then processed in paraffin for the purpose of histologic evaluation.

Results

1. Thirty human TMJ's were imaged, dissected in either the sagittal or coronal plane and examined histologically. One joint was lost in preparation and was subsequently not included in this study. A total of twelve joints exhibited clinically normal anatomy in relation to condyle eminence, fossa and disc morphology. The other seventeen joints exhibited a range of degenerative joint changes which included anteromedial, anterior and lateral disc displacements, discal perforations and abnormal bone pathology.

2. The diagnostic accuracy of sagittal and coronal MRI's when compared to sagittal anatomic sections showed that when the sagittal and coronal T1 weighted MR images were compared with the sagittal anatomical sections for normal joints, an accurate diagnosis was made in 8 joints from the sagittal images. However in 3/6 of the coronal images of the same joints an inaccurate diagnosis of a pathological change was made. Except for one joint, T1 weighted images failed to image discal perforations. Articular surface changes were well imaged by sagittal and coronal MRI's which provided a three dimensional representation remodelling and degenerative joint pathology.

3. The diagnostic accuracy of sagittal and coronal MRI's when compared to coronal anatomic showed that the four joints which demonstrated normal anatomy were accurately interpreted by coronal MR images and the complementary sagittal images. Five of the six joints which had an anteriorly displaced disc could be diagnosed by a coronal image. Articular surface changes due to remodelling or degenerative changes in the joint were accurately imaged in all joints by coronal MRI's which provided an accurate outline of subtle changes in contour of the cortical bone from the lateral to medial aspect of the joints.

4. Sagittal and coronal T2TSE image were highly accurate when compared to the anatomic and histologic sections. T2TSE images provided an accurate representation of the disc, articular surfaces and retrodiscal tissues for the normal joint. Considering the reduced image time for this sequence and the detail provided it would be considered the preferred imaging sequence. Coronal images were valuable in imaging remodelling and degenerative changes in the head of condyle which were not so sensitively imaged by sagittal MRI's.

Summary

1. MR imaging of the TMJ has a high diagnostic accuracy and should be considered as the prime imaging modality for soft and hard tissue changes of the TMJ. However MR imaging is dependent on technical factors such as magnetic field strength, gradient coil strength, software and surface coils to achieve a high quality image.

The small number of false diagnoses in this study were consistently related to underestimation of the pathologic conditions. All of the false diagnoses were false negative's and included an underestimation of disc displacements, disc deformations or osseous changes. The underestimations were usually due to the inability of MR imaging to depict the most lateral or most medial part of the joint. The most lateral and most medial parts of the joint were not depicted with the same high quality images as the central zone.

Although the diagnostic accuracy in this study was high, it may be possible to further improve the MR images. One possibility would be to use MR imaging sections that are thinner than 3mm. In this way volume averaging of oblique structures would be reduced, and the image quality of the most lateral and most medial parts of the joint would be

improved. Another way to improve MR imaging would be to use a smaller field of view, resulting in higher spatial resolution.

2. The most accurate imaging modality for normal and pathologic joints was the sagittal and coronal T2 weighted sequences which were highly sensitive to articular surface changes, disc displacements and perforations. When the images were compared to the histologic sections of the same joint this accuracy was highlighted.

The results also showed that the use of sagittal MR images alone does not provide sufficient accuracy in the evaluation of disc position and articular surface changes. Consequently a full MR examination of the TMJ for positional disc abnormalities and osseous changes should include imaging in both coronal and sagittal planes.

DECLARATION

This work contains no material which has been accepted for the award of any other degree or diploma in any university or other tertiary institution and, to the best of my knowledge and belief, contains no material previously published or written by another person, except where due reference has been made in the text.

I give consent to this copy of my thesis, when deposited in the University Library, being available for loan and photocopying.

Part of the material contained within this thesis has been published in the Journal of Orofacial Pain, Volume 10, Number 3, 1996.

Caroline Crowley
1997

ACKNOWLEDGMENTS

I wish to express my sincere gratitude to Dr. David Wilson, Associate Professor in Oral Pathology, The University of Adelaide, for his dedicated supervision and continuous encouragement. His consistent infectious enthusiasm, guidance and valued criticism have been a constant source of inspiration.

I wish to thank Dr. Tom Wilkinson, Senior Lecturer in Prosthodontics, The University of Adelaide for his guidance and encouragement over many years in the field of the TMJ.

Special thanks to Mrs. Sandra Powell for her expert technical assistance and constant patience when explaining laboratory procedures and computer programmes. I am also indebted to Mr. Peter Dent for help in the area of photography.

To Professor Rudi Slavicek, Prosthodontic Department, University of Vienna, I extend my gratitude for access to his research laboratories. I also acknowledge Associate Professor Eva Piehslingher, Prosthodontic Department, University of Vienna for her enthusiasm and assistance in obtaining the cadavers and MRI's in Vienna. To Assistant Professor Christian Czerny, Department of Radiology, Vienna, and Professor L. Wicke, Department of Radiology, Vienna for their MRI assistance.

I wish to extend my sincere thanks to Professor Mick Sage, Department of Radiology, Flinders Medical Centre, Adelaide for his support and encouragement in facilitating the use of the Hospital's MRI unit in this project. I also express my sincere thanks to Dr. Andrew Whyte, Department of Radiology, Flinders Medical Centre, Adelaide for his expert guidance and assistance in interpretation of the MRI's.

ABBREVIATIONS

ADD	anterior disc displacement
cm	centimetre
CR	centric relation
g	gram
H+E	haematoxylin and eosin
HCL	hydrochloric acid
LDD	lateral disc displacement
MDD	medial disc displacement
mg	milligram
ml	millilitre
mm	millimetre
msec	milliseconds
MW	molecular weight
NEX	number of excitations
TE	echo time
TR	repetition time
μm	micrometre

CHAPTER ONE

INTRODUCTION

INTRODUCTION

Magnetic resonance imaging is a non-invasive, non-irradiating diagnostic procedure that has the potential to produce high quality tomographic images in any plane with excellent soft tissue resolution. Contrast between tissues in MR images is not dependent on tissue density but reflects variations in molecular structure and tissue characteristics allowing discrimination between osseous, muscular, fibrous, adipose and vascular tissue.

Magnetic resonance imaging has been used in the evaluation of soft and hard tissue abnormalities of the TMJ since 1985. The diagnostic applicability of this MR imaging technique has been illustrated by only a relatively few arthrographic and surgical comparisons. Besides the small number of reports with direct correlations between imaging methods, there are other limitations to previous reports. Arthrography by itself is not 100% accurate, and during surgery it is difficult to be sure if observations are accurate since the joint is deep and only the lateral part can be exposed. A cross sectional view of the different mediolateral parts of the joint is not easily attained during surgery. In addition histologic evaluation of normal and pathologic joints and the sensitivity and accuracy of magnetic resonance in imaging these changes has not been reported.

The objectives of the present investigation were:

1. To illustrate the accuracy of midsagittal and central coronal T1 Weighted MR images when compared to their corresponding anatomic and histologic sections.

2. To provide a comparative analysis of TMJ's based on macroscopic assessment of joint dissections and diagnosis by T1 Weighted MR images.

3. To compare T1SE, T1GE, T2SE and T2TSE MR images with corresponding anatomic slices and histologic sections.

CHAPTER TWO

REVIEW OF THE LITERATURE

CHAPTER TWO

REVIEW OF THE LITERATURE

2.1.   ANATOMY AND HISTOLOGY OF THE NORMAL HUMAN TEMPOROMANDIBULAR JOINT

2.2.   ANATOMICAL VARIATIONS IN ANATOMY AND HISTOLOGY

2.3.   CLASSIFICATION OF TEMPOROMANDIBULAR JOINT DISORDERS

2.4.   ANATOMY AND HISTOLOGY OF THE PATHOLOGICAL HUMAN TEMPOROMANDIBULAR JOINT

2.4.a. REMODELLING

2.4.b. OSTEOARTHROSIS/OSTEOARTHRITIS

2.4.c.   INTERNAL DERANGEMENT

2.5.   INDICATIONS FOR IMAGING THE HUMAN TEMPOROMANDIBULAR JOINT

2.6.   HISTORICAL PERSPECTIVE OF MAGNETIC RESONANCE IMAGING

2.7.   BASIC PRINCIPLES OF MAGNETIC RESONANCE IMAGING

2.8.   PULSE SEQUENCE SELECTION

2.9.   CLINICAL AND CADAVER MAGNETIC RESONANCE IMAGING STUDIES OF THE HUMAN TEMPOROMANDIBULAR JOINT

REVIEW OF THE LITERATURE

Temporomandibular joint disorders affect up to 25% of the general population. Recent improvements in imaging techniques allow an accurate and non-invasive assessment of the joint. The classical signs and symptoms of TMJ disorders include pain, tenderness, clicking and locking. Imaging studies to confirm a diagnosis should be considered if the clinical diagnosis is equivocal or if a standard course of conservative therapy is unsuccessful and additional treatment is required. An imaging study for confirmation of the diagnosis is often requested by third party payers when prolonged care is planned that will be costly. Legal considerations are often a source of imaging studies as many patients presenting with joint dysfunction have a history of jaw trauma. In general the diagnosis is obtained clinically in the majority of cases and the imaging study is done for confirmation and documentation prior to therapy.

Ten years ago the arthrogram was the popular imaging modality. In the early 1980's computed tomography (CT) was introduced as a non-invasive replacement for the painful arthrogram. Magnetic resonance imaging (MRI) was introduced shortly after as a non invasive imaging modality which was able to aquire images with soft and hard tissue detail without exposing the patient to ionising radiation or known biological hazards,

2.1. ANATOMY AND HISTOLOGY OF THE NORMAL HUMAN TEMPOROMANDIBULAR JOINT

The TMJ is the freely moving (diarthrodial) articulation between the condyle of the mandible and squamous portion of temporal bone. The condyles of the TMJ sit in an articular fossa and are surrounded by a capsule. The anterior aspect of the TMJ is limited by the articular eminence, the posterior aspect by the squamotympanic fissure and plates, the lateral aspect by ligaments and muscle attachments and the medial aspect by the medial wall of the fossa which is formed by a portion of the temporal bone. The condyle and the fossa are separated by an articular disc. The disc is limited anteriorly by a capsule and posteriorly it is attached to the retrodiscal tissues. Laterally and medially the disc attaches to the poles of the condyle by ligaments which are reinforced laterally and medially by discal (collateral) ligaments.

Condyle

The features of the adult condyle were reported in an autopsy study by Oberg, Carlsson and Fajers (1971) of 102 TMJ's from subjects aged 20-93 years. These investigators reported that the condyles studied had an average mediolateral width of 20 mm and an antero-posterior length of 10 mm. Both dimensions included the articular soft tissues. The condyle is not symmetrical. The medial pole of this semicylindrical body projects well beyond the medial surface of the ramus, while the lateral pole extends only slightly laterally. A shallow concavity, the pterygoid fovea, is located on the anteromedial aspect of the mandibular neck. It is here that the inferior head and most fibres of the superior head of the lateral pterygoid insert into the mandible (DuBrul 1980, Mahan et al 1983, Wilkinson 1988).

There is a large degree of variation among human condyles, both in shape and in the angle at which the condyle bears to the ramus of the mandible. In any individual the left condyle may not have the same form as the right condyle. In studies by Moffett (1962); Yale, Allison and Hauptfuehr (1966) and Yale (1969), the longitudinal axis of the condyles were reported to converge posteriorly. The angle this created with the frontal plane varied from 0 to 30 degrees, while the angle between the longitudinal axis and the frontal plane varied between -45 degrees and +35 degrees with an average angulation of +5 degrees.

The direction of the longitudinal axis of the condyle is important in interpreting MRI and radiological images of the TMJ as is the knowledge of the shape of the osseous components of the joint. However when interpreting images it must be borne in mind that there may be differences in the shape of the joint components with and without soft tissue coverings due to variations in thickness of the soft tissues (Bean, Omnell and Oberg 1977; Hansson et al 1977). The form of the condyle varies widely from one individual to another. The superior outline in the mediolateral plane is frequently (approx 60%) rounded or convex, but occasionally it is flat or straight (20-30%). In children the condyle is frequently rounded, especially when viewed from in front or above (Yale et al 1966; Oberg et al 1971). When viewed from the superior the shape of the condyle varies from oval to round with a flat surface posteriorly to kidney shape with a concave shape posteriorly.

Temporal Components - Articular Eminence and Mandibular Fossa

The articular eminence runs obliquely from the posterior root of the zygomatic arch to the medial aspect of the joint. It is strongly convex anteroposteriorly and slightly concave mediolaterally. The posterior slope of the eminence is much steeper than the gradual slope anterior to the crest of the eminence which is referred to as the preglenoid plane.

The mandibular fossa is the concave area bounded medially by a narrow bony wall, anteriorly by the posterior slope of the articular eminence and posteriorly by the post glenoid process, or tubercle. The fossa is bordered by the post glenoid tubercle and the origins of the zygomatic process. The postglenoid process is an inferior extension of the temporal squama directly posterior to the most lateral part of the fossa and anterior to the opening into the external acoustic meatus. The tympanic plate lies posteriorly to this process and the rest of the mandibular fossa lies medially. It meets the squamosum at the squamotympanic fissure, which runs mediolaterally behind the depth of the fossa.

The mandibular fossa, like the condyle and articular eminence, exhibit wide morphologic variation (Ricketts 1950). The autopsy study by Oberg et al (1971) showed that the articular surface of the fossa is oval. It is wider mediolaterally and anteroposteriorly than the condyle, measuring 23 and 19 mm respectively. The roof of the fossa are thin, frequently translucent to light, and are not built to withstand loading from the condyle (Hylander 1979). The postglenoid process is non articulating in humans (DuBrul 1980). The joint capsule attaches to the entire anterior surface of the postglenoid process, and the retrodiscal tissues are interposed between it and the condyle. Thus, the condyle does not

normally make contact with the postglenoid process even during complete retrusion of the mandible (DuBrul 1980).

In newborn infants the articular surface is almost flat. It is the growth of the temporal component during childhood and adolescence that forces the articular surface of the disc into the S shape which is seen in sagittal sections. The steepness of the adult articular eminence varies among individuals, but the inclination averages 60 degrees, with a standard deviation of 5 degrees and in the frontal plane the articular fossa is concave (Oberg 1971).

Articular Surface of the Condyle and Temporal Components

The articular tissues of both the condyle and temporal articulating surfaces are composed of dense fibrous connective tissue and fibrocartilage, not hyaline cartilage. The reason for this resides in unique developmental characteristics of the TMJ and has certain functional advantages. Hyaline cartilage is uniquely constructed to withstand compressive and torsional loading and is less able to withstand shearing forces (Moss 1966). However, dense fibrous connective tissue can withstand shearing forces much better than compressive forces. Under normal circumstances shearing forces predominate over compression forces in the human TMJ and thus fibrous connective tissue is the appropriate functional tissue in the TMJ.

The articular surface consists of a layer of dense collagenous tissue, the articular zone, which is thickest in the superior and anterior surface of the condyle and the posteroinferior surface of the articular eminence (Oberg 1964; Richards 1984). Hansson et al (1977)

reported from a histological study of 115 TMJ's from age 1 day to 93 years that these tissues have the potential to become cartilaginous under functional loading. Beneath the fibrous outer layer lies a zone of undifferentiated mesenchyme forming the proliferative zone and inferiorly is the intermediate zone. Beneath this is a cartilage zone consisting of a layer of fibrocartilage containing chondrocytes and a matrix of collagen fibrils and other extracellular matrix components including proteoglycans. The proliferative zone, the intermediate zone and the cartilage layer form the soft tissue growth zone between the surface collagen and the compact bone. The soft tissue zone is most active in the condyle (Blackwood 1966; Carlsson, Oberg and Bergman 1967).

The growth zone in the articular tissues depends on the presence of undifferentiated mesenchymal cells to play a pivotal role in the growth and functional development of the TMJ. In circumstances of slow growth there is differentiation of the mesenchymal cells into preosteoblasts and osteoblasts which form bone on the inferior aspect of the growth zone whereas in conditions of rapid growth there is differentiation of cells into prechondrocytes and hypertrophic chondrocytes (Oberg 1964). The preosteoblasts, osteoblasts and prechondrocytes form the transitional layer. The rate of growth of the articular tissues is to a large extent related to the hypertrophyic cartilage cells (Oberg et al 1969). Growth is rapid until 14-15 years of age after which it progressively decreases until adulthood (Bjork 1966). There is controversy as to whether this zone in the condyle should be regarded as a primary growth centre or whether its purpose is mainly that of adaptive remodelling (Thilander et al 1976). Inferior to the cartilage zone is the cortical bone zone and cancellous bone zone.

Hansson and Nordstrom (1977) reported that in adults the composition and thickness of the TMJ articular surface layers varies with the degree of remodelling that has or is occurring which in turn depends on age and functional loading. A cartilage layer develops from the undifferentiated mesenchyme in response to functional loading of the joint on the superior and anterior aspect of the condyle and posteroinferior surface of the articular eminence. In the peripheral parts of the condyle and the temporal surface where there is minimum functional loading, cartilage formation rarely occurs.

Due to variations in the thickness of the cartilage layer, the thickness of the soft tissue layers covering the condyle and articular eminence also varies. They are thickest (0.5 mm) superiorly and anteriorly over the condyle, and posteroinferiorly in the articular eminence. It is thinnest (0.1 to 0.2 mm) over the posterior aspect of the condyle and on the floor of the articular fossa (Hansson and Nordstrom 1977). As already stated these variations are due mainly to variations in thickness of the cartilage layer and correspond to areas exposed to maximum and minimum functional load respectively.

Articular Disc

The articular disc is a firm, but, flexible structure that will accommodate to the incongruities that exist between the shape of the articular surface of the condyle and those of the articular eminence. In the normal joint the shape of the disc is determined by the morphology of the condyle and temporal components. For this reason the disc is relatively flat planed in newborns. Changes in shape of the condyle and temporal components which occur during adolescence result in the development of a disc with a biconcave appearance having an anterior thick zone, intermediate thin zone and a posterior thick band. Posteriorly

the disc continues as the retrodiscal tissues which connect to the temporal bone and the posterior aspect of the condyle. Anteriorly the disc blends with the capsule. Laterally the disc is attached to the medial and lateral poles of the condyle by collateral ligaments where it blends into the lateral connections of the capsule.

Rees (1966) studied 12 human cadaver TMJ and reported that the inferior disc surface is concave and oval in shape like the condyle, with which it is in contact, with its long axis placed transversely. The superior surface is convex posteriorly but anteriorly it is saddle shaped, being slightly convex from side to side and slightly concave from anterior to posterior.

Hansson and Nordstrom(1977) demonstrated that the disc is thinnest (approximately 1 mm) in the central zone and thickest (2 to 4 mm) in the anterior and the posterior regions and divides the area between the condyle and articular fossa into superior and inferior joint spaces.

Scapino (1983) studied the histological appearance of three serially sectioned TMJ's from subjects whose age ranged from 23 to 75 years. Scapino described the collagen fibre organisation within a normal disc as consisting centrally of predominantly anteroposterior coursing fibre bundles which interlace with transversely orientated fibres in the thickened anterior and posterior bands. Burgeson (1984) described similar features and reported that the collagen was type I collagen. Manzione, Katzberg and Manzione 1984 and Osborne 1985 reported that the discs of human TMJ's are composed of fibrocartilage. This fibrocartilage is composed predominantly of type I collagen in contrast to type II collagen of hyaline cartilage (Morimoto, Hashimoto and Suetsugu 1987; Gage, Francis and Triffit

1989). Gage et al 1990 reported from a histological study of eight human TMJ's that the anterior, cental and posterior bands consisted of type I collagen and the retrodiscal tissues contained type III collagen.

Retrodiscal Tissues

The retrodiscal tissues form a rhomboid with its apex being the posterior band of the disc, a superior stratum inserting into the squamotympanic fissure, an inferior stratum attaching to the posterior part of the neck of the condyle and the fibres of the posterior capsule forming the base on the parotid gland (Wilkinson and Crowley 1993). Rees (1966) described the retrodiscal tissues as a "bilaminar zone" because the loose stretchable upper stratum contained elastin and the non stretchable lower stratum contained relatively few elastin fibres. Rees reported that, posteriorly, the upper and lower strata blended with the fibres of the posterior capsule that could be seen running from the temporal bone to the mandible. In this study of fresh human postmortem material, Rees observed that the retrodiscal tissues expanded to fill the glenoid fossa as it was vacated by the condyle and suggested that venous engorgement of the retrodiscal tissues could facilitate these volume changes. It was suggested that the return of the disc when the condyle moved backwards on closure was caused by its attachment to the condyle, and that this was aided by a mechanism of elastic recoil of the upper stratum of the retrodiscal tissues.

Osborne (1989) expanded on the concept that in the closed position a venous pool occupied the plexus medial to the condyle and that on opening, this pool moved posteriorly to the vessels of the plexus behind the condyle, which resulted in balancing of tissue pressure.

Scapino (1991) described the histology of the retrodiscal tissues as containing upper and lower fibro-elastic strata and a intermediate zone consisting of a venous plexus supported in a fibro-elastic framework. Wilkinson and Crowley (1994) reported that the primary function of the retrodiscal tissues was to provide a volumetric compensatory mechanism for pressure equilibration that was still active in joints demonstrating disc displacement and degenerative changes. The concept of the upper stratum having a specialised elastic recoil mechanism was not supported by this study.

Synovial Membrane and Fluid

It was reported from a histological study of human cadaver TMJ's by Hylander (1979) that synovial membrane lines the inner capsular surface and is most abundant on the superior and inferior surfaces of the retrodiscal tissues and all surfaces not under shearing or compressive load. The synovial membrane may form folds over the retrodiscal tissues when the joint is in the closed position. The synovial membrane is smooth with several small villi that increase in number and size with age.

In a review of the literature by Schmid and Ogata (1967) the synovial membrane was reported to consist of an intimal layer which is adjacent to the joint space and a subintimal layer. The intima is highly cellular and contains numerous thin walled vessels. The subintimal layer is composed of fibrous and adipose tissue and is poorly vascularised. The TMJ synovial intima comprises two cell types. Type A cells which are phagocytotic and Type B cells which are involved in large molecule synthesis

The synovial cells produce a fluid mainly consisting of plasma dailysate with a polysaccharide protein complex, a proteoglycan containing hyaluranic acid (Ward 1980). The main functions of the synovial membrane were thought to be secretion, phagocytosis, nutrition of the avascular tissues within the joint and regulation of the movement of solutes, electrolytes and proteins. Synovial fluid acts as a lubricant for the joint surface and is a secondary source of nutrients for the avascular superficial aspects of the condyle and temporal bone, and the dense central part of the disc. It was hypothesised by DeBont (1994) that compression of the synovium due to disc displacement or joint osteoarthritis may impair its function, cause loss of lubrication and retard joint movement (Gedikogher et al 1986).

The cellular component of synovial fluid consists of phagocytic cells which function to remove free fragments from the joint space produced due to wear and tear of the joint surfaces during normal joint function (Toller 1961; Schmid and Ogata 1967; Athansou et al 1988). These fragments and metabolites pass back through the synovial membrane into the lymphatic system.

Capsule

The capsule is a thin, loose, densely fibrous structure which encloses the articular surface of the temporal component of the fossa, condyle and articular disc and defines the anatomical and functional boundary of the joint. The articular capsule surrounds the articular surface of the condyle and blends with the periosteum of the mandibular neck. It attaches separately below the medial and lateral attachments of the disc to the medial and lateral poles of the condyle. Laterally, it adheres to a small bony elevation, the articular

tubercle, on the outside of the root of the zygomatic process, and runs along the lateral edge of the eminence, mandibular fossa and postglenoid process. Posteriorly it attaches to the tip and anterior surface of the postglenoid process and extends medially along the raised anterior lip of the squamotympanic and petrosquamosal fissures. Its medial attachment runs along the sphenosquamosal suture. Anteriorly it blends with the anterior thick zone of the disc.

Ligaments

The articular capsule is reinforced laterally by strong tight fibres that make up the temporomandibular (lateral) ligament. A comparable reinforcement is not present on the medial side of the joint. DuBrul (1980) described the temporomandibular ligament as consisting of a superficial fan shaped layer of obliquely orientated collagen fibres and a deeper narrow band of collagen fibres that run in a more horizontal direction. The superficial portion attaches broadly to the outer surface of the root of the zygomatic arch and converges to attach to the condyle inferior to and posterior to its lateral pole. The deeper band joins the articular tubercle to the lateral condylar pole and posterolateral portion of the articular disc.

The principal biomechanical function of the TM ligament , acting singly or with its contralateral equivalent, is to check or limit movements of the condyle-disc complex. The anatomical arrangement of this ligament and the capsule between the temporal bone and the disc permits a wide range of antero-inferior movement between condyle and disc in the superior joint space. However the relative movement between the condyle and disc is small

because the inferior part of the capsule and the inferior collagen layer of the retrodiscal tissues firmly attach the disc to the condyle.

The mediolateral movements of the joint are limited by lateral ligaments, which stabilises the condyle in laterotrusion. The accessory ligaments are the sphenomandibular and stylomandibular ligaments. The stylomandibular ligament limits the antero-protrusive movement of the mandible. Ramford and Ash (1971) have postulated these ligaments play important roles in regulating mandibular position and movement in dysfunctional states.

Muscular Involvement of the TMJ

The muscles involved with mandibular movement and which generate movements of the TMJ are the temporalis, masseter, lateral and medial pterygoids, and the suprahyoid and infrahyoid groups. The supra-hyoid muscles include the digastric, myloyoid and geniohyoid muscles. These muscles maintain a coordinated movement of the mandible during the movements of speech, swallowing and mastication.

Sicher (1950) and Eriksson (1983) reported on the difficulty in interpreting the mechanics of the TMJ because movements of the mandible are not dependent on the interplay between the shape of the articulating bones and ligaments, but by interplay between the muscles. Normal articular movements are constant in, and characteristic of, each individual because of their autonomic muscular patterns.

2.2.   ANATOMICAL VARIATIONS IN ANATOMY AND HISTOLOGY

The range of variation in the normal appearance and position of the structures of the TMJ must be known to allow an accurate interpretation of images using the various available modalities. Diagnosis is thus based on the clinician's ability to differentiate between the normal variation of joint structures and pathological appearances.

Condyle

There is significant variation in the shape of the condyle and the angulation of the latero-medial pole axis.

1) The shape of the head of a sample of condyles when viewed from the front was classified by Yale et al (1966) as flat (25.2%), convex (58.3%), angled (11.6%), rounded (3.0%) and miscellaneous (1.9%).

2) Viewed from the superior aspect, the condyle varies considerably in shape.

3) The latero-medial pole axis in the horizontal plane is generally angled to the posterior. Yale et al (1966) showed that the range was between 0 and 30 degrees. In the vertical plane the latero-medial pole axis generally sloped to the inferior. The range was between (+) 35 and (-45) degrees, but the average was (+) 5 degrees. In total 11.2% had a negative angulation, 28.8% had a zero angulation and 60% had a positive angle. Variation of angulation within the same individual occurred in 51.9% in the horizontal plane and 48.2% in the vertical plane. In 26% both horizontal and vertical angles were symmetrical. The study by Yale et al (1966) showed there was no variation between races. However concurrent with an increase of the individuals age was an increasing frequency of flat condyles and a reduced frequency of convex condyles.

Condyle and Fossa Dimensions

A cadaver study by Oberg et al (1971) showed that within the age group 20 to 93 years, the antero-posterior width of the condyle ranged between 5.5 and 16 mm with an average of 9.8 mm. The corresponding temporal dimension averaged 19.1 mm with a range of 12 to 23 mm. In the latero-medial dimension the condyle averaged

19.8 mm with a range of 12 to 23 mm. The temporal component averaged 23 mm, ranging between 18 and 28 mm.

Postnatally the condyle appears to grow more in a mediolateral than in an anteroposterior direction. The average width of the condyle in a small group of individuals aged 0-9 years has been found to be about 80%, and the condyle length only about 65% of that found in adults. In a 10 to 19 year old group the corresponding figures were 98% and 88% respectively (Oberg et al 1971).

Articular Disc

Hansson and Nordstrom (1977) reported the findings of an autopsy study of 48 right TMJs from subjects whose age ranged from 1 day to 93 years that were considered normal by macroscopic examination and not exhibiting any signs of arthrosis or deviations in form. Sections were taken perpendicular to the pole axis at four different positions: lateral, latero-central, medio-central and medial. In general the posterior aspect of the disc was thickest: in the centre it was 2.9 mm (+/-0.58 mm), laterally it was 1.9 mm (+/- 0.68) and medially 2.31 mm (+/-0.64). The central part of the disc was thinnest (1.08 mm, +/-0.4 mm), and even throughout, but slightly thicker medially (1.3 mm, +/-0.44). The anterior part of the

disc was even in thickness (2.03 mm, +/-0.55 mm) from the lateral to the medial aspect. In general the more medially placed the cut, the less was the variation in thickness in either the posterior, central or anterior portions of the disc. The lateral thinning out of the adult disc in the middle and posterior dense parts is probably due to increased functional loading in these areas as the disc in children does not show this lateral decrease.

Soft Tissues

The soft tissue layers over the articular surfaces of both the condyle and temporal fossa have been described by Moffett (1962), Blackwood (1966) and Hansson et and Nordstrom (1977). In general the articular tissues can be described as relatively thin ranging from 0.3 to 0.4 mm in thickness. In the condyle they were thicker over the anterior and superior surfaces (0.45 mm, +/-0.15 mm) than they were over the posterior surface (0.25 mm, +/-0.17 mm). The dimensions were slightly greater more medially (0.45 mm, +/-0.16 mm), than laterally (0.37 mm, +/-0.13 mm). The temporal fossa showed an even thickness through both lateral and medial zones. On the eminence the soft tissue layer was thickest over the posteroinferior slope (0.45 mm, +/- 0.18 mm) and thinnest in the apex of the articular fossa (0.07 mm, +/- 0.05 mm). The thicker zones correspond to the areas that are heavily loaded during function. The thickness of these tissues is dependent on an increase in the amount of cartilage tissue at the same time as the undifferentiated mesenchyme disappears in these parts. The thinner layers posteriorly on the condyle and in the roof of the fossa in the temporal component with an intact undifferentiated mesenchyme at a greater age relates to the small functional load in these areas.

2.3.   CLASSIFICATION OF TEMPOROMANDIBULAR JOINT DISORDERS

Classifications of TMJ disorders can take the form of symptomatic clinical classifications, tissue specific classifications or general classifications. In the clinical classification systems there is a paucity of descriptive histopathology describing clinical conditions (Bell 1983) and frequently treatment regimes are incorporated into the classification (Okeson 1993). The general TMJ disorder classifications tend to parallel the classifications used in rheumatology, incorporating a classification system that reflects musculoskeletal disorders in other parts of the body.

The clinical classification system proposed by Bell (1983) divided temporomandibular disorders into five main groups. These included acute muscle disorders, disc interference disorders of the joint, inflammatory disorders of the joint, chronic mandibular hypomobilities and growth disorders of the joint. In order to separate clinically presenting TMJ disorders within each particular class, certain clinical features were considered. These included features within the history that were aetiologically significant, symptoms of masticatory pain, symptoms of restriction of mandibular movement, symptoms of interference during mandibular movement, symptoms of acute malocclusion and radiographic confirmation if required.

The clinical classification proposed by Okeson 1993 separated all TMJ disorders into four broad categories having similar clinical characteristics: masticatory muscle disorders, temporomandibuar joint disorders, chronic mandibular hypomobility disorders and growth disorders. Each of these categories was further divided according to dissimilarities that were clinically identifiable. Each subcategory had a proposed treatment regime.

The general classification system proposed by DeBont and Stegegna (1993) distinguished articular disorders from non articular disorders. Articular disorders included non inflammatory chondro-osteoarthropathies, growth disorders, arthritides, diffuse connective tissue disorders and miscellaneous articular disorders. Non articular disorders included muscle disorders, growth disorders and miscellaneous non articular disorders.

The classification proposed by Bell (1983) separates TMJ disorders into distinct clinical groups and further division based on certain clinical features is included.

1. Acute Muscle Disorders

      Masticatory muscle splinting

      Masticatory muscle spasm

      Masticatory muscle inflammation

2. Disc Interference Disorders of the Joint

      Class I interference (at closed joint position)

      Class II interference (as translatory cycle begins)

      Class III interference (during normal cycle)

      Class IV interference (partial dislocation anterior to cycle)

      Spontaneous anterior dislocation

3. Inflammatory Disorders of the Joint

      Synovitis and capsulitis

      Retrodiscitis

      Inflammatory arthritis

4. Chronic Mandibular Hypomobilities

      Contracture of elevator muscles

      Capsular fibrosis

      Ankylosis

5. Growth Disorders of the Joint

      Aberration of development

      Acquired change in structure

      Neoplasia

Classification proposed by Okeson JP. In Management of Temporomandibular Joint Disorders and Occlusion 3rd edition, 1993, Mosby Year Book, St. Louis, pp:310. This classification separated clinically recognisable TMJ disorders and proposes treatment guidelines for each group.

I. Masticatory muscle disorders

       1. Protective co-contraction

       2. Local muscle soreness

       3. Myofacial pain

       4. Myospasm

       5. Myositis

II. Temporomandibular joint disorders

1. Derangement of the condyle-disc complex

       a. Disc displacement

       b. Disc dislocation with reduction

       c. Disc dislocation without reduction

2. Structural incompatibility of the articular surfaces

       a. Deviations in form

       b. Adhesions

       c. Subluxation

       d. Spontaneous dislocation

3. Inflammatory disorders of the joint

       a. Synovitis

       b. Capsulitis

c. Retrodiscitis

d. Arthritides

    i. Osteoarthritis

    ii. Osteoarthrosis

    iii. Polyarthritides

e. Inflammatory disorders of associated structures

III. Chronic mandibular hypomobility

1. Ankylosis

    a. Fibrous

    b. Bony

2. Muscle contracture

3. Coronoid impedance

IV. Growth disorders

1. Congenital and developmental bone disorders

    a. Agenesis

    b. Hypoplasia

    c. Hyperplasia

    d. Neoplasia

2. Congenital and developmental muscle disorders

    a. Hypotrophy

    b. Hypertrophy

    c. Neoplasia

Classification proposed by DeBont LGM and Stegegna B, in Pathology of Temporomandibular Joint Internal Derangement and Osteoarthrosis. Int. J. Oral Maxillofacial Surg 1993;22:71-74. This classification was based on a general division of disorders.

I. Non inflammatory chondro-osteoarthropathies

a. Osteoarthrosis and internal derangement

-Chondromalacia

-Internal derangement

b. Mechanical derangement's

-Internal derangement's

Osteochondritis dissecans

Disc displacement

-Condyle eminence mobility disturbances

Subluxation

Luxation

Hypermobility syndromes

Capsular fibrosis

Ankylosis

c. Bone and cartilage disorders with articular manifestations

Avascular necrosis

II Growth disorders

Non-neoplastic

Developmental

Hypoplasia

Hyperplaia

Dysplasia

Acquired

Condylosis

Juvenile ostoeathrosis or rheumatoid arthritis

Neoplastic

Pseudotumors

Benign

Malignant

III Arthritides

Primary

Rheumatoid arthritis

Other arthritides

Secondary

Synovitis

Capsulitis

Crystal induced arthropathy

IV Diffuse connective tissue disorders

Systemic lupus erythematous

Mixed connective tissue disease

Polymyositis

Scleroderma

Sjogrens syndrome

Rheumatic fever

Polymyalgia rheumatica

Arteritis temporalis

V. Miscellaneous articular disorders

Nonarticular disorders

I. Muscle disorders

Myofacial pain

-Regional

-Generalised

Muscle fibrosis

-Contracture

Chronic muscle strain

-Bruxism

Muscle inflammation

-Tenomyositis

-Infection

Motor function disorders

-Orofacial dyskinesia

-Cramp/spasm

Miscellaneous muscle disorders

-Degenerative

-Myasthenia

-Myotonia

-Neoplasm

II. Growth disorders

Eagles syndrome

Coronoid impingement syndrome

Neoplasia

III. Miscellaneous non articular disorders

2.4. ANATOMY AND HISTOLOGY OF THE PATHOLOGICAL HUMAN TEMPOROMANDIBULAR JOINT

The classification systems proposed present a diverse range of pathologies that may affect the TMJ and for which a patient may present for treatment. However the main subgroups that present in cadavers and which can be imaged by MRI include internal derangement with joint dysfunction, remodelling and degeneration of the joint articular surfaces.

2.4.a. REMODELLING

Synovial joints cease to grow when individuals are approximately 20 years old. However, structural changes occur in both the soft and mineralised tissues of synovial joint components after growth has ceased. This reflects functional demands on the joint structures. In optimal conditions a remodelling joint is characterised by slowly occurring morphologic changes. In this way components adapt to each other and assist in maintaining joint function.

Johnson (1962) in a histologic study of adult joints described remodelling that affected adult joints as progressive, regressive and circumferential. Progressive remodelling results from formation of chondrocyte clusters and increased proteoglycan production. Furthermore, bone may be added to the subchondral plate through apposition in existing osteons as well as through vascular invasion of cartilage and endochondral ossification (Sokoloff 1982). Regressive remodelling involves chondrolytic removal of cartilage proteoglycans and loss of chondrocytes due to cell degeneration and necrosis, resorption of subchondral bone, and metaplastic conversion of soft tissue into cartilage. Circumferential remodelling can be regarded as a peripheral progressive remodelling occurring due to the increase in cartilage and subsequent ossification of the capsule or ligament insertions which eventually leads to osteophytic lipping of the joint margins.

In 1974 Moffett et al published an investigation to ascertain whether the temporomandibular joints were remodelled in the same way as that found by Johnson for a number of other joints in man. They studied 34 TMJ's obtained at autopsy of subjects aged 45 to 81 years. They found that each preparation displayed histological signs of

remodelling in some area of the articular tissue and the subchondral bone. In many preparations it was obvious that the process had produced typical changes in the contours of the joint, while in others the remodelling could be identified only histologically. It was found that remodelling in the human TMJ was mainly of progressive and regressive types and that the rate and extent was dependent on functional or mechanical factors and not age. It was reported that remodelling, progressive as well as regressive, may become extensive and lead to deviations in the form of the joint components which can interfere with joint function. The structural changes may also evolve in a pathological direction developing into osteoarthritis.

Mongini (1972) studied the macroscopic appearance of 100 skulls from subjects aged 18-67 years at death and reported that remodelling of the TMJ's was significantly associated with an increasing number of lost teeth and increasing age. He concluded that remodelling is the result of stresses to which the condyle is subjected during normal functional activity. Mongini (1975) also studied 100 skulls from subjects aged 20-53 at death and with complete dentition's but with variously abraded natural dentition's and reported that dental wear influenced condylar shape due to bone remodelling.

Moffett et al (1964) related the mechanism of progressive remodelling to the development of fibrous cartilage in the TMJ. The transformation of the fibrous articular tissue into fibrocartilage was observed only in those parts of the joint which were considered to be articulating or pressure bearing, namely the anterior part of the condyle and the posterior slope and the crest of eminence. It was thought to be likely that the same functional stimuli which induce this differentiation are also responsible for the proliferative response of the articular tissue and the underlying bone. This may manifest itself as an alteration or

reshaping of the outline of the articular tissue. Moffett hypothesised that the thickening of the articular surface and the cartilage due to progressive remodelling results in expansion of the calcified zone, resorption of the calcified tissue, ingrowth of vessels from the underlying bone, and finally advancement of the subchondral bone plate towards the articular surface. These authors proposed that regressive remodelling is initiated by bone resorption at the junction of the cartilage. In the resorption area the subarticular bone is replaced by vascular mesenchyme. Beneath the covering articular layer, which may remain intact, repair of the subarticular bone can take place by formation of new cartilage and bone, thereby forming a new surface contour.

Blackwood (1966) reported in a comprehensive histological study of 530 TMJ's from different age groups that the TMJ was affected by the same types of remodelling in most of the adult joints. Blackwood concluded that it is the undifferentiated mesenchyme cells of the proliferative zone that are responsible for dimensional changes in the articular surface, while the fibrous surface layer does not participate in the process and is only passively involved in the underlying changes. Blackwood hypothesised that the mesenchyme cells differentiate into chondrocytes which produce the collagen and proteoglycans of the matrix and also the glycoproteins and enzymes. Blackwood (1966) confirmed his earlier findings in a continuing study in which he also included microradiography of 45 TMJ's of subjects aged 37-90 years. He reported that it is the undifferentiated mesenchyme in the proliferative zone that are responsible for TMJ remodelling and that this layer of cells has a capacity to proliferate and differentiate throughout life. The chondrocytes in the fibrous cartilage layer produce the collagen and the proteoglycans of the matrix. Blackwood hypothesised that remodelling compensated for the changing relationship of the jaws which resulted from occlusal wear or through loss of teeth.

Oberg (1971) examined the gross anatomy and the subsequent histology of 102 TMJ's from subjects aged 20-93 years and observed advanced deviations in form due to remodelling in 57 joints. Twenty three percent of joint temporal components and 42% of the condyles exhibited deviations in form. Remodelling was evident in 40% of the joints of the 20-39 year old age group whereas in the joints of people above 40 years extensive remodelling was seen in about 60% of the joints.

Hansson et al (1977) and Hansson and Nordstrom (1977) examined 115 TMJ's from human cadavers whose age ranged from 1 day to 93 years. The thickness of the soft tissue in the sagittal plane was measured microscopically in 22 of the TMJ's which exhibited deviations in form in the anterior, central and posterior parts of the joint. The soft tissue layers were thickest and the undifferentiated mesenchyme was thinnest in the lateral parts of the superior aspect of the condyle, laterally on the anterior and posterior-inferior slopes of the articular eminence and posteriorly in the mediocentral part of the disc. This was reflected in the statistically highly significant negative correlation found between the amount of undifferentiated mesenchyme and the thickness of the soft tissue layer, a finding which suggests that the undifferentiated mesenchyme is utilised for remodelling of the soft tissue layers with deviations in form developing as a result. The occurrence of undifferentiated mesenchyme and the total thickness of the soft tissue layers reflects the functional loading of the joint components. The researchers supported the theory that increased biomechanical loading stimulated the growth of the cartilage from the undifferentiated mesenchyme with simultaneous thickening of the soft tissue layer. The depletion of the undifferentiated mesenchyme in TMJ's with deviations in form indicated that the ability of joints to retain the capacity to proliferate and repair under functional loading may be impaired. This is in agreement with the findings of a macroscopic

investigation of autopsy material by Bean, Omnell and Oberg (1977) who postulated that

deviations in form of the TMJ may be related to variations in thickness of the soft tissues.

2.4.b. OSTEOARTHROSIS/OSTEOARTHRITIS

Osteoarthrosis can be defined as a primarily noninflammatory disease of movable joints characterised by deterioration and abrasion of the articular soft tissue surface, and by simultaneous remodelling in the underlying bone (Sokoloff 1982). Osteoarthritis has been defined as osteoarthrosis with synovitis (Okeson 1993). Therefore use of the term osteoarthritis implies inflammation of the synovium, capsule and articulating tissues caused by waste products and inflammatory mediators.

The aetiology of osteoarthrosis is not yet properly understood. Age is a predisposing factor as both the frequency and extension of the macroscopic lesion increase with age (Oberg et al 1971; Kopp 1978) but there is no evidence of any functionally important age dependent alterations in joint tissue indicating that age would play a primary etiologic role. The most significant factor is thought to be mechanical loading of the joint (Hansson 1977). Autopsy studies have revealed a correlation between tooth loss and macroscopic lesions of OA of the TMJ (Oberg et al 1971). Other factors which may also increase the load carried by the TMJ are age, muscular hyperactivity (bruxism), unilateral chewing, deformity following trauma and congenital defects.

It has been postulated that osteoarthrosis of the human TMJ starts in the articular surface of the condyle or fossa (Contepomi and Farkas 1976). A second hypotheses is that microfractures resulting in hardening of the subchondral bone precipitate lesions in the articular surface (Radin et al 1973). A third hypotheses is that osteoarthrosis is the result of simultaneous changes in both the articular surface and the subarticular bone (Telhag 1973).

Osteoarthrosis of the TMJ can be classified according to depth and surface extension of changes. The lesion is considered deep when the soft tissue surface is damaged down to the subarticular hard tissue, or the disc has been perforated. The lesions are generally focal in nature and seldom extend over the whole joint surface. The lesions are most frequently localised to the lateral part of the condyle and temporal components. The medial aspect of the joint is seldom affected.

The TMJ disc lacks the reserve remodelling capacity of the articular tissues and is frequently involved first in osteoarthrosis. Longstanding increased compressive forces on the disc leads to thinning, cell necrosis, intercellular matrix degradation and eventually perforation. Thinning of the disc will also increase the strain on the other opposing components exacerbating changes in these areas.

In the human TMJ the earliest microscopic change associated with osteoarthrosis at the articular joint surface is fibrillation, splitting, clefting and thinning of the collagen fibrils of the articulating surface (Freeman 1972). This is reportedly associated with degradation of proteoglycans and subsequent loss of glycosaminoglycans (Ineroth 1978). In this context it has been suggested that chondrocyte damage leads to release of proteolytic enzymes from lysosomes which results in degradation of proteoglycans (Ali and Evans 1973). The major consequence of the degradation of proteoglycans is reduced resistance to compressive forces generated during joint function. The depletion of glycosaminoglycans makes the tissues softer and easily deformed and this subjects the collagen to abnormally high strains (Freeman and Kempson 1973). The process may progress to more severe forms of tissue disintegration that affects deeper regions of the articular cartilage and ultimately leads to complete cartilage destruction and exposure of the subchondral bone. The release of

necrotic cartilage tissue containing proteoglycan macromolecules can elicit a foreign body response and cause low grade synovitis and capsulitis.

It has been postulated that the cancellous subchondral bone acts like a shock absorber (Radin et al 1973). When this bone has to absorb increased load due to cartilage destruction, fatigue micro fractures can occur. In addition destructive changes such as osteolysis, invasion of granulation tissue and osteoporosis are thought to occur further reducing the ability of the TMJ to withstand functional loading (Lereim and Goldie 1975). Concurrent with these changes new bone formation can lead to osseous outgrowths called osteophytes (Jeffery 1973). Bone cysts may occur in cases of severe TMJ destruction.

Extra-articular tissue responses to TMJ osteoarthrosis include muscle responses and changes in occlusion. The muscle responses may include muscle splinting and disuse atrophy. Occlusal responses may include some occlusal disturbances such as a late developing anterior open bite and, as a result of a shortening of the ascending ramus, a tilting of the occlusal plane often associated with some chin deviation towards the affected side.

Symptoms associated with osteoarthrosis in the TMJ such as pain, stiffness and reduced mobility have been attributed to secondary inflammation of the capsular tissues. It has been hypothesised that proteoglycans released into the synovial fluid during rapid degradation and breakdown of the joint surfaces are capable of causing chronic synovitis characterised by increased vascularity, oedema, accumulation of fibrin, increased fibroblastic activity and extravasation of phagocytic mononuclear clear cells (DeBont 1991; Stenga 1994). The synovitis in turn can cause further destruction of the articular surface due to release of

proteolytic enzymes (collagenase, cathepsins, plasminogen) from the lysosomes of degenerating cells. It has been suggested that the increased lysosome content in joints with osteoarthrosis occurs as a response to the increased phagocytic activity by the synovial cells in affected joints (Hammerman 1966).

It has also been postulated that an inflammatory response is produced by pyrophosphate which is found in high concentrations in joints with osteoarthrosis as the amount of pyrophosphate correlates well with the severity of osteoarthrosis. In osteoarthrotic joints calcium pyrophosphate crystals are formed which are often deposited in the cartilage tissue (Carlsson, Hassler and Oberg 1974). Free crystals in the synovial fluid have the potential to initiate an acute inflammatory response (McCarty 1975).

REMODELLING AND OSTEOARTHROSIS/OSTEOARTHRITIS

Remodelling of the TMJ can be defined as rebuilding of the subarticular soft and hard tissue layers mainly related to proliferative processes, while osteoarthrosis represents changes associated with a breakdown of the articular surface layer.

It has been suggested that remodelling and osteoarthrosis occur concomitantly in studies by Moffett et al (1974), Blackwood (1966), Boering (1966) and Oberg et al (1971). Reports indicated that if the demands on the remodelling activity in the TMJ exceed the capacity for repair that osteoarthrotic lesions may develop (Blackwood 1966). Throughout life the TMJ articular cartilage and the underlying bone display a shifting equilibrium between changes in form and function. Increased loading may stimulate remodelling, involving increased synthesis of proteoglycans and collagen fibrils. Overloading may disturb the equilibrium between form and function, giving rise to tissue breakdown (DeBont and Stegegna 1993).

2.4.c. INTERNAL DERANGEMENT

Internal derangement of the TMJ affects all tissues of the joint and may present as either an anteriorly displaced, anteromedially displaced, laterally displaced or perforated disc. There is almost universal consensus that internal derangement and osteoarthrosis of the TMJ occur concomitantly (Hansson and Oberg (1977); Katzberg et al (1983); Hellsing and Holmlund (1985); Westesson et al (1984); Westesson (1985); DeBont et al (1986). However, opinions differ as to the cause and effect relationship between the two disorders. The prevailing view seems to be that joint degeneration proceeds faster and to a more severe degree in cases of persisting internal derangement (Westesson et al 1984; Westesson 1985). De Bont et al (1986) stated that internal derangement was one of the accompanying signs of osteoarthrosis but Stegegna et al (1989) considered osteoarthrosis the basic disorder.

DeBont (1993) in a study of human cadaver TMJ's presented the hypotheses that internal derangement is highly correlated with TMJ osteoarthrosis and osteoarthritis. The author suggested that cartilage breakdown may affect the sliding properties of the joint surfaces and that deterioration of the synovial fluid gives rise to frictional and adhesive wear. These alterations impair the movement of the disc and may cause disc hesitation. In turn this later phenomenon may induce joint stiffness and repetitive stretching of the disc attachments. Subsequently the discal attachments may gradually elongate to an extent that permits disc displacement.

Several problems arise when evaluating the validity of the hypotheses postulated by these studies. Autopsy studies (Westesson 1984; DeBont 1986) usually involve joints from aged

individuals who, based on probability alone, might have suffered from degenerative disease more often than young people. Also, some histologic studies (Solberg 1985) fail to include a histologic examination to identify early signs of degeneration. Results from inspection of surgical specimens (Scapino 1983; Hall 1984; Isberg et al 1986; McCoy et al 1986; Blaustein and Scapino 1986; Kurita et al 1989) may be biased by the fact that joint surgery is performed only in severe cases of painful internal derangement which resists conservative treatment. Finally radiographic examination (Westesson 1985) often may not disclose mild osteoarthrotic changes and will not disclose changes due to degeneration and normal articular remodelling.

In joints demonstrating internal derangement with anterior disc displacement the following changes in the joint may be evident.

Disc

Scapino (1983) reported that in joints with displaced discs the bulk of the posterior band lay anterior to the condyle with the central part of the disc below or anterior to the articular eminence. The anterior position of the disc was reflected by the apparent increase in the maximum length of the anteroinferior part of the joint capsule and adjacent joint recess. In addition the disc overlays more of the lateral pterygoid muscle than is normal and could be folded around the thin central band in an upward/superior fold or a downward/inferior fold. The author demonstrated that thickening of the posterior band occurred in displaced discs. The degree of thickening varied from one joint to another, and within the same joint at various positions along the lateral and medial margins. Observations of disc thickening and folding in anatomical sections made by Steinhardt (1933), Blackwood (1969) and Crowley

et al (1996) coincided with the arthrographic findings of Wilkes (1978), Blascke (1980) and Katzberg et al (1980).

Histologicaly the disc adapts to its anterior position. Observed histologic signs that suggest remodelling of the disc include rearrangement of collagen fibres (Scapino 1983), decrease in cellularity (McCoy 1986) and the appearance of a proliferative surface layer (Kurita et al 1989).

Anterior Attachment of the Disc

In anteriorly displaced discs, the anterior band is positioned much further anteriorly than normal. Scapino (1983) showed that both the temporal ligament attachment and the position of the attachment to the superior surface of the superior belly of lateral pterygoid had shifted forward. Thus the anterior extent of the inferior joint cavity was longer, a characteristic used in arthrographic diagnosis of disc displacement (Wilkes 1978; Katzberg et al 1980).

Retrodiscal Tissues

In anteriorly displaced discs, the anterior one third of the retrodiscal tissues are located between the articular surface of the condyle and articular eminence, and not located posterior to the condyle as it is normally. In the retrodiscal tissues, fibrosis (Scapino 1983; Wilkinson and Crowley 1993), thickening of the arterial walls (Hall 1984), hyperplastic tissue formation (McCoy 1986; Blaustein and Scapino 1986), hyaline degeneration (Isberg

1986), enhanced staining for sulfated glycosaminoglycans (Blaustein 1986), splitting (Kurita et al 1989) and perforations (Isberg and Isacsson 1986) have been described.

Steinhardt (1933), Blackwood (1966), Scapino (1983) and Wilkinson and Crowley (1994) observed fibrosis of the anterior retrodiscal tissues which had been described as remodelling due to compressive loading of the posterior attachment which in turn had been displaced anteriorly over the head of the condyle. The potential for venous engorgement of the retrodiscal tissues as described by Rees (1954) and observed by Steinhardt (1933), Scapino (1983) and Wilkinson and Crowley (1994), was still present in joints demonstrating a displaced disc despite the retrodiscal tissues assuming a "pseudodisc" like appearance.

Synovial Membrane

DeBont et al (1993) described that when a disc is displaced anteriorly it causes increased pressure on the synovial membranes resulting in variations in the production and composition of synovial fluid and the passage of fluids from the joint cavity back into the lymphatic system. This pressure effect reportedly occurs anteriorly and posteriorly and may cause a significant reduction of synovial membrane function. In turn this may impair joint function and cause a progressive increase in the debris content of the fluid and in the erosion rate of the articular region.

Capsule and Ligaments

Scapino (1983) reported that in joints with a displaced disc the shift in the tissue mass results in an increase in the length of the anteroinferior part of the joint capsule and the adjacent joint recess. This causes an apparent elongation of the anterior recess of the inferior joint space which has been suggested to corresponded to the magnitude of the disc displacement (Katzberg et al 1980). The further the disc is displaced the greater the potential for stretching the lateral ligament and the capsule in the affected zones which may reduce the stability of the joint.

The Condyle and Temporal Articulating Surfaces

An increase in the thickness of the articular tissues associated with disc displacement has been consistently reported by researchers (Blackwood 1966; Hansson and Nordstrom 1977; DeBont 1993). Remodelling is frequently seen on the latero-posterior part of the articular eminence, and the latero-anterior part of the condyle in joints with displaced discs. Progressive and regressive remodelling in all TMJs with displaced discs has been reported, but in general the integrity of the articular tissue was not affected (Scapino 1983). Disturbed fibre organisation has been described and although Scapino (1983) did not find these changes consistently, this investigator believed they were a result of altered functional loading. However Steinhardt (1933), Westesson (1985) and DeBont (1986) reported that articular surface degenerative changes occured consistently in association with disc displacement.

2.5. INDICATIONS FOR IMAGING THE TEMPOROMANDIBULAR JOINT

The treatment of disorders of the TMJ is hampered by a relative inability to visualise the structures involved. An ideal imaging technique should provide information about the status of the osseous structures and soft tissues at rest and during function. A number of diagnostic techniques exist to assist the process of clinical diagnosis of TMJ disorders. The alternatives for joint imaging include conventional radiography, CT, arthrography and MRI. An imaging study of the joint is warranted:

1) when the diagnosis of internal derangement is in doubt and must be established before therapy is initiated.

2) if the diagnosis is not in doubt but confirmation is required for medicolegal reasons.

3) preoperatively for disc surgery.

4) where therapy has failed and doubt about the diagnosis arises.

However, controversy exists as to which technique is most accurate in assessing dysfunction (Kaplan 1989; Katzberg et al 1983). The use of plain radiographs is limited due to an inability to detect disc displacement, the superimposition of structures over the area of interest, non visualisation of the medial and superior portion of the condyle, excessive exposure to ionising radiation and the fact that osseous anatomy is best visualised. Further, Nilner and Peterson (1995) recently concluded that no single radiographic finding accurately correlated with treatment outcome in patients with TMJ disorders and that plain radiography had only a minor role in determining the management of these patients. A radiographic examination may be used to exclude other dental and jaw pathology that might be causing referred pain to the area.

Laminography, which developed as an alternative, eliminates the superimposition of bony structures and allows more accurate assessment of joint spaces because of the ability to visualise the joint at varying depths. However laminography only depicts bony changes and involves patients in extensive exposure to ionising radiation.

Arthrography has the advantage of allowing visualisation of the dynamic relationships between osseous and soft tissue joint components, including evidence of perforation of the disc (Murphy 1981). The disadvantage of arthrography is that it is an invasive procedure which is frequently associated with postoperative pain, limitation of movement and transient crepitis following the procedure. In addition reports by Ryan et al (1990) and Watt-Smith et al (1993) indicated that disc perforations were overdiagnosed using arthrography.

Computerised tomography (CT) provides a non invasive method of evaluating TMJ anatomy and function which images bony changes. However, intra-articular soft tissues are poorly visualised and the patient is exposed to ionising radiation. CT is not recommended for imaging the disc as the tendinous attachment of the lateral pterygoid muscle often has a similar appearance (Dixon 1991; Wilkinson and Maryniuk 1983).

Magnetic resonance imaging (MRI) has developed as an imaging modality, applicable to the TMJ, which has the potential to aquire three dimensional, multiplane images without exposing the patient to ionising radiation or known biological hazards.

MR images of the TMJ have been reported to provide visualisation of both the soft and hard tissues, confirmation of location and deformation of the disc, identification of

degeneration and inflammation of the surrounding tissues and provides a technique to allow for assessment of the joint components in function (Katzberg 1989; Westesson 1992). In addition simulated "cine" mode images have been obtained that introduce the ability to record TMJ dynamics non invasively (Burnett et al 1987). One reason that MR has become the focus of intensive research is the possibility that it may provide physiological and possibly biochemical tissue specific information as well as anatomic information (Roberts 1990).

In summary the various imaging modalities provide varying sensitivity in imaging the soft and hard tissues of the normal and abnormal TMJ as illustrated in the following table.

Characteristic	Conventional radiography	Arthrography	CT	MR
Disc Position	No	Yes	Yes	Yes
Perforation	No	Yes	No	No
Disc Dynamics	No	Yes	No	No
Disc Shape	No	No	No	Yes
Bony Changes	Yes	Yes	Yes	Yes

Table correlating the accuracy of conventional radiography, arthrography, CT and MR in diagnosing disc position, disc perforations, disc dynamics, disc shape and bony changes in the human TMJ.

2.6. HISTORICAL PERSPECTIVE OF MAGNETIC RESONANCE IMAGING

As early as 1924 the magnetic properties within the nuclei of cells had been postulated as an explanation for the small structures found in the atomic spectra. Within 15 years Rabi et al (1939) were successful in performing experiments on molecular beams. In the mid 1940's two groups of investigators working independently (Bloch et al 1946; Purcell 1946) simultaneously obtained magnetic resonance signals from the nuclei of liquids and solids. For the next three decades the techniques of *in vitro* high resolution nuclear magnetic resonance spectroscopy (NMR) were refined and incorporated into most biochemistry and physics laboratories.

Damadian (1971) made an important contribution when he observed that the relaxation times of protons within malignant tissues were longer than those of normal tissues. This was an early demonstration of the alterations in molecular nuclei of tissues that have undergone malignant transformation. However, these were *in vitro* studies, and the variations in relaxation times (T1 and T2) within complex molecular systems were imperfectly understood. It is now known that changes in the relaxation times are difficult to relate to specific disease (Fullerton 1988).

In 1973 Lauterbur successfully produced a two dimensional image by the induction of local interactions employing nuclear magnetic resonance. Lauterbur used secondary coils to add a gradient to the main magnetic field which spatially encoded to NMR signal and enabled the computer construction of images.

2.7. BASIC PRINCIPLES OF MAGNETIC RESONANCE IMAGING

Physical Basis

Nuclei with an odd number of protons possess spin or angular momentum and a charge. Therefore, they act like magnets with north and south poles and a magnetic moment oriented along this axis. These magnetic dipole nuclei are randomly orientated in the absence of an external magnetic field but when they are placed in a field they attempt to align with it. More nuclei align in the parallel, lower energy orientation than the higher energy level antiparallel orientation. Therefore net magnetisation is in the same direction as the external field. However, in reality the nuclear magnetic moments are not perfectly aligned with the external field, and they begin to precess about its axis. Precessional frequency is a product of the strength of the external magnetic field and a constant which is unique for each nuclear species. This precessional frequency is also called the resonance or Larmor frequency which is dependent on the nuclide and the strength of the external magnetic field.

There are numerous elements that can be imaged by MR. Any nucleus with an odd number of either protons or neutrons can produce an MR signal. However, MR is primarily applied to the imaging of hydrogen due to its high natural abundance and its high sensitivity to MR signal.

A collection of precessing nuclei will have a macroscopic magnetisation owing to the summation of individual magnetic moment vectors. To detect a signal in MR, energy is required to cause the macroscopic magnetisation to change direction with respect to the

external magnetic field, and to induce resonance. This occurs when radiofrequency (RF) energy is added at the Larmor frequency, causing the protons to be excited to a higher energy level resulting in parallel to antiparallel magnetic moment transitions. If an appropriate RF pulse is delivered, the macroscopic magnetisation can be rotated by 90 degrees, thus producing transverse magnetisation which is perpendicular to the main magnetic field. As the nuclei recover their alignment by relaxation processes, they produce radiosignals as they emit the absorbed energy that is proportional to the magnitude of the initial alignment. Tissue contrast (ie, differences in signal) develops as a result of the different rates at which nuclei realign within the magnetic field.

To accurately spatially localise RF signals in order to construct a MR image, gradient fields are superimposed on the static field. Surface coils placed in planes at right angles to the main magnetic field provide a gradient such that each volume (called a voxel) in space within the field has a slightly different magnetic field associated with it than the protons in any other voxel. If different areas within the object experience slightly different magnetic field strengths, the resonance frequency produced will vary according to spatial location. Surface coils have revolutionised MRI of the TMJ as the S/N ratio is increased, resolution is better and image quality has improved (Harms et al 1985). Using dual surface coils improves efficacy by imaging both joints in the time it would take to do one side.

The spatially encoded signals are measured after a defined time period has elapsed (TE) and the images are transformed by computers using either the two dimensional or three dimensional Fourier transformation process (2DFT and 3DFT) to produce a free induction decay signal (FID). The main advantage of the 3DFT technique is that it allows sections to

be made as thin as 1.25mm compared to 2 to 3mm with the 2DFT technique (Wilk and Harms 1988, Wilk et al 1988).

Magnetic Resonance Signal

The strength of the MR signal is proportional to nuclear density, nuclear motion (flow) and the relaxation times T1 and T2 (Hasso et al 1990; Payne 1996). Nuclear Density is the number of protons in a given volume (voxel) that contribute to the signal. Nuclear Motion results from the change in location of the protons during the time the study is in progress. T1 (spin lattice or longitudinal relaxation time) is the time required to regain longitudinal magnetisation following a 90 degrees RF pulse; that is the time to relax to the minimal energy state which is tissue dependent since different tissues allow exchange of energy at different rates. T2 (spin-spin or transverse relaxation time) is the time that the resonating protons remain coherent and precess in phase following a 90 degrees radiofrequency pulse. T2 decay is due to magnetic interactions that occur between spinning protons. Each tissue type has unique T1 and T2 values.

2.8. PULSE SEQUENCE SELECTION

A single free induction decay (FID) signal is not sufficient to generate an acceptable MR image, and repeated FIDs are only occasionally used. The two most commonly utilised pulse sequences are the gradient recalled echo (GRE) and spin echo (SE) techniques, both of which rely on two separate RF pulses with collection of information (echo) only after the second pulse.

Spin Echo

Spin echo sequences allow the examiner to use both T1 and T2 magnetic resonance images (Katzberg 1989; Tasaki and Westesson 1993). The repetition time (TR) and echo time (TE) are parameters controlled by the operator, and they can be used in relation to the T1 and T2 values in the tissues to optimise image contrast and resolution, a process called "weighting". A long TR and short TE produce proton density weighting. A short TR and short TE produce T1 weighted images (T1W). T1W images are best for examining the normal temporomandibular joint. T2W images (long TR and long TE) are best for detecting inflammation and effusions of the joint (Curtin 1988). Spin echo uses an initial RF pulse of 90 degrees flip angle with a subsequent refocussing pulse of 180 degrees. This sequence requires a relatively long TR to ensure recovery of the protons from the RF pulses, resulting in lengthened acquisition time.

On T1 weighted images, tissues that have a short T1 such as fat, appear bright, whereas tissues that have long T1, such as fluid appear dark. On T2 weighted images, tissues with long T2, such as fluid and cysts appear bright, whereas tissues that have a short T2 such as

muscle appear dark. On proton density weighted images, tissues with increased proton density appear moderately bright.

Gradient Echo

Gradient recalled sequences (GREs) differ from SE sequences in many ways. Very short TR's are possible with GREs because the RF pulse angles are less than 90 degrees, thus shortening image acquisition time. Gradient recalled techniques refocus the echo rather than the 180 degree pulse as is the case with the spin echo sequences (Moon 1973). The formation of an echo with these sequences requires the application of two gradient pulses. The application of the frequency encoding gradient during the echo immediately dephases the spin along the X-direction. To correct for this dephasing, an inverted gradient pulse is first applied prior to read out, which produces a compensatory phase shift of opposite sign. The first pulse is called a dephasing gradient and the second is a rephasing gradient. The pair of dephasing and rephasing gradients constitute a gradient reversal, which results in the formation of a gradient echo at the echo time. When using GRE sequences, another signal variable is obtained (T2*) that is equivalent to the effective transverse relaxation time and that is always shorter than the "true" T2 (Walter 1988).

The advantage of a gradient echo MR image is that unlike conventional spin echo pulse sequences which use a 90 degree flip angle for excitation, the flip angle may be varied for the gradient echo image (Hasso et al 1991). Small flip angles only slightly reduce the longitudinal magnetisation so that spins can almost fully remagnetise between RF pulses, even with short TR. As a result, faster imaging is possible than with spin echo sequences. The reduced flip angle also affects contrast. Because T1 effects are diminished with small

flip angles, these images are predominantly weighted towards proton density. Since the effects of T1 differences on the longitudinal magnetisation become more pronounced as the flip angle is increased, gradient echo images acquired with short TR and large flip angles are predominantly T1 weighted.

Gradient echo sequences lack a refocussing RF pulse which results in images generated which are sensitive to artefacts from magnetic field inhomogenicities (Conway et al 1989; Schellhas 1988). This sensitivity may be utilised in the detection of lesions. Haemorrhage and calcification can produce variations in local magnetic field homogenicity leading to localised signal loss on gradient echo scans. This signal behaviour may aid in the detectability of these lesions. In addition signal from flowing blood is increased compared with that of conventional spin echo sequences.

A variety of GRE sequences are frequently used to visualise temporomandibular joint dynamics in the pseudodynamic (cine) fashion. In particular gradient refocussed acquisition in the steady state (GRASS), fast imaging with steady precession (FISP) and low angle shot (FLASH) are methods that can obtain rapid images, since the time required for each image is roughly 25 seconds (Burnett 1987; Conway et al 1989). The advantage of these methods is that they can eliminate some of the motion artefacts prevalent in some in standard T1W images. In the "cine" mode they can depict the exact time of disc recapture as the mouth is being opened and may aid in distinguishing normal variants from pathologically displaced discs. The disadvantage of these imaging sequences is that the signal to noise ration is decreased so that the image are somewhat inferior (Conway 1989).

Intensity of the Magnetic Resonance Signal

When viewing MR images, hyperintense signals (echoes) are displayed as white, while hypointense echoes are displayed as black. Since T1 represents a growth curve, a short T1 will produce an intense MR signal on a T1 weighted image as recovery of the longitudinal magnetisation will have occured. Conversely, a long T1 will produce a signal of low intensity. A long tissue T2 will produce an intense signal on a T2 weighted image, because less decay of transverse magnetisation will have occured in a given time. Therefore a short T2 will be represented by a MR signal of low intensity. Therefore to interpret MR images it is important to be aware of the pulse sequence technique utilised.

2.9. CLINICAL AND CADAVER MAGNETIC RESONANCE IMAGING STUDIES OF THE HUMAN TEMPOROMANDIBULAR JOINT

Recent studies of TMJ patient groups comparing clinical, arthrographic, CT and surgical findings with sagittal or coronal MR images have reported that this new imaging modality provides excellent visualisation of both soft and hard tissues (Katzberg et al 1986; Roberts 1985; Kaplan 1987; Donlon 1987; Helms 1986; Katzberg 1985; Harms 1985 and Wilk 1986). Difficulties in interpretation of the images have been reported in joints with a combination of anterior and medial or lateral displacements of the disc (Westesson et al 1987; Westesson et al 1987). In addition perforations (Moses et al 1989), adhesions (Watt-Smith et al 1993) and articular surface changes (Dixon 1991; Watt-Smith et al 1993) have been reported to be poorly imaged.

The cadaver model provides an opportunity to compare T1 and T2 weighted MR images with the corresponding anatomic and histologic sections. Cadaver studies also allow the accuracy and sensitivity of MRI to be assessed against a "gold standard" prior to its introduction into clinical practice (Westesson et al 1987; Schwaighofer et al 1990; Tasaki and Westesson 1993).

NORMAL TEMPOROMANDIBULAR JOINT

Articular Surfaces

In clinical and cadaver studies comparing sagittal and coronal T1 weighted MR images with surgical or anatomical findings it was reported that cortical bone which had no signal

intensity provided an accurate outline of the glenoid fossa, articular eminence and surface of the mandibular condyle (Hasso et al 1991; Wilk and Harms 1986; Harms et al 1985; Katzberg 1989; Schwaighofer et al 1990; Tasaki and Westesson 1993). High signal intensity was present in the central portion of the head of the condyle and in the centre of the articular eminence due to marrow fat. On a normal T2 weighted image the cortical bone had a very low signal and the marrow had an intermediate to low signal (Schellhas 1989; Harms 1985). Normally no high signal structures were seen within the joint in a T2 weighted image giving it a grainy appearance.

Disc

Clinical and cadaver studies have shown that disc position and shape can be well imaged in T1 and T2 weighted sagittal and coronal images because the densely collagenous fibrous connective tissue of the disc has an intermediate to dark MR signal which provides good contrast between the low signal of the osseous and muscular components of the joint (Katzberg 1986; Westesson et al 1987; Roberts et al 1985; Roberts et al 1991; Payne and Nakielny 1996). Tasaki (1993) and Katzberg (1988) showed that in coronal MR images the disc had an arc like configuration with the medial margin of the disc attaching to the medial pole of the condyle and with the lateral margin attaching to the lateral pole and highlighted against the high signal parotid gland and skin. Cadaver studies by Schwaighofer et al (1989) and Katzberg et al (1988), comparing sagittal and coronal MR images with anatomical sections, revealed a 86% and 83% respective accuracy of MRI in the evaluation of disc position. It was suggested by both these studies that coronal images of normal joints provided little additional information.

Controversy exists in determining whether MR imaging accurately demonstrates the margin between the disc and its posterior attachments in the TMJ. Roberts et al (1990) in a cadaver study assessing the MR signal from different TMJ tissue stated that the boundary between the intermediate zone and the posterior band of the disc can be mistaken for the boundary between the posterior band and the posterior attachment. This would lead to the conclusion that the disc is in a more anterior position. A valid interpretation of the disc position requires a clear identification of the structures involved. However Scapino (1991) in a study comparing the MR images of TMJ cadavers suggested that regional differences in the distribution and organisation of connective tissue, fat and vascularity within the disc and retrodiscal tissues allows for good contrast in MR images.

Retrodiscal Tissues

Clinical and cadaver studies showed the vascular retrodiscal tissues in sagittal T1 images presenting as an area of intermediate signal bounded by the low signals of the condyle and fossa and anteriorly by the posterior band of the disc (Scapino 1991; Roberts 1990; Tasaki 1993). The retrodiscal tissues in T2 weighted images had a high signal (Wilk 1986; Schellhas 1989). Sagittal images of normal joints clearly demonstrated the junction of the retrodiscal tissues with the fibrous, low signal disc. The dense fibrous posterior capsule of the joint forms the posterior boundary of the retrodiscal tissues and has been described in T1 and T2 weighted sagittal images as a low signal band running from the condyle to the squamotympanic fissure (Crowley et al 1996).

Muscles

Clinical and cadaver studies have shown that in cental and medial T1 and T2 weighted sagittal and coronal images the superior and inferior bellies of the lateral pterygoid muscle have a mildly hypointense signal of uniform intensity (Harms and Wilk 1987; Schellhas et al 1987; 1988; Schellhas 1989). Tendons were well delineated by their very low intrinsic signal, which contrasted sharply with adjacent muscle and fat. The medial reflection of the temporalis muscle can be visualised as a vertical muscular structure just anterior to the lateral pterygoid muscles (Katzberg et al 1986).

PATHOLOGICAL JOINTS

Anterior disc displacement

MR imaging is extremely useful in imaging internal derangement's. Research comparing MR images with clinical findings report that it has been used to diagnose disc displacements with great accuracy (Roberts et al 1985; Katzberg et al 1985; Harms et al 1985; Cirbus et al 1987). Because of the ability of MR imaging to image hydrogen protons, it has been reported that information about the state of disc hydration may be ascertained which can aid in classifying the degree of disc abnormality (Helms et al 1989). Katzberg et al (1988) in a clinical study reported on the need to obtain complementary sagittal and coronal images to provide a three dimensional view of the joint and to assist in the identification of pure lateral and medial displacements which were previously difficult to identify. Anterior, anterolateral and anteromedial disc displacements have frequently been

reported to be associated with findings of degenerative joint disease in clinical studies (Katzberg et al 1988; Westesson 1985)

The accuracy of MR in depicting disc position and reducibility in joints with an anterior disc displacement when correlated with cadaver findings has been reported to range from 88% to 100% (Watt-Smith et al 1993; Tasaki and Westesson 1993; Rao et al 1990). Katzberg et al (1988) in a combined cadaver and clinical study reported that rotational anteromedial and medial disc displacements are more common than anterolateral or lateral disc displacements. Joints with anteriorly displaced discs have been reported to be diagnosed on both T1 and T2 weighted sagittal images by a low signal anterior to the head of the condyle which represents the distorted and displaced disc and distension of the joint capsule (Harms 1985). It has also been reported (Drace 1990) that identification of the anteriorly positioned junction of the posterior band of the disc and the retrodiscal tissues allowed identification of an anteriorly displaced disc. Katzberg (1988) reported on the importance of coronal MR images in the identification of disc displacements when either the disc is not evident on the sagittal plane of imaging or if the fossa is empty. The author reported that precise location of the displaced disc required a series of sequential sections from lateral to medial and at least one central coronal section. Curtin (1988) also emphasised the importance of coronal images in the detection of medial or lateral disc displacements.

Controversy exists as to whether it is possible to diagnose an anteriorly displaced disc from a MR image. As previously stated Katzberg (1988) has suggested that if the disc is not clearly demonstrated on the sagittal plane of imaging or if the fossa is empty, then a coronal image is needed. Recent research (Crowley et al 1996) indicates that it is possible

to identify an anteriorly displaced disc by accurate imaging of the junction between the disc and retrodiscal tissues although in joints with a anterior disc displacement the anterior retrodiscal tissues assume a "pseudo-disc" like appearance.

Errors were reported in interpreting sagittal images that failed to image medial and lateral disc displacements, however these abnormalities were depicted in coronal images (Westesson 1987). Difficulties frequently occur in distinguishing the capsule and disc in coronal and sagittal MR images of joints with thinned and displaced discs (Tasaki 1993; Crowley et al 1996).

Perforations

In clinical studies comparing MR images with surgical findings, disc perforations have been reported to be visualised as a separation in the disc fragments and frequently the high signal in T2 weighted images of fluid between the fragments has been identified (Harms 1985; Wilk 1986). It has been reported that the earliest evidence of a perforation is the loss of demarcation between the disc and the retrodiscal tissues (Curtin 1988). Watt-Smith et al (1993) in a study comparing arthrotomagraphic and MR images with surgical findings in 50 TMJ's showed a 78% sensitivity and 98% specificity for the detection of perforation, in contrast to other authors who have reported in a comparison of MRI with surgical findings that MRI fails to image disc perforations (Donlon 1987; Katzberg 1986; Helms 1986; Moses et al 1989). It has been suggested (Harms 1985; Watt-Smith et al 1993) that the possibility of missing small perforations will be reduced as MR technology improves and it becomes possible to obtain narrower and contiguous sections.

Mobility/Adhesions

Watt-Smith et al (1993) in a study comparing arthrotomographic and magnetic resonance images of 50 TMJ with surgical findings have reported that it is not possible to directly demonstrate adhesions by MRI. In a cadaver study by Crowley et al (1996) the authors reported that it was not possible to detect adhesions by T1 weighted images. However to date there has been little research investigating the sensitivity and specificity in detecting adhesions by MRI.

Articular surface changes

Articular surface changes which have been reported to be imaged by MRI include condylar flattening, osteophyte "beaking" on the anterior aspect of the condyle, cortical thickening and erosions (Harms 1987; Katzberg 1989). However, an *in vivo* study comparing MR images with surgical correlations demonstrated a poor detection rate of 13% (Watt-Smith et al 1993). It was reported that the susceptibility artefact, and poorer spatial resolution of the fast gradient echo pseudodynamic method make it less sensitive at detecting bony changes compared to the static spin echo method. Previous clinical studies have indicated that the most frequent misinterpretation of MR images occured in joints with a combination of anterior and medial or lateral disc displacement and articular surface changes (Westesson 1987). Clinical studies have suggested that an improved accuracy can be achieved if coronal images are combined with sagittal images to provide a accurate three dimensional image of joint articular surfaces (Schellhas 1988; Katzberg 1988; Katzberg 1989).

Schwaighofer (1990) when comparing coronal and sagittal MR images with cryosectional anatomy reported that coronal images clearly depicted erosions and flattening of the head of condyle while sagittal images showed osteophytes better. In a study by Westesson et al (1987), when sagittal MR images alone were compared with cadaver sections, the accuracy in detecting bone abnormalities was recorded to be as low as 60%. However, in a recent study comparing human cadaver TMJ cryosections with sagittal and coronal MR images, Tasaki and Westesson (1993) reported a 93% accuracy in the assessment of osseous changes. The authors reported that errors occured in joints where the MRI's were interpreted as demonstrating remodelling when the anatomical sections showed degenerative changes.

Certain MR signal characteristics seen in the head of the condyle have been described as representing the pathological condition of avascular necrosis (AVN) and osteochondritis dessicans (OCD) (Schellhas 1989). However, it is necessary to assess whether this signal represents the pathology described or whether it is representative of normal features such as subcortical cyst like spaces or condensed cortical bone.

CHAPTER THREE

MATERIALS AND METHODS

MATERIALS AND METHODS

3.1. SOURCES OF CADAVER MATERIAL

3.2. MAGNETIC RESONANCE IMAGES

3.3. DISSECTION OF CADAVER MATERIAL

3.4. PREPARATION OF TMJ SLICES FOR HISTOLOGY

3.5. PHOTOGRAPHY

3.6. METHODS OF ANALYSIS

3.6.a. COMPARISON OF T1 WEIGHTED MAGNETIC RESONANCE IMAGES WITH ANATOMICAL SECTIONS

3.6.b. COMPARISON OF T1 WEIGHTED SPIN ECHO, T1 WEIGHTED GRADIENT ECHO, T2 SPIN ECHO AND T2 TURBO SPIN ECHO WITH CORRESPONDING ANATOMIC AND HISTOLOGIC SLICES

MATERIALS AND METHODS

GENERAL INTRODUCTION

This study was based on analysis of human material which was subjected to the following:

1. The TMJ's of whole human heads were imaged in both the sagittal and coronal planes using magnetic resonance imaging (MRI).

2. The TMJ's were then dissected from the cadaver heads, decalcified and sliced in either the sagittal or the coronal plane to produce blocks of tissue that matched the MR images.

3. The TMJ blocks were then processed in paraffin for the purpose of histologic evaluation.

The details of these processes are described in subsequent sections.

3.1.   SOURCES OF CADAVER MATERIAL

The human TMJ's used in this study were derived from sources in Adelaide, Australia and Vienna, Austria. Five whole human cadaver heads were obtained from the Anatomy Department of the University of Adelaide and nine whole human cadaver heads were obtained from the Anatomy Department of the University of Vienna. The Adelaide and Vienna heads had been embalmed in situ with a mixture of formaldehyde (6-8%), phenol (8 %), white spirit (20%) and glycerine (15%).

No information relating to the age and sex distribution of the specimens was available. In addition, it was not possible to determine the cause of death or to obtain an antemortem history relating to signs and symptoms of TMJ dysfunction.

3.2. MAGNETIC RESONANCE IMAGES

MR imaging procedures were undertaken at sites in Adelaide, Australia and Vienna, Austria as follows:

3.2.1. Adelaide, Australia, MRI's

Adelaide specimens were imaged at either Wakefield Street Hospital or Flinders Medical Centre.

3.2.1.a. Wakefield Street Hospital Specimens

Two whole heads and their TMJ's were studied in the sagittal plane with a 0.5 Tesla magnetic resonance imaging system (Philips Gyroscan T5) with the body coil as the transmitter and bilateral TMJ surface coils as the receiver's. Bilateral TMJ images could therefore be obtained with the cadaver heads centred midsagittally and each surface coil positionally angled and secured over the subjacent TMJ.

A short T1 weighted, 200 msec repetition time, 20msec echo time, 7mm slice thickness, 1.5mm gap, 25cm field of view axial sequence was performed to localise the joints and to establish the parasagittal plane of orientation at right angles to the long axis of the condyle for each joint.

Sequential sagittal images were then obtained through the entire width of the joint from the lateral to medial pole using the following imaging parameters:

3mm slice thickness,

0mm interslice gap,

17cm field of view,

425msec repetition time,

30msec echo time,

spin echo,

multislice,

cephalometrically corrected parasagittal images.

3.2.1.b. Flinders Hospital Specimens

Three whole heads and their TMJ's were studied in the sagittal and coronal planes using a 1.5 Tesla magnetic resonance imaging system (Siemens) with the body coil as the transmitter and bilateral TMJ surface coils as the receiver's. For bilateral TMJ examinations, the heads were positioned supine in the bilateral TMJ coil/head holder and centred midsagittally. Different parameters and pulse sequences were used in the same plane of orientation and at the same slice depth and thickness in both planes.

Scan 1: T1 Weighted Spin Echo (T1SE)

Sagittal and Coronal Planes for Right and Left Joints

TR: 450msec

TE: 15msec

Number of phases encoded: 256

NEX: 3

Field of view: 16cm

Slice thickness: 3mm

Interslice gap: 0.1mm

Scan Time: 8.35mins

Scan 2: T1 Weighted Gradient Echo (T1GE)

Sagittal and Coronal Planes for Right and Left Joints

TR: 450msec

TE: 15mesc

Numbers of phases encoded: 256

NEX: 1

Field of view: 16cm

Slice thickness: 3mm

Interslice gap: 0.1mm

Scan Time: 4.21mins

Scan 3: T2 Weighted Spin Echo (T2SE)

Sagittal and Coronal Planes for Right and Left Joints

TR: 2000msec

TE: 90msec

Number of phases encoded: 160

NEX: 1

Field of view: 16cm

Slice thickness: 3mm

Interslice gap: 0.1mm

Scan Time: 8.35mins

Scan 4: T2 Weighted Turbo Spin Echo (T2TSE)

Sagittal and Coronal Planes for Right and Left Joints

TR: 3000msec

TE: 90msec

Number of phases encoded: 160

NEX: 2

Field of view: 16cm

Slice thickness: 3mm

Interslice gap: 0.1mm

Scan Time: 5.07mins

3.2.2. Vienna, Austria, MRI's

Ten whole heads and their TMJ's were studied in the parasagittal and coronal planes using a 0.5 Tesla magnetic resonance imaging system (Philips Gyroscan S5) with the body coil as the transmitter and a single 10cm round surface coil as the receiver. With this configuration, a relatively uniform object excitation was achieved with the large body coils, while the smaller, sensitive volume of the surface coil allowed the signal to noise ratio to be increased in the vicinity of the coil. With the surface coil a 23 cm field of view could be used without incurring image degradation from aliasing artefacts. For bilateral TMJ examinations, the human cadaver heads were centred midsagittally in the head holder. Each surface coil was then positionally angled and secured over the subjacent TMJ.

3.2.2.a. Sagittal MRI's

A short T1 weighted, 400 msec repetition time, 30msec echo time, 5mm slice thickness, 1.5mm interslice gap, 23cm field of view, spin echo, multislice images were obtained to establish the parasagittal plane at right angles to the long axis of the condyle.

Sequential sagittal T1 weighted MR images were then obtained through the entire width from the lateral to the medial pole of each condyle with the following imaging parameters:

3mm slice thickness,

0 interslice thickness,

23cm field of view,

400msec repetition time,

30msec echo time,

spin echo,

multislice images,

cephalometrically corrected parasagittal images.

3.2.2.b. Coronal MRI's

All 20 TMJ's were imaged in the coronal plane from the anterior part of the disc to the posterior part of the fossa. Sequential T1 weighted MR images were obtained parallel to the transverse condylar axis with the following imaging parameters:

3mm slice thickness,

0 interslice thickness

23 cm field of view,

400msec repetition time,

30msec echo time,

spin echo,

multislice images.

3.3. DISSECTION OF CADAVER MATERIAL

The dissection techniques used to obtain the TMJ blocks from both the Adelaide cadaver heads and the Vienna cadaver heads were identical.

After sagittal and coronal MR scans were obtained, the cranium and contents were removed using a fine tooth metal blade bandsaw on a radius 15mm above each external acoustic meatus and parallel to the Frankfurt horizontal. A block of tissue bound anteriorly by the posterior wall of the maxilla, superiorly by the middle cranial fossa, posteriorly by the external acoustic meatus, inferiorly by the ramus of the mandible and medially by the medial pterygoid plate was obtained by sectioning with the fine tooth metal blade bandsaw.

After dissection the blocks containing the joints were washed in constantly running water for 1-4 days to remove the oils from the preserving fluid which was necessary prior to fixation, decalcification and infiltration of wax. The end point for washing was determined by olfactory means and also by feel as the preserving fluid had both a distinctive smell (phenol) and feel (glycerine and white spirit). On removal of the embalming fluid, postfixation of specimens was effected by immersing in 10% neutral buffered formalin for 2-4 days depending on the size of the block.

The post-fixed blocks were then decalcified by immersion in decalcification solution which contains decalcifying agent and a chelating agent (Appendix 1). The end point for decalcification was determined radiographically when there was evidence of complete decalcification. The blocks were radiographed at daily intervals until decalcification was

complete. Following decalcification the blocks were washed for a minimum of 24 hours up to 72 hours in running tap water.

These TMJ blocks were then trimmed to a 6cm square block and placed in a locally designed and manufactured perspex joint holder (Crowley et al 1996). This acrylic joint holder prevented movement of the TMJ block and maintained the same angulation while sequential 3mm slices were cut through each TMJ block.

The TMJ blocks were placed in the holder and all right TMJ's were dissected in the parasagittal plane and all left TMJ's were dissected in the coronal plane at 3mm intervals. Exceptions to this rule were the 4 joints imaged at Wakefield Street Hospital which were all sectioned in the sagittal plane as no corresponding coronal MRI's were available.

After preparing slices from each TMJ block, the slices were then transferred to 10% neutral buffered formalin as a storage medium for variable periods up to several weeks or months. Alternatively if the specimens were to be photographed they were washed briefly in running water, followed by immersion in 70% alcohol to revive the colour and lessen formalin inhalation. Specimens were then left in 70% alcohol if they were going to be dehydrated and processed immediately or again placed in 10% neutral buffered formalin as a long term storage medium.

3.4.   PREPARATION OF TEMPOROMANDIBULAR JOINT SLICES FOR HISTOLOGY

All specimens were processed by hand under vacuum. Each slice of TMJ was dehydrated, infiltrated with wax and embedded in Surgipath^R embedding medium (Appendix 2).

Once the blocks were embedded in Surgipath^R embedding medium they were trimmed by removing the excess wax. Histological sections 9 microns in thickness were obtained on a microtome. They were subsequently floated onto chromic acid cleansed gelatinised glass slides (Appendix 3). One or two sections from each block were stained with Haematoxylin and Eosin (H&E) (Appendix 4) and one or two sections close to the sections chosen for H&E staining were stained with a Trichrome (Appendix 5) staining method.

3.5. PHOTOGRAPHY

3.5.1. Macrophotography of Magnetic Resonance Images

The MR images were photographed using a Nikon FA camera with a 55mm macro lens. Kodak RPC black and white positive film was used and standard processing procedures were employed (Appendix 6) before the images were printed through a Leitz 35mm enlarger onto Ilford Multigrade 3 paper (Appendix 7).

3.5.2. Macrophotography of Dissected Cadaver Material

Colour Prints

The anatomical TMJ dissections were photographed using a Nikon FA camera with a 55mm macro Nikon lens. Fuji colour HGII negative film, 100ASA was used. The film was processed at a minilab using the C41 processing technique.

Colour Slides

Colour slides were obtained using a Nikon FA camera with a 105mm micro Nikon lens. Ektachrome Kodak 160ASA Tungsten film was used. The film was processed at the Institute of Medical and Veterinary Science (IMVS) through a mini lab using the E6 processing technique.

3.5.3. Microphotography

The histologic sections were photographed using an Olympus BH Microscope Camera with a daylight filter and photographic attachments which included the Olympus Light Camera body to match the Microscope Camera, autoresponsive box. and a Kelvin colour temperature meter. Ektachrome slide film at 100ASA film speed was used. The film was processed at the Institute of Medical and Veterinary Science Photography Department using the E6 processing technique.

3.6. METHODS OF ANALYSIS

3.6.1. COMPARISON OF T1 WEIGHTED MAGNETIC RESONANCE IMAGES WITH ANATOMIC SLICES
(Vienna and Wakefield Street Hospital MRI's)

This phase of the study was designed to compare photographs of the mid-coronal and mid-sagittal anatomical slices of the TMJ with corresponding sagittal and coronal MR images. In the sagittal plane, line drawings of these prints were used to correlate the position of the discal-retrodiscal junction between the corresponding anatomic and MR sections. In the coronal plane, line drawings of these prints were used to correlate between the head of condyle between the corresponding anatomic and MR sections.

Sagittal and coronal anatomic slices were evaluated for the following:

1. Disc position and shape

2. Disc perforation

3. Articular surface changes

Each coronal and sagittal anatomical joint slice was then assessed as exhibiting:

1. Normal joint anatomy

2. Disc displacement

3. Perforation

4. Articular surface changes

Normal joint anatomy

A classification of normal joint anatomy required fulfilment of the following criteria:

1. The articular tissues of the temporal and condylar components were smooth.

2. The posterior band of the disc was situated above or slightly anterior to the head of the condyle.

3. The disc was biconcave in sections (perpendicular to its long axis) cut through the central and mediocentral regions and biconcave or rectilinear in profile in the laterocentral region.

4. There was no fissuring, fraying or perforation.

Disc displacement

Disc displacements were classified into the subgroups of antero-medial, lateral or medial disc displacements. The central feature of an anteromedial disc displacement was the location of the posterior band of the disc anterior or anteromedial to the condyle. A medial disc displacement was diagnosed when the bulk of the disc was herniated over the medial pole of the condyle with no anterior component. The lateral discal ligament was elongated and a thinned posterior band of disc remained at the 12 or 1 o'clock position in central sections. A lateral disc displacement occured when the bulk of the disc was positioned over the lateral pole of the condyle and the medial discal ligament was elongated.

Disc Perforation

This subgroup included any anatomical slices that demonstrated a perforation in the disc in sagitally or coronally sectioned joints.

Articular surface changes

This group incorporated those joints affected by remodelling and the pathologic osteoarthrotic/osteoarthritic processes. A classification of articular surface changes subsequent to osteoarthrosis incorporated the range of conditions affecting the articular fibrocartilage. This subgroup included normal variations in the joint, initial degenerative changes, advanced degenerative changes and finally to destroyed cartilage. The macroscopic appearances of these changes included lipping caused by osteophyte formation, sclerosis, concavities, surface flattening and erosions, subchondral cyst formation and deformation of the disc.

The results of analysis of the anatomic slices were then tabulated on a proforma (Appendix 8).

Observations of the sagittal and coronal MR images were subsequently correlated with the findings derived from examination of sagittal and coronal anatomical slices (Appendix 9). With the anatomical findings used as the morphologic standard, it was then possible to assess and tabulate the diagnostic accuracy in assessing the disc position, disc perforations and articular surface changes in sagittally dissected joints by sagittal and complementary coronal MR images. Likewise the diagnostic accuracy in assessing the disc position, disc

perforations and articular surface changes in coronally dissected joints by coronal and complementary sagittal MR images was also assessed (Appendix 10).

3.6.2. COMPARISON OF T1 WEIGHTED SPIN ECHO, T1 WEIGHTED GRADIENT ECHO, T2 SPIN ECHO AND T2 TURBO SPIN ECHO WITH CORRESPONDING ANATOMIC AND HISTOLOGIC SLICES

(Flinders Hospital MRI's)

The anatomic slices of the six joints were assessed using the criteria described in the previous section (3.6.1.) and each joint was categorised as exhibiting normal anatomy, disc displacement, disc perforation or articular surface changes.

The corresponding histologic sections were then viewed under the microscope for evidence of pathology in the discal-retrodiscal complex and articular surfaces. Joint regions evaluated separately were the anterior and posterior slopes of the condyle; the articular eminence and mandibular fossa of the temporal component; the disc; and the posteroinferior, posterosuperior, anteroinferior and anterosuperior disc attachments. In all these regions, histologic signs suggesting disintegration of articular tissues; deviations in form; and ongoing progressive, regressive and circumferential remodelling were recorded. Each joint was graded with respect to prominence and extension along the surfaces (Appendix 11).

Each coronal and sagittally sectioned joint was characterised as exhibiting:

1. Normal joint anatomy

2. Disc displacement

3. Disc perforation

4. Articular surface changes

-Articular tissue disintegration (osteoarthritis/osteoarthrosis)

-Progressive/regressive/circumferential remodelling

-Deviation in form

1. Normal joint anatomy

A joint was classified as normal if it exhibited the following criteria:

1. The disc consisted of condensed, avascular collagen fibres. The fibres centrally take a predominantly anteroposterior course and interlace with the transversely orientated fibre of the anterior and posterior bands.

2. The retrodiscal tissues consist of highly vascular, loosely organised fibro-elastic connective tissue.

3. The articular surfaces consisted of an outer fibrous tissue layer, a fibrocartilage zone, a cortical bony end plate and cancellous bone zone.

2. Disc displacement

Each joint was assessed as to whether it demonstrated histologic features of disc displacement. The histologic features investigated included rearrangement of collagen fibres and decrease in cellularity of the disc. The retrodiscal tissues were examined to see if there was any signs of fibrosis, reduction in vascularity, hyperplastic tissue formation, hyaline degeneration, splitting and perforation.

3. Disc perforation

The discal tissues were examined to determine whether there was any histological features indicating perforation.

4. Articular surface changes

Each joint was examined histologically to determine whether it demonstrated features of either remodelling or articular tissue degeneration based on classifications proposed by Hansson and Oberg 1977 and DeBont 1994. Remodelling was subclassified into the subgroups of progressive, regressive or circumferential remodelling.

Remodelling

Progressive remodelling was scored positive if chondrocyte clusters were evident in the articular zone. Bone may have been added to the subchondral plate through apposition as well as through vascular invasion of the cartilage and endochondral ossification.

Regressive remodelling was scored positive if there was evidence of loss of chondrocytes in the cartilage layer due to cell degeneration and necrosis, resorption of the subchondral bone and conversion of the fibrous connective tissue into cartilage.

Circumferential remodelling was considered as a peripheral, progressive remodelling consisting of cartilagenisation and subsequent ossification of capsule or ligament insertions which eventually lead to osteophytic lipping of the joint margins.

Articular tissue disintegration- (osteoarthrosis/osteoarthritis)

Histologic characteristics of disintegration of the articular zone included:

- fibrillation of the articular connective tissue layer,

- decrease in number of mesenchymal cells in the articular layer,

- irregular border between the subchondral bone and cartilage.

MRI Comparison

Following classification of the sagittal and coronally sectioned joints based on their anatomical and histologic features, each joint was compared to its corresponding MRI's. The four different MRI sequences (T1SE, T1GE, T2SE, T2TSE) were then assessed to determine which sequence provided the most accurate representation of the anatomical slices and histologic sections in the coronal and sagittal planes.

In addition, for sagittally sectioned joints, the contribution of the coronal MR images in providing a three dimensional image of the joint was assessed. Likewise the contribution of sagittal images in coronally sectioned joints was also assessed.

CHAPTER FOUR

RESULTS

CHAPTER FOUR

RESULTS

4.1. SELECTION OF ANATOMIC AND HISTOLOGIC MATERIAL FOR ANALYSIS

4.2. ILLUSTRATION OF ACCURACY OF MIDSAGITTAL AND CENTRAL CORONAL MAGNETIC RESONANCE IMAGES WHEN COMPARED TO ANATOMIC AND HISTOLOGIC SECTIONS

4.3. COMPARATIVE ANALYSIS OF TMJ'S BASED ON MACROSCOPIC ASSESSMENT OF JOINT DISSECTIONS AND DIAGNOSIS BY MAGNETIC RESONANCE IMAGING

4.4. COMPARISON OF T1SE, T1GE, T2SE AND T2TSE MAGNETIC RESONANCE IMAGES WITH CORRESPONDING SLICES AND HISTOLOGIC SECTIONS

RESULTS

INTRODUCTION

The results of the study are described in four separate sections as follows:

1. Selection of anatomic and histologic material for analysis.

In this section the rationale for choosing midsagittal and central coronal anatomic slices and histologic sections is described.

2. Illustration of accuracy of midsagittal and central coronal MR images when compared to anatomic and histologic sections.

The purpose of this section is to demonstrate the visual concordance of chosen MRI slices and the corresponding anatomic slices and histologic sections.

3. Comparative analysis of TMJ's based on macroscopic assessment of joint dissections and diagnosis by MRI.

In this section the results of analysis of all joints based on assessment of anatomic specimens and corresponding MR images is presented.

4. Comparison of T1SE, T1GE, T2SE and T2TSE MR images with corresponding anatomic slices and histologic sections.

(Flinders Hospital MRI's)

In this section the results of a comparison of four imaging sequences relative to corresponding anatomic slices and histologic sections were presented.

4.1. SELECTION OF ANATOMIC AND HISTOLOGIC MATERIAL FOR ANALYSIS

In this section the rationale for choosing midsagittal and central coronal anatomic slices and histologic sections is described.

4.1. Sagittal material

As was described in the material and methods section, specimens were anatomically sliced and histological sectioned in both sagittal and coronal planes. MR images of the samples from the three Centres were performed in both sagittal and coronal planes using a variety of imaging sequences which generated a large number of MR images.

Preliminary analysis of the anatomical and histological sections from the lateral, midsagittal and medial aspect of the joint showed the midsagittal slice best illustrated the anatomic and histologic features representative of coronally and sagittally sectioned joints demonstrating normal and pathologic joint anatomy. This is illustrated in the following examples of joints showing normal and pathologic features sectioned in both the sagittal and coronal planes (Figs 1-2).

Therefore in this study although medial and lateral anatomical slices and MR images were examined and reviewed, the midsagittal and central coronal anatomic slice was chosen as the standard source for histological analysis and comparison with corresponding MR images. However, as described in Section four for two pathological joints lateral and medial anatomic and histologic sections were also reviewed.

4.1.1. Sagittally sectioned joint showing normal anatomy

Joint 2R3 (Wakefield Memorial Hospital)

This joint demonstrates the features (from lateral to medial) necessary for the joint to be classified as normal (Figs 1a, 1d and 1g). The articular surfaces of the condyle and fossa were smooth, the "bow-tie" shaped disc was positioned at the one o'clock position and no fissuring, fraying or perforation of the disc was evident. The medial anatomic slice was assessed as accurately representing the normal joint features and little additional diagnostic information was obtained from the additional slices.

Examination of histologic sections of the same joint from lateral to medial showed that the medial section was representative of the joint's histologic features (Figs 1b, 1d and 1f). In all slices the disc consisted of densely collagenous fibrous connective tissue and the junction with the vascular, fibro-elastic retrodiscal tissues at the one o'clock position could be seen. In all slices the fibrous connective tissue outer layer and cartilage zone were thickened on the head of condyle, articular eminence and anterior fossa.

Fig. 1a.

A lateral sagittal anatomic section through a right TMJ (Joint 2R-Wakefield Memorial Hospital). This joint demonstrates normal anatomy with the junction of the highly vascular retrodiscal tissues with the posterior band of the disc at the twelve o'clock position (white arrow). The disc (D) has a bow tie like appearance. The articular surfaces of the condyle (C) and fossa (F) are smooth.

Fig. 1b.

Photomicrograph of a lateral sagittal histologic section of the same right TMJ (Joint 2R-Wakefield Memorial Hospital) as seen in Figure 1a. The junction of the densely collagenous, thickened disc with the highly vascular retrodiscal tissues can be seen (white arrow). The articular covering of the condyle and eminence appear normal. (Trichrome stain, Mag X 7.5).

Fig. 1c.

A midsagittal anatomic section through the same right TMJ as Figure 1a (Joint 2R-Wakefield Memorial Hospital). This slice shows the same anatomic features as Figure 1a with the posterior band of the disc at the one o'clock position (white arrow). The disc (D) has a bow tie like appearance and the retrodiscal tissues appear less vascular. The articular surfaces of the condyle (C) and fossa (F) are smooth.

Fig. 1d.

Photomicrograph of a midsagittal histologic section of the same right TMJ (Joint 2R-Wakefield Memorial Hospital) as seen in Figure 1b. The junction of the densely collagenous disc with the vascular retrodiscal tissues can be seen (white arrow). The articular covering of the condyle and eminence is thickened. (Trichrome stain, Mag X 8).

Fig. 1e.

A medial sagittal anatomic section through a right TMJ (Joint 2R-Wakefield Memorial Hospital). This joint demonstrates the same anatomic features of normal joint anatomy as the previous slices. The disc (D) has a bow tie like appearance and the retrodiscal tissues appear less vascular. The condyle is reduced in thickness anteroposteriorly.

Fig. 1f.

Photomicrograph of a medial sagittal histologic section of the same right TMJ (Joint 2R-Wakefield Memorial Hospital) as seen in Figure 1c. The disc is reduced in thickness and the junction with the less vascular retrodiscal tissues can be seen. The articular covering of the condyle and eminence is thickened. (Trichrome stain, Mag X 8.5).
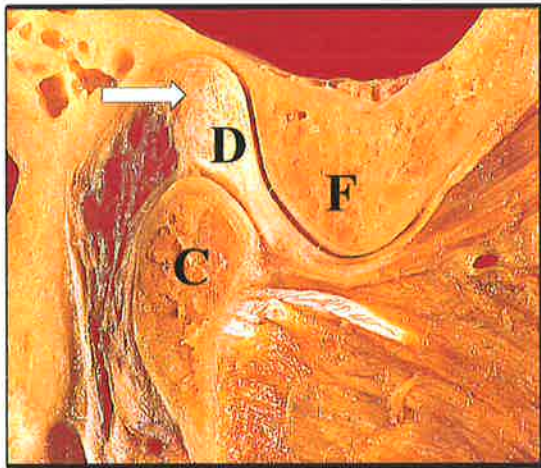
Fig. 1a.

Fig. 1b.
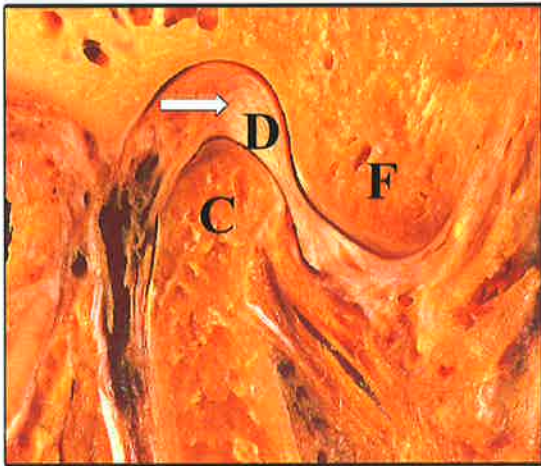
Fig. 1c.
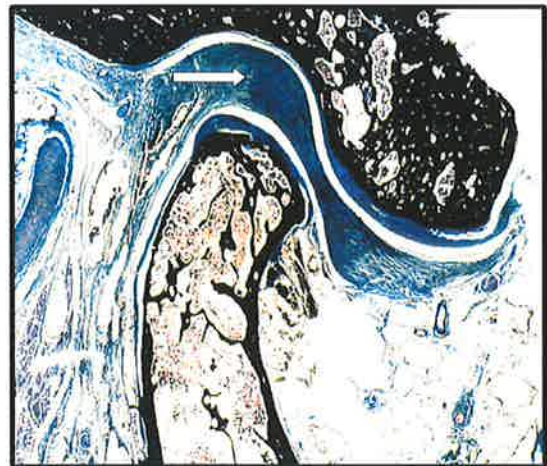
Fig. 1d.
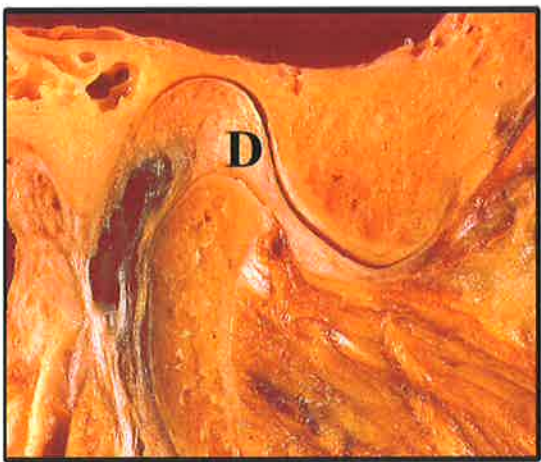
Fig. 1e.
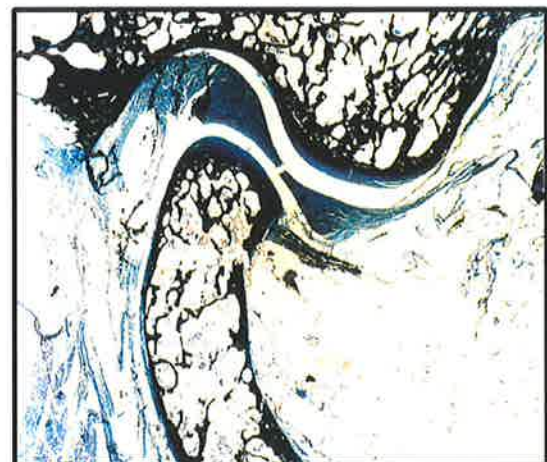
Fig. 1f.

4.1.2. Sagittally sectioned joint demonstrating disc displacement, perforation and articular surface changes

Joint 1L (Wakefield Memorial Hospital)

Anatomic slices from the lateral to medial pole of this joint showed a diverse range of pathology which was best represented by the medial anatomic slice (Figs 2a, 2d and 2g). Lateral anatomic slices showed the disc to be thinned, perforated and displaced anteriorly, however articular surface changes in the condyle could not be seen (Fig. 2a). Central midsagittal anatomic slices showed the retrodiscal tissues to be thinned over the head of condyle, the disc was perforated and displaced and articular surface changes were evident in the head of condyle (Fig. 2d). Medial anatomic slices showed the retrodiscal tissues to be elongated over the remodelled head of condyle and the disc was displaced anteriorly but not perforated (Fig. 2g).

Histologic sections of the same joint showed that remodelling and degenerative changes in the head of the condyle could be seen from the medial to lateral aspect of the joint (Figs 2b, 2b and 2h). The displaced disc and its junction with the "pseudodisc" like retrodiscal tissues could be seen in all sections, however the perforation was only evident in lateral sections.

Fig. 2a.

A lateral sagittal anatomic section through a right TMJ (Joint 1L-Wakefield Memorial Hospital). This slice shows thinning and elongation of the discal-retrodiscal tissues over the head of the condyle. Anteriorly a perforation is evident (white arrow).

Fig. 2b.

Photomicrograph of a lateral sagittal histologic section of the same right TMJ (Joint 1L-Wakefield Memorial Hospital) as seen in Figure 2a. The junction of the fibrous disc with the vascular retrodiscal tissues can be seen (arrow). The remnant of discal tissues can be seen anterior to the perforation. Remodelling in the head of the condyle can be seen (open arrow). (Trichrome stain, Mag X 8.5).

Fig. 2c.

A midsagittal anatomic section through a right TMJ (Joint 1L-Wakefield Memorial Hospital). The perforated disc can be seen anteriorly and the bulk of the disc is posterior. The junction with the vascular retrodiscal tissues can be seen (white arrow). The retrodiscal tissues can be seen elongated over the head of the remodelled condyle (C).

Fig. 2d.

Photomicrograph of a midsagittal histologic section of the same right TMJ (Joint 1L-Wakefield Memorial Hospital) as seen in Figure 2d. This section is just medial to the anatomic slice in Figure 2c and the perforation is now no longer evident. The junction of the fibrous disc with the pseudodisc like retrodiscal tissues can be seen (arrow). Remodelling of the head of the condyle (C) is evident with anterior beaking occurring. (Trichrome stain, Mag X 8.5).

Fig. 2e.

A medial anatomic section through a right TMJ (Joint 1L-Wakefield Memorial Hospital). The bulk of the disc (D) can be seen anteriorly displaced anteriorly with the posterior band thickened. The perforation is no longer evident in medial slices. The retrodiscal tissues can be seen elongated over the head of condyle (C). The condyle demonstrated extensive articular surface changes with remodelling of the surface contour (arrow).

Fig. 2f.

Photomicrograph of a medial histologic section of the same right TMJ (Joint 1L-Wakefield Memorial Hospital) as seen in Figure 2g. The fibrous disc (D) can be seen anteriorly over the head of condyle. The fibrous retrodiscal tissues can be seen over the thinned head of condyle (C). (Trichrome stain, Mag X 8.5).
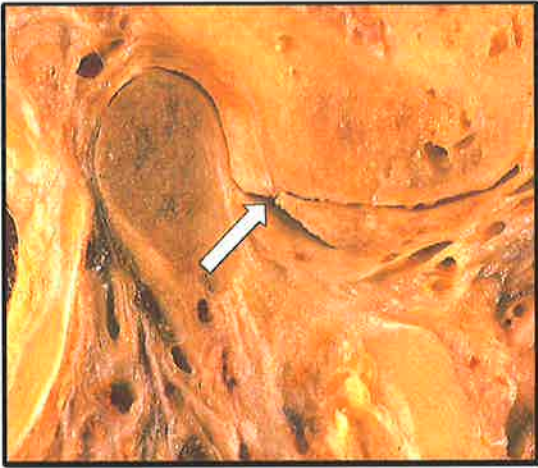
Fig. 2a.
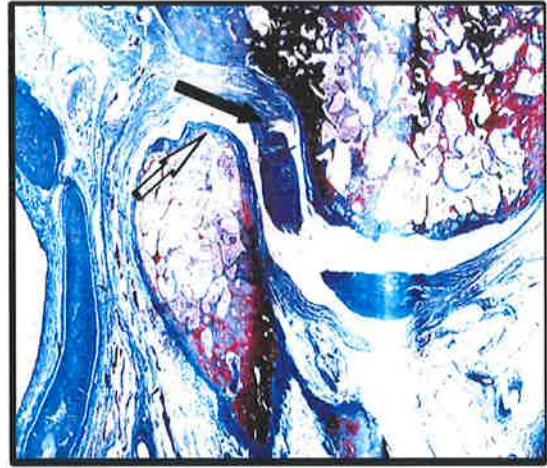
Fig. 2b.
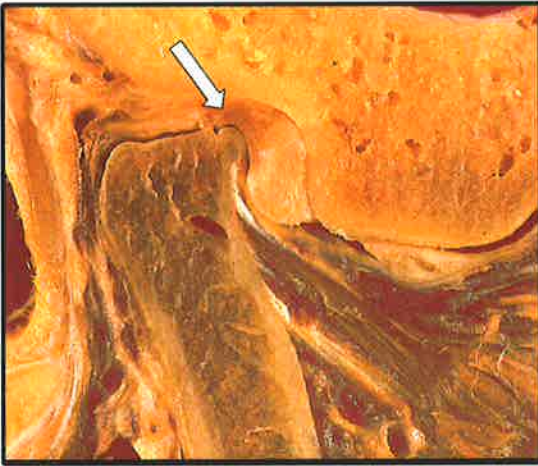
Fig. 2c.

Fig. 2d.
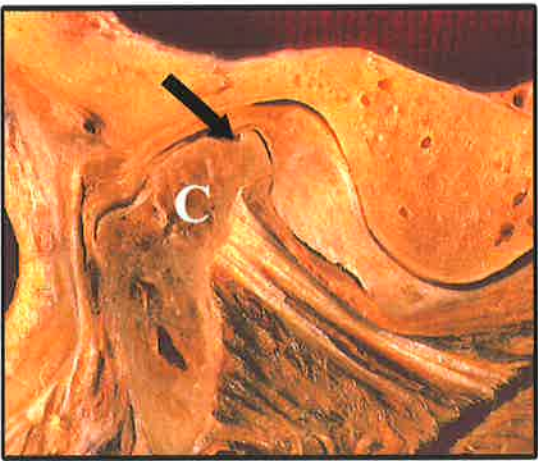
Fig. 2e.
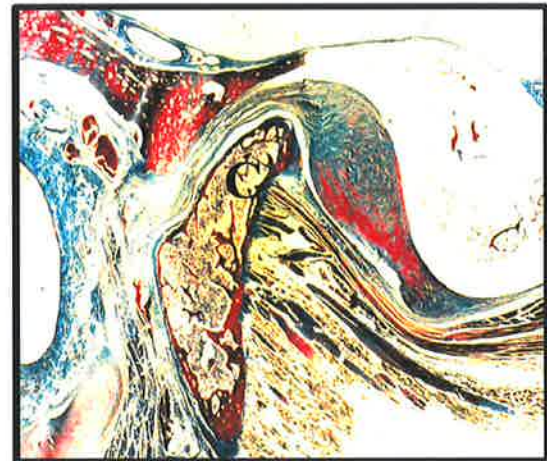
Fig. 2f.

4.2. Coronal material

Because of the architecture and anatomy of the TMJ the most diagnostically useful images were the central coronal images. Anterior coronal and posterior coronal slices provided only limited additional diagnostic information about the joint, however the central coronal anatomic slice, histologic section and MR image was found to be representative of both normal and pathologic joint anatomy.

Accordingly for the purpose of this study and in general, midcoronal MR images of the joint were used for comparison with gross anatomical and histological sections.

4.2.1. Coronally sectioned joint showing normal anatomy

Joint 12L (Vienna)

In a coronally sliced joint demonstrating normal anatomy the central slice best illustrated the normal joint features (Figs 3a and 3b). Anterior coronal slices showed the lateral pterygoid muscle inserting into the pterygoid fovea, the disc being of even thickness over the condyle and blending with the capsule medially and laterally. Anterior coronal slices did not clearly demonstrate whether articular surface changes were occurring. Posterior coronal slices showed the smooth articular surfaces of the condyle and fossa and the even thickness disc in position over the head of condyle.

Fig. 3a.

A anterior coronal anatomic slice through a left TMJ (Joint 12L-Vienna). This joint demonstrated normal anatomical features with disc (D) positioned over the head of condyle (C). The medial and lateral capsules can be seen inserting into the head of condyle. The lateral pterygoid muscle (LP) can be seen inserting into the head of condyle inferiorly.

Fig. 3b.

A posterior coronal anatomic slice through a left TMJ (Joint 12L-Vienna). The normal joint anatomy can be seen with the disc (D) of even thickness over the smooth head of condyle (C).
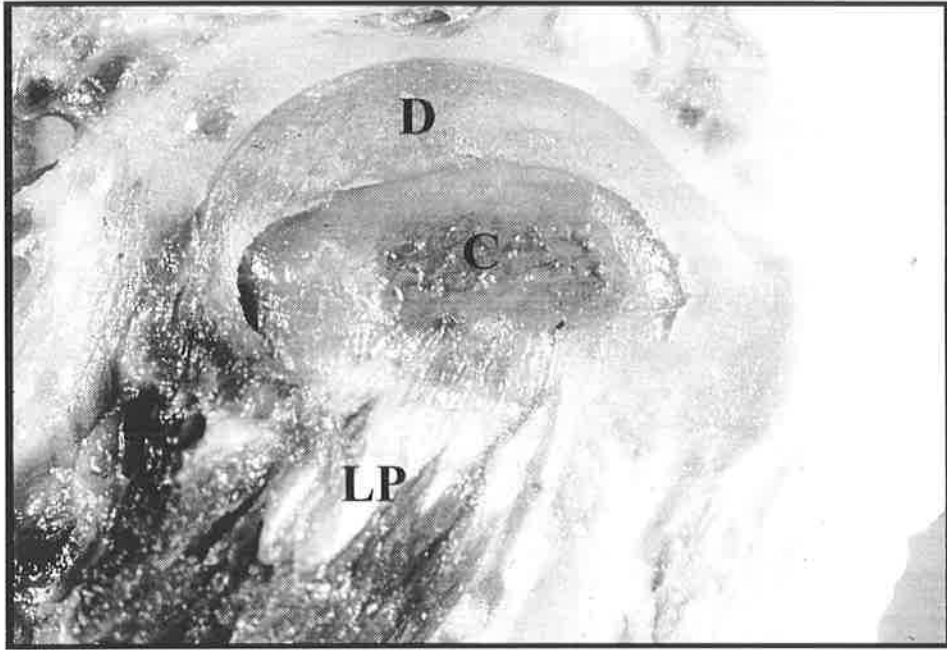
Fig. 3a.
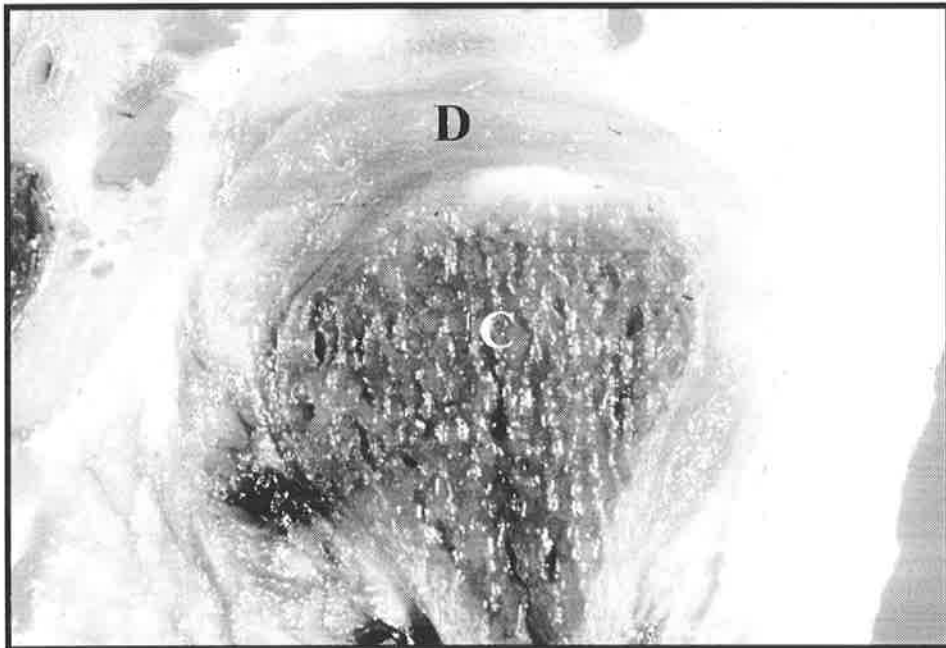
Fig. 3b.

4.2.2. Coronallly sectioned joint showing disc displacement, lateral perforation and articular surface changes

Joint 1L (Flinders Medical Centre)

The anterior coronal slice best showed the disc anteriorly displaced but failed to illustrate the articular surface changes occurring and the perforation laterally (Fig. 4a.). The central coronal slice shows the perforation with the bulk of the disc displaced anteromedially as well as providing a accurate image from lateral to medial of the articular surface changes (Fig. 4b.). The posterior coronal slice failed to show articular surface changes, the disc displacement or perforation (Fig. 4c)

Fig. 4a.

A anterior coronal anatomic slice through a left TMJ (Joint 1-Flinders Medical Centre). The neck of condyle (C) can be seen with the lateral pterygoid muscle medially (LP). The outline of the fossa (F) can be seen with the bulk of the disc (D) displaced anteriorly.

Fig. 4b.

A central coronal anatomic slice through a left TMJ (Joint 1-Flinders Medical Centre). The condyle (C) and fossa (F) can be seen articulating on each other laterally (arrow). The lateral pterygoid muscle (LP) can be seen inserting into the head of condyle inferiorly. Superiorly a area of discal or retrodiscal tissues can be seen (white arrow).

Fig. 4c.

A posterior coronal anatomic slice through a left TMJ (Joint 1-Flinders Medical Centre). The posterior head of condyle (C) can be seen surrounded by the highly vascular retrodiscal tissues.
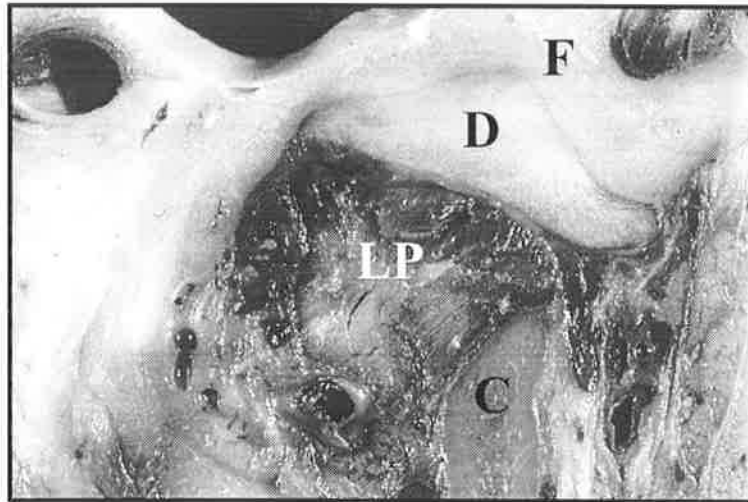
Fig. 4a.
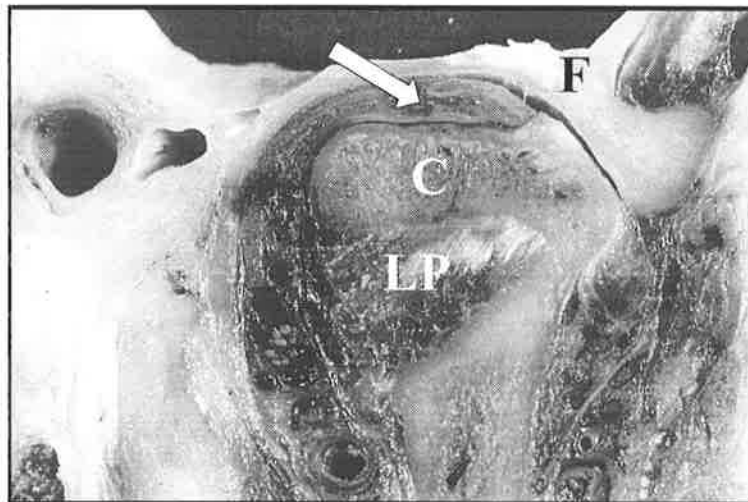
Fig. 4b.

Fig. 4c.

4.2. ILLUSTRATION OF THE ACCURACY OF MIDSAGITTAL AND CENTRAL CORONAL MAGNETIC RESONANCE IMAGES WHEN COMPARED TO ANATOMIC AND HISTOLOGIC SECTIONS

The purpose of this section is to demonstrate the visual concordance of chosen MRI slices and the corresponding anatomic slices and histologic sections.

Detailed analysis of all specimens relative to the diagnosis of normal joint or joint pathoses is presented in section 3 (Tables 1 and 2).

4.1. NORMAL JOINTS

4.1.1. Sagittally sectioned joint showing normal anatomy

Joint 2R3 (Wakefield Memorial Hospital)

This joint demonstrated the criteria required for the anatomic slices to be classified as normal (Fig. 5a). The articular surface of the temporal and condylar components were smooth. The junction of the biconcave disc with the retrodiscal tissues was situated at the one o'clock position. There was no evidence of disc fissuring, fraying or perforation. The lateral pterygoid muscle could be seen inserting into the pterygoid fovea.

Histologically the junction of the densely collagenous disc with the highly vascular, loosely organised fibro-elastic retrodiscal tissues could be seen at the one o'clock position (Fig. 5b). The articular joint surfaces appeared normal consisting of a fibrous connective tissue outer zone, a cartilage zone, a cortical bone zone and cancellous bone marrow. There was no evidence of any osteocartilagenous defects or lesions although the condyle demonstrated thinning of the cortical bony end plate on the antero-superior aspect. The fibrous articular covering was thickest over the superior surface of the condyle and the eminence and the posterior surface of the fossa.

In the sagittal T1 weighted MR image the cortical bone had a characteristic low signal which provided an accurate outline of the glenoid fossa, articular eminence and condyle (Fig. 5c). The low signal of the cortical bone was highlighted between the high signal image of the bone marrow and the intermediate signal of the intracapsular soft tissues. Disc position and shape was well imaged as a classical "bow tie" because the densely collagenous fibrous connective tissue of the disc had an intermediate to low MR signal

which provided good contrast between osseous and soft tissue components of the TMJ. In sagittal sections, the vascular retrodiscal tissues presented as an area of high signal bounded by the low signal of the condyle and fossa. Anteriorly the contrast between the high signal retrodiscal tissues and the intermediate to low signal of the posterior band of the disc assisted in identifying the discal/retrodiscal junction. The lateral pterygoid muscle imaged as parallel bands of low signal and could be seen inserting into the pterygoid fovea which was identified by a discontinuity in the low signal cortical plates of the condyle. The higher signal bands of the central tendon and fatty tissue imaged between the low signal of the two heads of lateral pterygoid muscle.

Fig. 5a.

A sagittal anatomic section through a right TMJ (Joint 2R-Wakefield Memorial Hospital). This joint demonstrates normal anatomy with the posterior band of the disc at the one o'clock position (arrow). The disc (D) has a bow tie like appearance and the articular surfaces of the condyle (C) and fossa (F) are smooth.

Fig. 5b.

Photomicrograph of a sagittal histologic section of the same right TMJ (Joint 2R-Wakefield Memorial Hospital) as seen in Figure 5a. The junction of the densely collagenous disc with the vascular retrodiscal tissues can be seen (arrow). The articular covering of the condyle and eminence is thickened.

(Trichrome stain, Mag X 7.5).

Fig. 5c.

A T1 weighted MR image of the same sagittal section of Joint 2R as seen in Figure 5a. The disc has a typical low signal bow tie like appearance and the junction with the high signal retrodiscal tissues at the one o'clock position can be seen (arrow). The thickened articular surface of the condyle and eminence images as an increased low signal (white arrow).
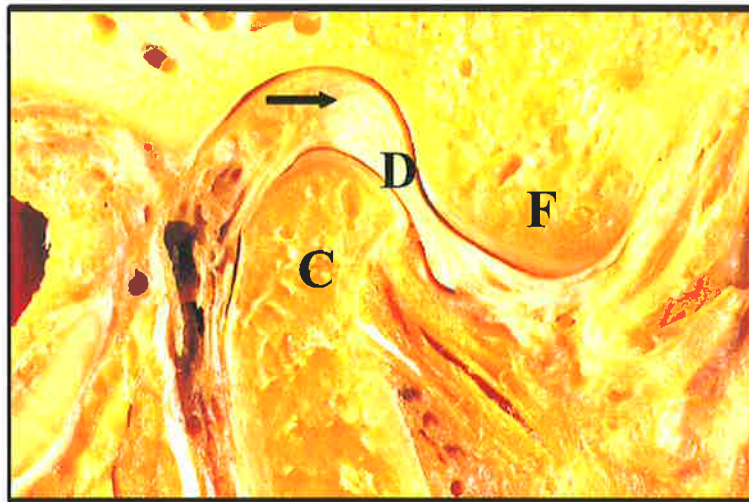
Fig. 5a.
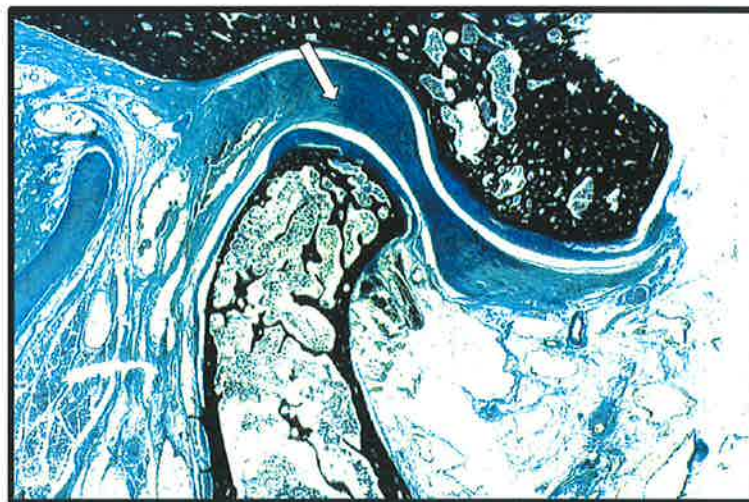
Fig. 5b.
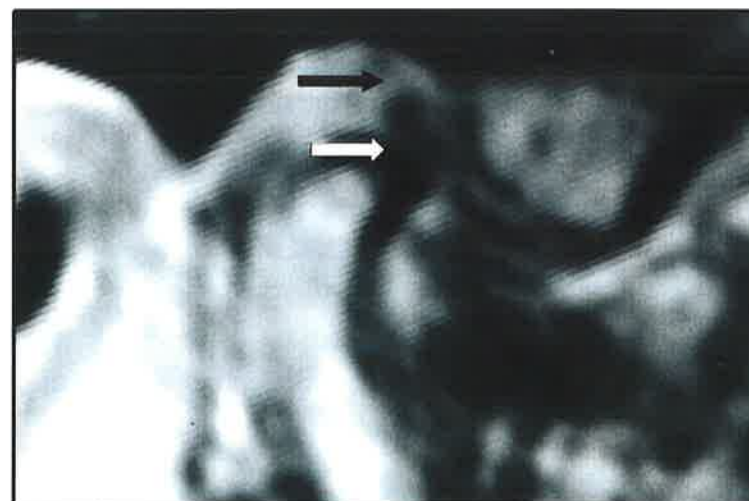
Fig. 5c.

4.1.2 Coronally sectioned joint showing normal anatomy

Joint 10L (Vienna MRI)

This joint demonstrated normal anatomy with a narrowing of the disc over the lateral pole (Fig. 6a). In coronal MR views the cortical bone of the condyle and fossa was well visualised with the dimensions of the disc accurately represented (Fig. 6b). The lateral capsule of the joint was clearly visible in the MR views highlighted against the bright signal image of the parotid gland and adipose tissue.

Sagittal MR views also illustrated normal TMJ structures with the "bow tie" of the disc well outlined between condyle and fossa (Fig. 6c). The junction between the posterior band of the disc and the retrodiscal tissues was at the one o'clock position and the foot of the disc was adjacent to the crest of the eminence.

Fig 6a.

A coronal anatomic section through the centre of the condyle of a left temporomandibular joint (Joint 10L-Vienna). This joint demonstrates normal anatomy but the disc is reduced in thickness over the lateral pole (white arrow). The lateral capsule (C) is seen running from the lateral pole of the condyle to the root of the zygoma.

Fig. 6b.

A T1 weighted MR image of the same coronal section of Joint 10L as seen in Figure 6a. The disc is well imaged as an area of medium density between the cortical plates of the condyle and the temporal component with reduced joint space over the lateral pole (white arrow). The lateral capsule is highlighted against the high signal adipose tissue (arrow).

Fig. 6c.

A T1 weighted mid sagittal MR image of Joint 10L. The junction of the low signal posterior band of the disc (white arrow) with the high signal retrodiscal tissues is at the 1 o'clock position and the disc is well outlined creating a "bow tie" effect.
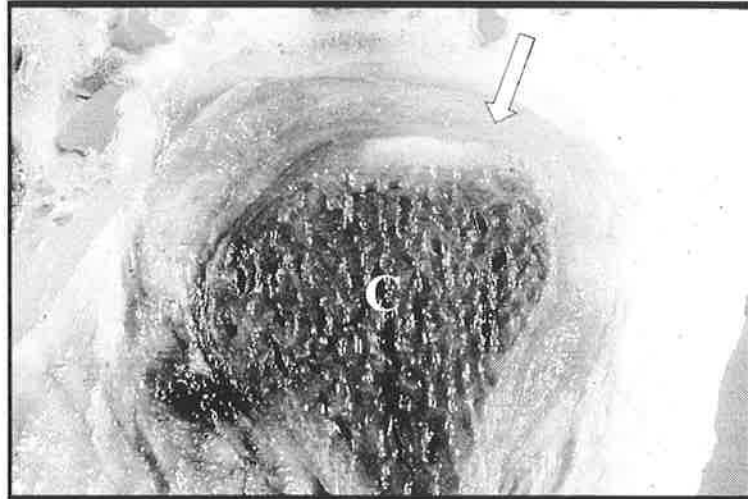
Fig. 6a.
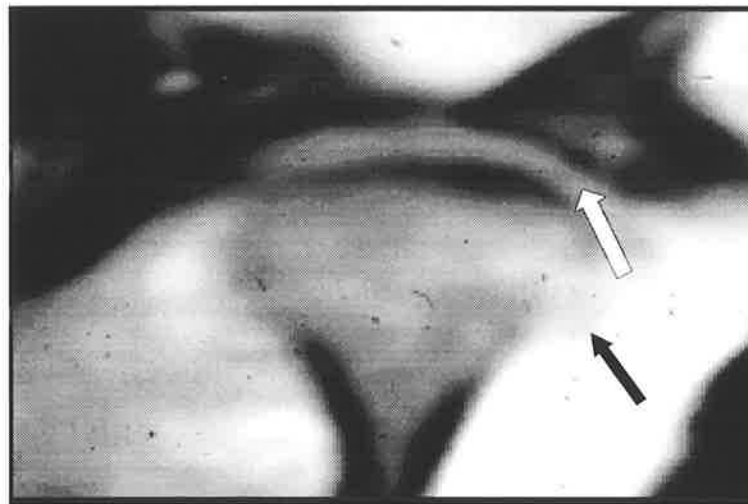
Fig. 6b.
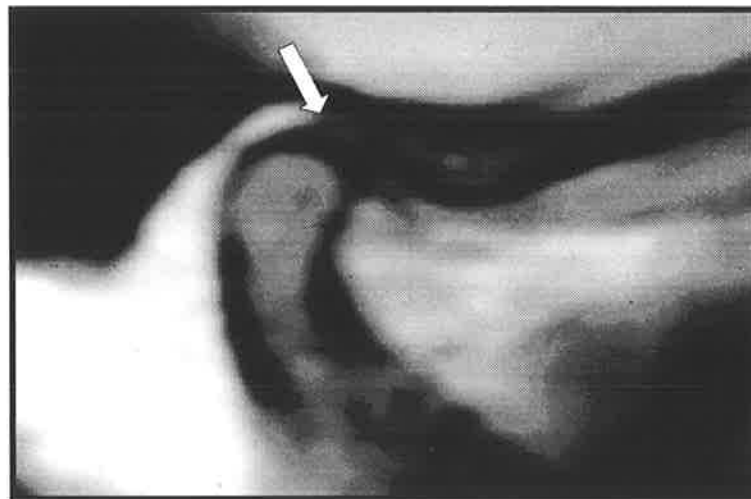
Fig. 6c.

4.2 PATHOLOGICAL JOINTS

4.2.1. Sagittally dissected joint showing discal perforation, osteocartilagenous changes and disc displacement.

Joint 1R2 (Wakefield Memorial Hospital MRI)

This sagittally dissected joint demonstrated a diverse range of pathology from the lateral to medial poles which included a lateral discal perforation, osteocartilagenous changes and an anteromedial disc displacement.

The anatomical slice demonstrated a discal perforation with the anterior discal remnant displaced anteriorly and the posterior band of disc situated at the one o'clock position over the concave head of condyle (Fig. 7a). The retrodiscal tissues appeared elongated anteriorly over the remodelled head of condyle. The attachment of the superior stratum of the retrodiscal tissues was positioned anteriorly which is typical of all lateral joint sections. The posterior surface of the articular eminence demonstrated erosive changes and the anterior fossa was vertical.

Histologic sections of the same anatomic slice showed the posterior retrodiscal tissues had retained a highly vascular, fibroelastic framework, while anteriorly they had developed a more fibrous, avascular appearance (Fig. 7b). The attachment of the superior stratum of the retrodiscal tissues to the glenoid fossa was positioned anteriorly. The discal tissues consisted of densely collagenous fibrous connective tissue. Fibrillation was evident in the disc and retrodiscal tissues. The condyle and articular eminence had a concave, eroded appearance with a vertical fossa. All articular surfaces exhibited extensive remodelling and

degenerative changes. Examination of the articular surfaces showed osteoarthrotic changes in the cartilage layer which include fibrillation and an increase in the number of chondrocytes. In localised areas the fibrous articular covering and articular cartilage was absent and the interface between the subchondral bone and calcified cartilage was irregular. Anterior condylar lipping with laying down of cartilage was evident anteriorly.

Sagittal MR images of the joint demonstrated the discal perforation as localised low signal areas anteriorly and posteriorly representing the discal remnants (Fig. 7c). The higher signal area between the two localised area possibly reflected joint fluid accumulation subsequent to perforation of the disc. The vascular retrodiscal tissues imaged as high signal and the junction with the discal tissues at one o'clock could be identified. The cortical bone contour of the concave condyle and steeply vertical anterior fossa was accurately imaged. The eminence and condyle which histologically had a paucity of cortical bone was imaged by higher MR signal. The bone marrow in both the eminence and fossa imaged with high signal.

Fig. 7a.

A sagittal anatomic section through a right TMJ (Joint 1R-Wakefield Memorial Hospital). This joint has a perforated (P), displaced disc and the articular surface have undergone degenerative and remodelling changes. The posterior band of the disc and retrodiscal tissues are elongated and compressed over the head of the condyle (arrow). The anterior remnant of the perforated disc can be seen (D).

Fig. 7b.

Photomicrograph of a sagittal histologic section of the same right TMJ (Joint 1R-Wakefield Memorial Hospital) as seen in Figure 7a. There is fibrous remodelling of the anterior two thirds of the retrodiscal tissues (arrow) that are interposed between the condyle (C) and roof of the glenoid fossa (F). This section was taken just medial and at the medial edge of the perforation shown in Fig. 7a. Note the irregular topography of the condyle and anterior lipping present (white arrow).

(Trichrome stain, Orig Mag X 7.5).

Fig. 7c.

A T1 weighted MR image of the same sagittal section of Joint 1R as seen in Figure 7a. The junction of the low signal disc with the high signal retrodiscal tissues can be seen (white arrow). The perforated disc images as two localised low signal areas separated by a high signal area (arrow). The low signal pterygoid muscle (P) can be seen inserting into the pterygoid fovea surrounded by high signal fatty tissue.

Fig. 7a.
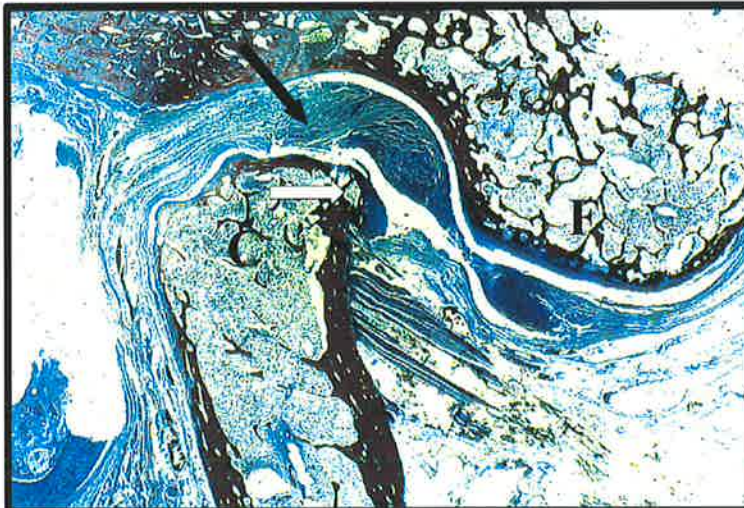
Fig. 7b.
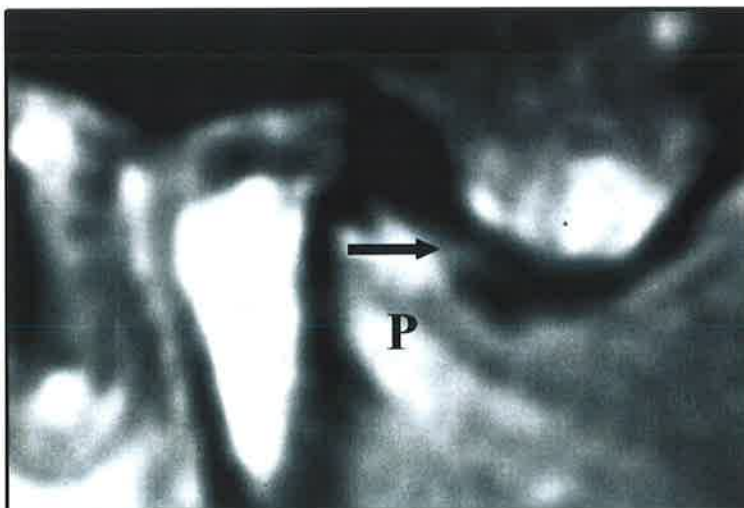
Fig. 7c.

2.2.2. Coronally dissected joint showing antero-medial disc displacement with remodelling.

Joint 2L6 (Vienna MRI)

Coronal anatomic slices demonstrated an antero-medial disc displacement with marked remodelling of the head of the condyle (Fig. 8a). The discal and retrodiscal tissues had undergone structural changes to conform to the altered condylar shape. The bulk of the disc was positioned medially with the medial discal ligament elongated and folded on itself forming a hernia sac. Histologic sections of the same anatomic slice demonstrated the remodelling in the head of the condyle with thinning of the articular surface (Fig. 8b.). The bulk of the fibrous disc was positioned over the medial aspect of the condyle.

Coronal MR images accurately represented the irregular contour of the articular surface of the condyle from the lateral to the medial pole (Fig. 8c). The anteromedially displaced disc was evident as an area of low signal over the medial surface of the condyle. The low signal of the discal ligament was seen folded on itself medially. In sagittal MR images the low signal mass anterior to the condyle confirmed the anteriorly displaced disc. The remodelling in the articular surface of the anterior slope of the condyle was under represented by the MR image.

Fig. 8a.

A coronal anatomic section through the centre of the condyle of a left temporomandibular joint (Joint 2L-Vienna). The joint demonstrates a anteromedially displaced disc (D) with the disc thinned and elongated over the lateral surface of the condyle (C) with elongation of the lateral discal ligament (arrow). The head of the condyle shows remodelling medially with folding of the medial discal ligament forming a hernia sac (white arrow).

Fig. 8b.

Photomicrograph of a sagittal histologic section of the same right TMJ (Joint 2L-Vienna) as seen in Figure 8a. Denudation of the bony end plate of the osteoporotic condyle is evident (C). The bulk of the disc (D) is displaced medially and the retrodiscal can be seen elongated over the lateral surface of the condyle (arrow). (Trichrome stain, Orig Mag X 9) .

Fig. 8c.

A T1 weighted MR image of the same coronal section of Joint 2L as seen in Figure 8a. The anteromedially displaced disc is evident as an area of low signal over the medial surface of the condyle and the discal ligament is seen folded on itself medially (arrow).
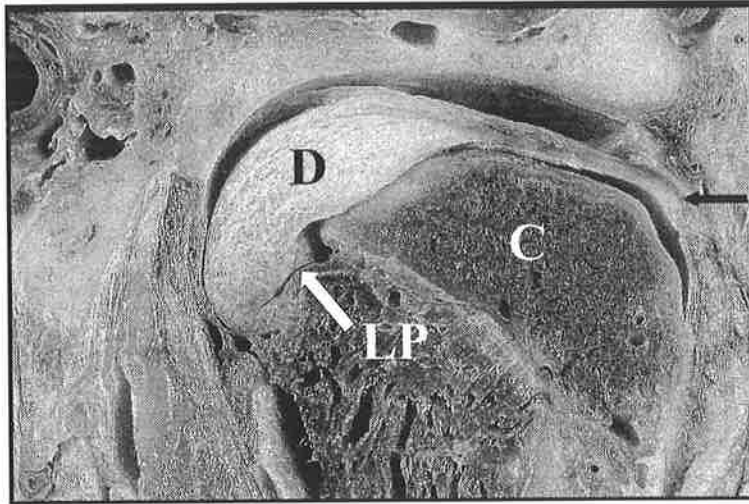
Fig. 8a.
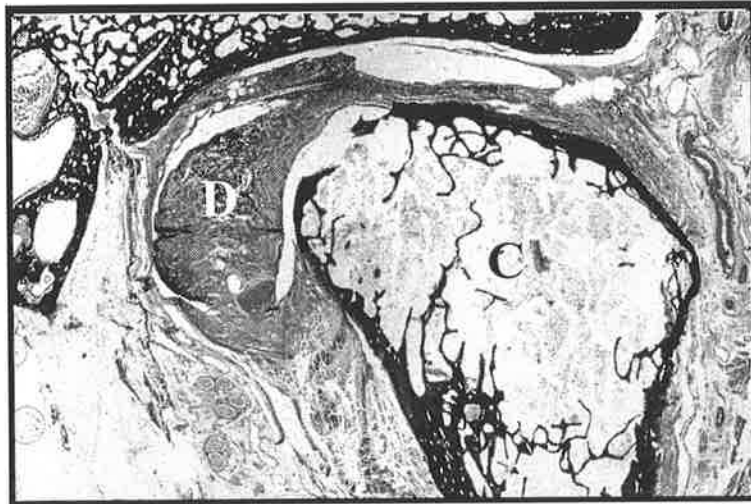
Fig. 8b.
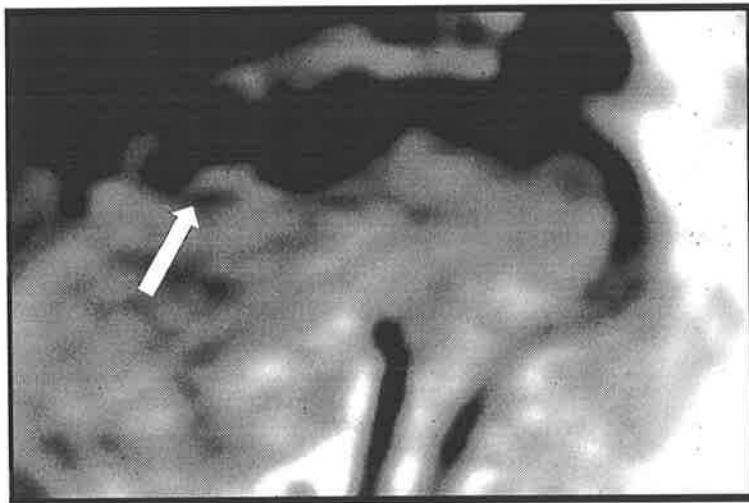
Fig. 8c.

Coronally dissected joint showing a laterally displaced disc

Joint 1L (Vienna)

A coronal anatomic cut through the posterior slope of the eminence demonstrated medial and lateral deviations in form and the discal tissue showed as an island inside the fossa (Fig. 9a). A coronal anatomic section through the crest of the condyle demonstrated a laterally displaced disc (Fig. 9b). It appeared that the bulk of the disc was displaced laterally with disruption of the medial discal ligament suggesting a possible traumatic aetiology.

In coronal MR images the same disc displacement was poorly imaged (Fig. 9c). A low signal mass adjacent to the lateral pole of the condyle was the only indication of the bulk of the disc.

Fig. 9a.

A coronal anatomic section through the articular eminence of a left temporomandibular joint (Joint 1L-Vienna). The disc (D) is seen as an island of soft tissue in a concavity of the posterior slope of the eminence (E). The superior and inferior lateral pterygoid muscles (LP) are cut transversely, anterior to their insertion in the pterygoid fovea.

Fig. 9b.

A coronal anatomic section through the centre of the condyle of the same joint as seen in Figure 9a (Joint 1L-Vienna). This section demonstrates a laterally displaced disc (D) with disruption of the medial discal ligament (L).

Fig. 9c.

A T1 weighted MR image of the same coronal section of Joint 1L as seen in Figure 9b. The severe lateral displacement is poorly imaged. A band of low signal is evident adjacent to the lateral pole of the condyle (arrow).
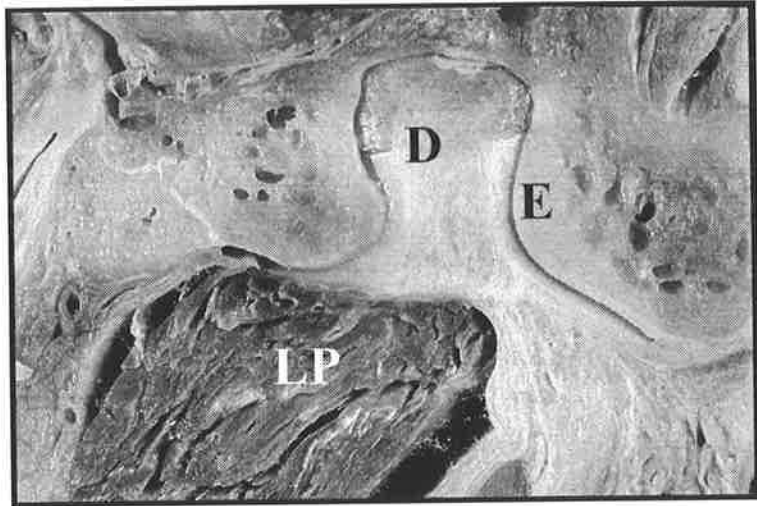
Fig. 9a.
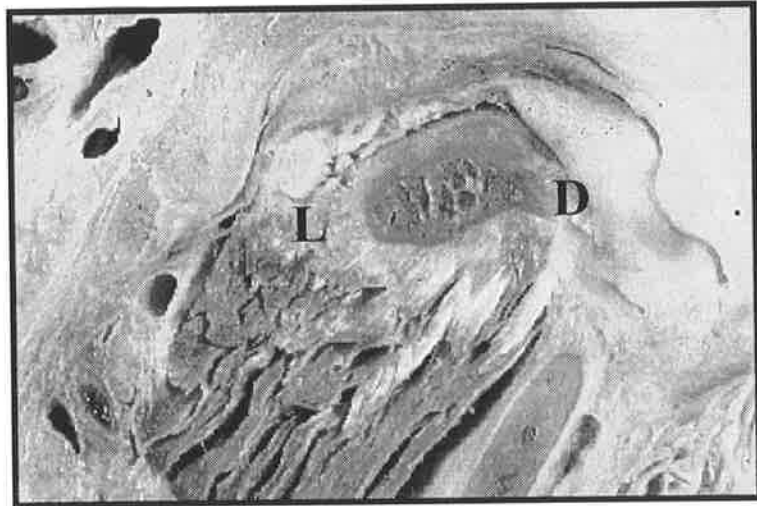
Fig. 9b.

Fig. 9c.

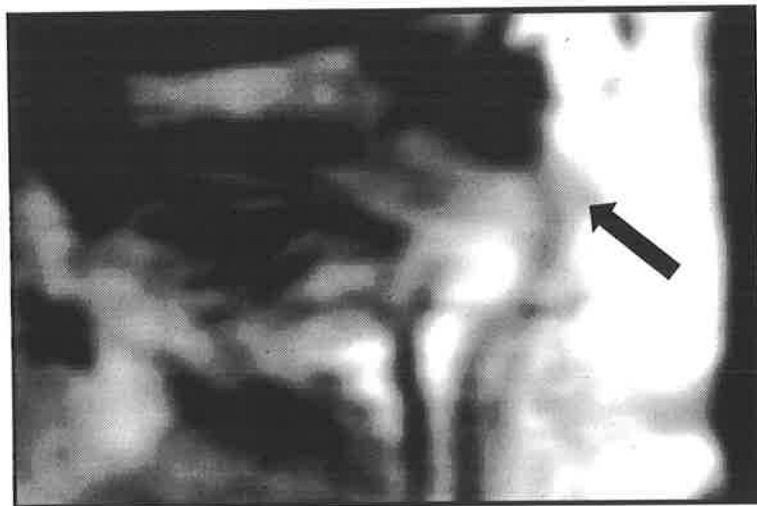## 4.3. COMPARATIVE ANALYSIS OF TEMPOROMANDIBULAR JOINTS BASED ON MACROSCOPIC ASSESSMENT OF JOINT DISSECTIONS AND DIAGNOSIS BY MAGNETIC RESONANCE IMAGING

Thirty human TMJ's were imaged, dissected in either the sagittal or coronal plane and examined histologically. One joint was lost in preparation and was subsequently not included in this study. A total of twelve joints exhibited clinically normal anatomy in relation to condyle eminence, fossa and disc morphology. The other seventeen joints exhibited a range of degenerative joint changes which included anteromedial, anterior and lateral disc displacements, discal perforations and abnormal bone pathology.

4.3.1. Sagittal anatomic sections

(Wakefield Memorial Hospital, Flinders Medical Centre and Vienna MRI's)

The results of analysis of sagittal anatomical sections are shown in Table 1. In summary 8/17 cadaver TMJ's demonstrated normal anatomy, 8/17 demonstrated an anteriorly displaced disc, 0/17 demonstrated a laterally displaced disc, 3/17 demonstrated a perforated disc and 5/17 demonstrated gross morphologic articular changes.

Sagittally Dissected Joints																		
	Vienna joints										Wakefield				Flinders			Total
Joint	1	2	3	4	5	6	7	8	9	10	1	2	3	4	1	2	3	
Normal Anatomy		✓	✓	✓	✓					✓			✓	✓		✓		8/17
Anterior Disc Displacement	✓						✓		✓		✓	✓			✓		✓	7/17
Medial Disc Displacement						✓												1/17
Lateral Disc Displacement																		0/17
Perforated Disc											✓	✓					✓	3/17
Articular Changes								✓	✓		✓	✓			✓		✓	5/17

Table 1. Table illustrating the diagnosis made for each joint examined in the midsagittal plane.

4.3.2. Coronal anatomic sections

(Flinders Medical Centre and Vienna MRI's)

The results of analysis of coronal anatomical sections are shown in Table 2. In summary 4/12 human cadaver TMJ's demonstrated normal anatomy, 6/12 demonstrated a anteriorly displaced disc, 1/12 demonstrated a laterally displaced disc, 2/12 demonstrated a perforated disc and 4/12 demonstrated a perforated disc.

Coronally Dissected Joints														
	Vienna Joints										Flinders			Total
Joint	1	2	3	4	5	6	7	8	9	10	1	2	3	
Normal Anatomy			◆		✓			✓		✓		✓		4/12
Anterior Disc Displacement		✓				✓	✓		✓		✓		✓	6/12
Medial Disc Displacement														
Lateral Disc Displacement	✓													1/12
Perforated Disc							✓						✓	2/12
Articular Changes		✓		✓		✓					✓		✓	4/12

Table 2. Table illustrating the diagnosis made for each joint examined in the coronal plane.

◆ Denotes lost in preparation.

4.3.3. Comparison of sagittally sectioned joints with sagittal and coronal MRI's

The diagnostic accuracy of sagittal and coronal MRI's when compared to sagittal anatomic sections are shown in Table 3. In summary when the sagittal and coronal T1 weighted MR images were compared with the sagittal anatomical sections for normal joints, an accurate diagnosis was made in 8 joints from the sagittal images. However in 3/6 of the coronal images of the same joints an inaccurate diagnosis of a pathological change was made.

Errors occured in joints where the coronal images suggested degenerative changes in the articular surface which were not evident in the sequential sagittal anatomic sections. The sagittal MRI's accurately imaged the 7 joints with a anteriorly displaced disc, however in one joint the coronal image failed to identify the disc displacement. Difficulties in interpreting this coronal MRI occurred as the displacement was not associated with a thinning of the disc laterally and reduction of joint space laterally. It was not possible to diagnose from the sagittal MRI the one joint in which the disc was displaced medially, however diagnosis was possible from the coronal image. Difficulties in interpreting the lateral sagittal images occured due to the thinness of the disc and retrodiscal tissue failing to image. However coronal sections of the same joint accurately demonstrated the elongated discal ligaments, reduced joint space laterally and bulk of disc medially. Except for one joint, T1 weighted images failed to image discal perforations. Articular surface changes were well imaged by sagittal and coronal MRI's which provided a three dimensional representation remodelling and degenerative joint pathology.

Joint Condition	Anatomical Diagnosis	Diagnosis by Sagittal MRI	Diagnosis by Complementary Coronal MRI
Normal Anatomy	8	8	3/6
Disc Position			
Disc Displacement	8	7	5
ADD	7	7	4/5
MDD	1	0	1
LDD	-	-	-
Perforation	3	1/1	
Articular Changes	6	6	4/4

Table 3. Accuracy of diagnosis of sagittally dissected joints by sagittal and complementary coronal MR images.

4.3.4. Comparison of coronally sectioned joints with sagittal and coronal MRI's

The diagnostic accuracy of sagittal and coronal MRI's when compared to coronal anatomic sections are shown in Table 4. In summary the four joints which demonstrated normal anatomy were accurately interpreted by coronal MR images and the complementary sagittal images. Five of the six joints which had an anteriorly displaced disc could be diagnosed by a coronal image.

Difficulties in interpretation occured in one joint where the displacement was predominantly anterior and the mid-condylar coronal section exhibited a normal anatomical relationship without reduction of the joint space laterally, elongation of the discal ligaments or positioning of the bulk of the disc medially. However the sagittal MR image suggested an anteriorly displacement and the combination of the sagittal and coronal images provided the three dimensional image of the joint. One joint demonstrated a laterally displaced disc, however neither the sagittal or coronal MRI accurately imaged this reflecting the difficulty in interpreting lateral images of the joint where the close relationship of the surface coil results in a poor quality image and lack of tissue contrast laterally. Two coronally sectioned joints demonstrated discal perforations. One joint had a severe perforation which could be diagnosed from the MR image as the extensive degenerative changes had resulted in the low signal articulating surfaces being positioned adjacent to each other with an absence of signal from discal tissue. The other joint demonstrating a perforation which could not be imaged by MRI, had a medially displaced disc with marked narrowing of the joint space over the lateral pole and perforation of the lateral discal ligament. Articular surface changes due to remodelling or degenerative changes in the joint were accurately imaged in all joints by coronal MRI's which provided an accurate outline of subtle changes in contour of the

cortical bone from the lateral to medial aspect of the joints. Sagittal MRI's of the same joints frequently failed to image early articular surface remodelling which would be imaged by coronal MRI's.

Joint Condition	Anatomical Diagnosis	Diagnosis by Coronal MRI	Diagnosis by Complementary Sagittal MRI
Normal Anatomy	4	4	4
Disc Position			
Disc Displacement	7	5	6
ADD	6	5	6
MDD	-	-	-
LDD	1	0	0
Perforation	2	1	0
Articular Changes	4	4	3

Table 4. Accuracy of diagnosis of coronally dissected joints by coronal and complementary sagittal MR images.

4.4. COMPARISON OF T1SE, T1GE, T2SE AND T2TSE MAGNETIC RESONANCE IMAGES WITH CORRESPONDING ANATOMIC SLICES AND HISTOLOGIC SECTIONS

(Flinders Hospital MRI's)

In this section the results of a comparison of four imaging sequences relative to corresponding anatomic slices and histologic sections were presented.

4.4.1. SAGITTALLY SECTIONED JOINTS

4.4.1.1. Normal joint (Joint 2)

(i) Anatomic slice

This joint demonstrated the criteria required for the TMJ to be classified as normal (Fig. 10a). The articular surfaces of the temporal and condylar components were smooth. The junction of the disc with the retrodiscal tissues was situated only slightly anterior to the crest of the condyle. The disc was biconcave in mediocentral and central regions and had a rectilinear profile in lateral sections. There was no obvious fissuring, fraying or perforation of the disc.

(ii) Histologic section

A central histologic section of the joint demonstrated features consistent with a normal joint although variations did exist (Fig. 10b). The fossa had a thin articular covering of fibrous connective tissue which was absent in places with exposure and localised perforation of the bony end plate. The fibrous articular covering of the condyle was thickened and cartilage metaplasia with denudation of the cortical bony end plate was

evident. The central cavity of the condyle consisted primarily of bone marrow. The disc consisted of condensed, avascular fibrous connective tissue and the junction at the one o'clock position with the highly vascular, fibro-elastic retrodiscal tissues was clearly evident.

(iii) T1 weighted spin echo sequence

The thicker cortical bone of the articular eminence and the thinned cortical bone of the fossa was imaged as low signal highlighted against the high signal bone marrow (Fig. 10c). The thin cortical bone of the crest of the condyle and thickened fibrocatilage layer was accurately imaged by medium signal. The disc was well imaged as a biconcave medium-low signal mass, limited anteriorly by the low signal capsule. The junction of the disc with the higher signal retrodiscal tissues was well imaged.

The complementary mid-condylar, coronal, T1SE image indicated that there was a uniform joint space from lateral to medial (Fig. 10g). Anatomically as the disc was at the one o'clock position the tissue on the superior aspect of the condyle would be retrodiscal tissue and this area imaged as intermediate to high signal. Bone detail of the head of the condyle was accurately imaged.

(iv) T1 weighted gradient echo sequence

The articular surface of the condyle imaged as a band of intense low signal failing to indicate the histological changes in the cortical bone of the condyle (Fig. 10d). The articular surface of the fossa and eminence also imaged as intense low signal reflecting a lack of imaging sensitivity to histologic detail. The disc position and shape was poorly imaged although the junction with the retrodiscal tissues could be identified.

A mid-condylar, coronal, T1GE image of the same joint failed to demonstrate bony detail in the condyle (Fig. 10h). The joint space from lateral to medial was uniform indicating that the disc was in place.

(v) T2 weighted spin echo sequence

The dense cortical bone of the articular eminence and the thin cortical bone of the fossa was well imaged as intense low signal (Fig. 10e). The patchy low signal image of the cortical bone on the crest of the condyle indicated the increase in fibrocartilage in this area. The biconcave shape of the disc was well imaged due to the high signal from the fluid in the joint spaces adjacent to the intermediate zone of the disc. The anterior capsule and its insertions was also well imaged. Posteriorly the junction with the high signal retrodiscal tissues at the one o'clock position was well imaged.

A mid-condylar coronal section of the same joint accurately imaged the cortical bone changes in the articular surface of the condyle (Fig. 10i). The uniform thickness of the joint space from lateral to medial gave the best indication that the disc was in position.

(vi) T2 weighted turbo spin echo

The cortical bone of the articulating surfaces was well imaged as intense low signal highlighted against the intermediate to high signal of the bone marrow (Fig. 10f). The disc position was accurately imaged with the high signal of the fluid in the joint spaces helping to define the disc. The anterior joint capsule and its insertions were well imaged as was the junction posteriorly with the high signal retrodiscal tissues.

The mid-condylar coronal section of the same joint accurately imaged the cortical bone of the articular surface (Fig. 10j). The uniform joint space from lateral to medial containing the intermediate signal retrodiscal tissues indicates the disc was in a normal position.

Conclusion

The T2TSE image was highly accurate when compared to the anatomic and histologic sections. It provided an accurate representation of the disc, articular surfaces and retrodiscal tissues for the normal joint. Considering the reduced image time for this sequence and the detail provided it would be considered the preferred imaging sequence.

Fig. 10a.

A sagittal anatomic section through a right TMJ (Joint 2-Flinders Medical Centre). The articular surfaces of the condyle (C) and fossa (F) are smooth. The junction of the disc(D) with the retrodiscal tissues is at the one o'clock position (arrow).

Fig. 10b.

Photomicrograph of a sagittal histologic section of the same right TMJ (Joint 2 -Flinders Medical Centre) as seen in Figure 10a. Thinning of the fibrous layer is of the articular fossa can be seen in localised areas. There is thickening of the cartilage zone and resorption of the bony end plate of the condyle (arrow). The junction of the fibrous disc (D) with the vascular retrodiscal tissues at the one o'clock position can be seen (white arrow). (Trichrome stain, Orig Mag X 8.5).

Fig. 10c.

A sagittal T1 weighted spin echo MR image of the same sagittal section of Joint 2 as seen in Figure 10a. The remodelling in the head of the condyle (C) images as medium signal (arrow). The disc images as a well defined medium-low signal (D) and the junction with the higher signal retrodiscal tissues can be seen (white arrow).

Fig. 10d.

A sagittal T1 weighted gradient echo MR image of the same sagittal section of Joint 2 as seen in Figure 10a. The outline of the condyle and fossa is well defined however the remodelling of the condyle is not evident. The junction of the disc with the retrodiscal tissues can be seen (arrow), however the disc outline is poorly defined.

Fig. 10e.

A sagittal T2 weighted spin echo MR image of the same sagittal section of Joint 2 as seen in Figure 10a. The outline of the condyle and fossa is clear and the remodelling in the head of the condyle is indicated by the patchy low signal on the superior aspect. The disc is well defined and the junction with the high signal retrodiscal tissues is clear.

Fig. 10f.

A sagittal T2 weighted spin echo MR image of the same sagittal section of Joint 2 as seen in Figure 10a. The remodelling in the head of the condyle images as an increased low signal of the surface layer. The disc position, shape and junction with the retrodiscal tissues can be seen.
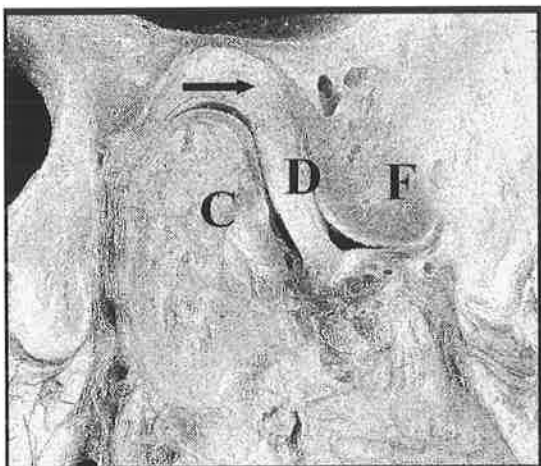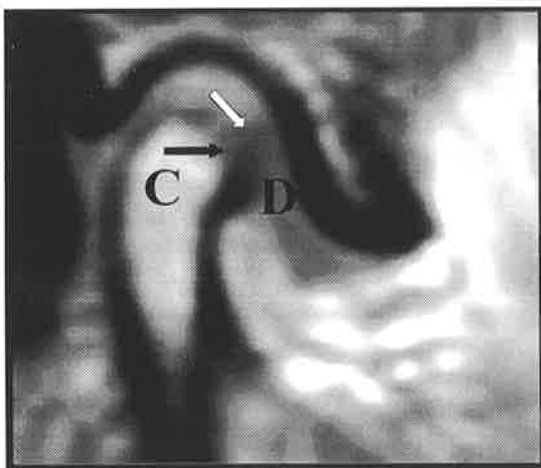
Fig. 10a.

Fig. 10b.

Fig. 10c.

Fig. 10d.

Fig. 10e.

Fig. 10f.

Fig. 10a.

A sagittal anatomic section through a right TMJ (Joint 2-Flinders Medical Centre). The articular surfaces of the condyle (C) and fossa (F) are smooth. The junction of the disc(D) with the retrodiscal tissues is at the one o'clock position (arrow).

Fig. 10b.

Photomicrograph of a sagittal histologic section of the same right TMJ (Joint 2 -Flinders Medical Centre) as seen in Figure 10a. Thinning of the fibrous layer is of the articular fossa can be seen in localised areas. There is thickening of the cartilage zone and resorption of the bony end plate of the condyle (arrow). The junction of the fibrous disc (D) with the vascular retrodiscal tissues at the one o'clock position can be seen (white arrow). (Trichrome stain, Orig Mag X 8.5).

Fig. 10g.

A coronal T1 weighted spin echo MR image through the centre of the condyle (C) of Joint 2. The even joint space which contains medium signal retrodiscal tissues indicated the disc is in place. The condyle and fossa are well defined.

Fig. 10h.

A coronal T1 weighted gradient echo MR image through the centre of the condyle of Joint 2. The condyle (C) articular surface is ill defined. The high signal area in the superior joint space would be retrodiscal tissues (arrow).

Fig. 10i.

A coronal T2 weighted spin echo MR image through the centre of the condyle of Joint 2. Remodelling in the head of the condyle is indicated by the heterogeneous low signal (arrow). The lack of elongation of the low signal medial discal ligament and the even joint space indicates the disc is in place.

Fig. 10j.

A coronal T2 weighted turbo spin echo MR image through the centre of the condyle of Joint 2. The remodelling is indicated by the patchy low signal of the head of the condyle (arrow).
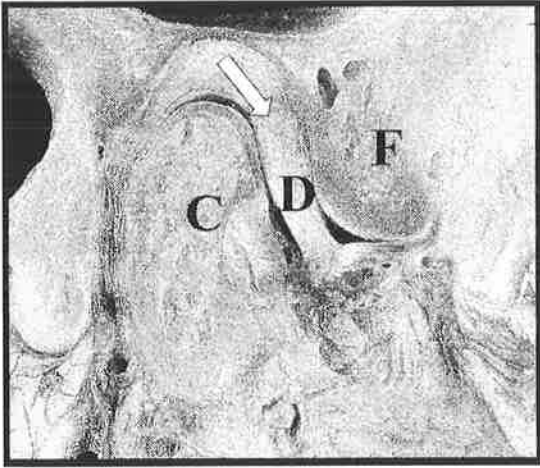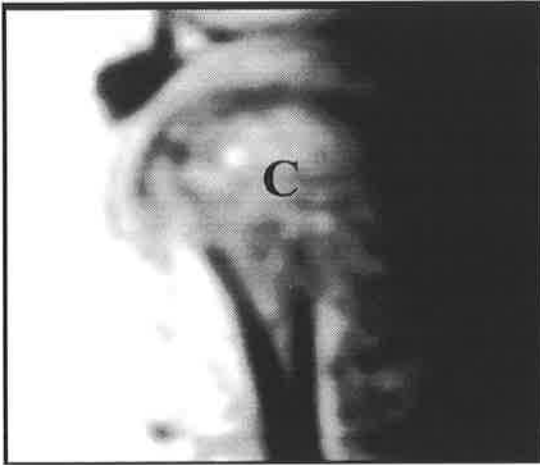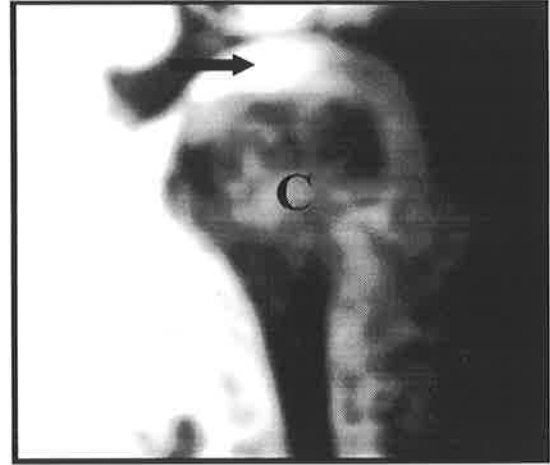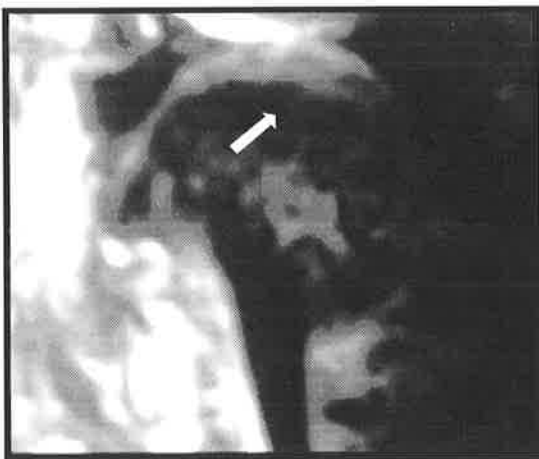
Fig 10a.

Fig 10b.
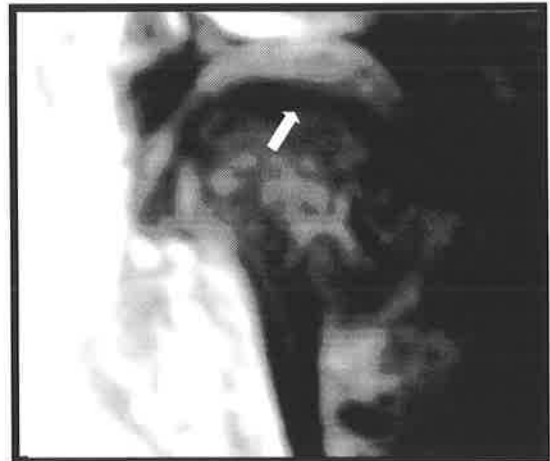

Fig. 10g.

Fig. 10h.

Fig. 10i.

Fig. 10j.

4.4.1.2. Remodelled joint with medially displaced disc (Joint 1)

(i) Anatomic slice

This sagittally dissected joint exhibited a range of pathology from the lateral to medial aspect of the joint (Fig. 11a). Remodelling of the condyle, fossa and articular eminence was evident in this joint. The condyle had developed anterior beaking and the articular eminence had a flattened appearance. In the most superior aspect of the anterior beak, it appeared that there was a subarticular cyst like cavity present. The disc and retrodiscal tissues had adopted a linear shape to maintain congruency of the remodelled articulating surfaces. Medially the disc was displaced over the thinned and narrowed condyle.

(ii) Histologic section

Histologically this joint exhibited osteoporotic changes in the condyle and temporal components with a reduction in cancellous bone (Fig. 11b). There was thinning of the articular fibrous connective tissue outer layer, cartilage zone and cortical bone of the articular surfaces. The fibrocartilage layer of the articular surfaces, though intact, demonstrated superficial fibrillation. The anterior beak of the condyle consisted of highly cellular fibrocartilage tissue which was undergoing calcification in areas. The cystic cavity seen in anatomic sections was an enlarged bone marrow space. The disc consisted of fibrous connective tissue and the anterior third of the retrodiscal tissues were elongated over the superior aspect of the condyle and had adopted a fibrous "pseudodisc" like appearance with reduced vascularity.

(iii) T1 weighted spin echo sequence

In the central MR image the bone marrow of the condyle imaged as high signal against the low signal outline of the cortical bone which was deficient on the superior flattened aspect (Fig. 11c). The remodelled anterior beak imaged as an area of intense low signal, however the cystic cavity seen in anatomical sections could not be identified. Medial sections accurately imaged the thinned condyle. The shape of the fossa and articular eminence was accurately outline by low signal of the cortical bone. The disc imaged as an area of medium-low signal anteriorly where the anterior capsule was well defined, however posteriorly the shape and junction with the retrodiscal tissues was ill defined. In medial images the bulk of the disc which was positioned over the head of the condyle could be identified.

A central coronal MR image of the same joint failed to image the remodelled head of condyle (Fig. 11g). The medially displaced disc was indicated by the reduced joint space laterally and the elongation of the medial capsule, however the displacement was difficult to identify.

(iv) T1 weighted gradient echo sequence

In sagittal MRI's the cortical bone outline of the condyle and fossa was accurately imaged (Fig. 11d). In central sections the low signal of the anterior beak of the condyle and the flattened superior surface was identified against the heterogeneous medium signal of the osteoporotic bone marrow. The narrowing of the condyle medially was also well imaged. In central sections the shape and position of the disc and its junction with the retrodiscal tissues posteriorly was poorly imaged. In medial sections of the same joint the medium low signal of the disc could be seen.

In a mid-condylar coronal section of the same joint, the only indication of the medial disc displacement was the increased joint space medially (Fig. 11h). It was not possible to identify the disc displaced over the medial pole. The extensive remodelling seen in sagittal anatomic and histologic sections was difficult to diagnose from the coronal image.

(v) T2 weighted spin echo sequence

The sagittal sequence from lateral to medial provided an accurate image of the fossa and articular eminence (Fig. 11e). The remodelled head of condyle which had a thin cortical bone end plate was well imaged showing flattening and osteophyte formation. The osteoporotic bone marrow imaged with a heterogeneous signal. In lateral sections the image of the thinned joint space and relative absence of disc indicated the displacement. In central sections the position and outline of the disc, the anterior capsule and its insertions and the junction with the retrodiscal tissues posteriorly was well imaged. In medial sections it was possible to identify the bulk of disc displaced over the narrowed head of condyle.

A mid-condylar coronal section of the same joint imaged the reduced joint space and absence of discal tissue laterally, the bulk of disc displaced medially and elongation of the medial discal ligament (Fig. 11i). The irregular low signal outline of the condyle indicated the articular surface had undergone remodelling but it under-represented the extent of the change. The bone marrow imaged with a heterogeneous signal intensity.

(vi) T2 weighted turbo spin echo sequence

The sagittal sequence imaged the articular surface remodelling of the condyle from lateral to medial (Fig. 11f). The lateral flattening, central osteophyte formation and medial narrowing were well imaged. The osteoporotic bone marrow imaged with a heterogeneous

signal. The disc position and shape was well imaged by sequential T2TSE MRI's. The discs thinness laterally, linear shape centrally and displacement medially could all be identified. In central and medial sections, anteriorly the capsule and its insertions and posteriorly the junction with the high signal retrodiscal tissues were well imaged.

Coronal section of the same joint imaged the remodelled head of condyle by the irregular low signal of the cortical bone from lateral to medial (Fig. 11j). The reduced joint space laterally, elongation of the discal ligament medially and the low signal of the discal tissues medially indicated the disc displacement.

Conclusion

The T2TSE provided the most diagnostic information for the shortest imaging time. In a joint which demonstrated articular surface remodelling and disc displacement the combination of the sequential sagittal and coronal images provided a three dimensional image of the joint.

Fig. 11a.

A sagittal anatomic section through a right TMJ (Joint 1-Flinders Medical Centre). The condyle has remodelled (C) and a large cystic like space can be seen in the head of the condyle (white arrow). The disc appears elongated and has lost its normal bow tie like appearance although the junction with the vascular retrodiscal tissues can be seen (arrow).

Fig. 11b.

Photomicrograph of a sagittal histologic section of the same right TMJ (Joint 1-Flinders Medical Centre) as seen in Figure 11a. The osteoporotic condyle (C) and fossa (F) do not demonstrate active remodelling as the articular surface consists of a thinned cartilage layer and bony end plate. The cystic like space seen in anatomic sections is not evident. The anterior retrodiscal tissues have assumed a fibrous pseudodisc like appearance (arrow). (Trichrome stain, Orig Mag X 7.5).

Fig. 11c.

A sagittal T1 weighted spin echo MR image of the same sagittal section of Joint 1 as seen in Figure 11a. The outline of the remodelled condyle (C) and fossa (F) can be seen. The junction of the low signal disc and high signal retrodiscal tissues is poorly defined. It is difficult to determine the outline of the disc.

Fig. 11d.

A sagittal T1 weighted gradient echo MR image of the same sagittal section of Joint 1 as seen in Figure 11a. The outline of the remodelled condyle (C) and fossa (F) is well imaged. The displaced disc and discal-retrodiscal junction cannot be identified.

Fig. 11e.

A sagittal T2 weighted spin echo MR image of the same sagittal section of Joint 1 as seen in Figure 11a. The outline of the articular surfaces of the condyle (C) and fossa (F) is evident. The remodelled anterior beak of condyle can be seen (arrow). The outline of the displaced disc and junction with the retrodiscal tissues is well defined (white arrow).

Fig. 11f.

A sagittal T2 weighted spin echo MR image of the same sagittal section of Joint 1 as seen in Figure 11a. The outline of the articular surfaces of the condyle and fossa is evident. The remodelled anterior beak of condyle can be seen (C). The outline of the displaced disc and junction with the retrodiscal tissues at the one o'clock position is well defined (white arrow). The central tendon of lateral pterygoid can be seen inserting into the pterygoid fovea.
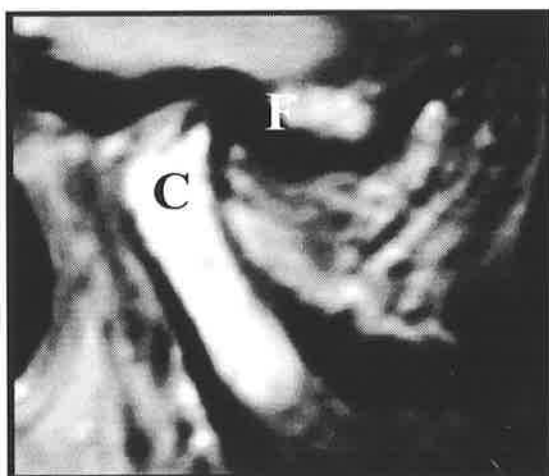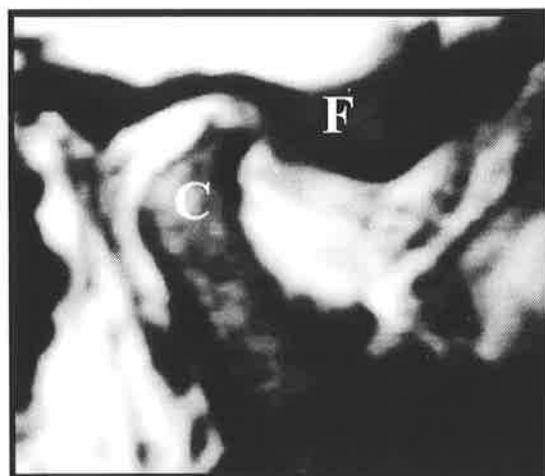
Fig. 11a.
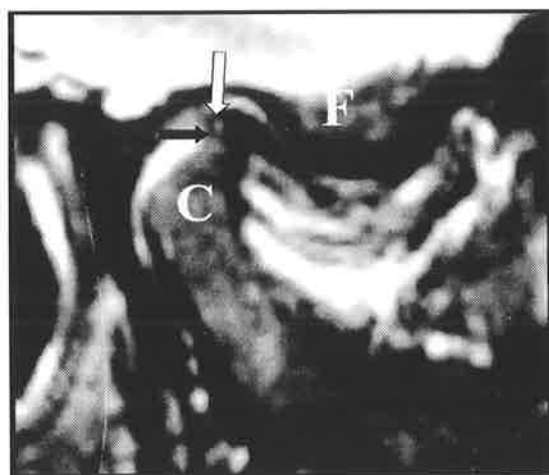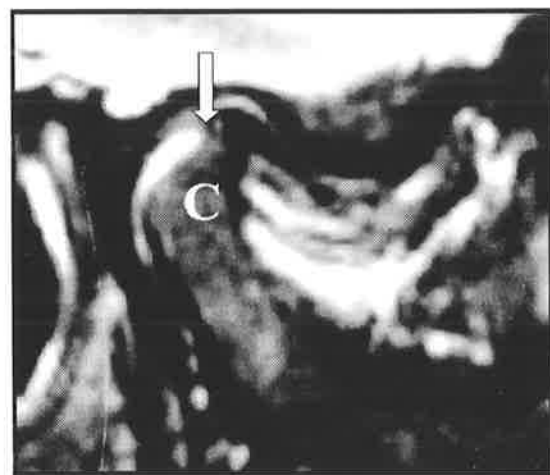

Fig. 11b.

Fig. 11c.

Fig. 11d.

Fig. 11e.

Fig. 11f.

Fig. 11a.

A sagittal anatomic section through a right TMJ (Joint 1-Flinders Medical Centre). The condyle has remodelled (C) and a large cystic like space can be seen in the head of the condyle (white arrow). The disc appears elongated and has lost its normal bow tie like appearance although the junction with the vascular retrodiscal tissues can be seen (arrow).

Fig. 11b.

Photomicrograph of a sagittal histologic section of the same right TMJ (Joint 1-Flinders Medical Centre) as seen in Figure 11a. The osteoporotic condyle (C) and fossa (F) do not demonstrate active remodelling as the articular surface consists of a thinned cartilage layer and bony end plate. The cystic like space seen in anatomic sections is not evident. The anterior retrodiscal tissues have assumed a fibrous pseudodisc like appearance (arrow). (Trichrome stain, Orig Mag X 7.5).

Fig. 11g.

A coronal T1 weighted spin echo MR image through the centre of the condyle of Joint 1. The irregular surface of the condyle (C) indicates that some remodelling is occurring. The disc space is reduced laterally (arrow) and the discal ligament is elongated medially (white arrow).

Fig. 11h.

A coronal T1 weighted gradient echo MR image through the centre of the condyle of Joint 1. The bony detail of the condyle and fossa is poor. The disc space is increased medially (white arrow).

Fig. 11i.

A coronal T2 weighted spin echo MR image through the centre of the condyle of Joint 1. Remodelling in the head of the condyle is well imaged by the irregularity in signal of the surface layer (arrow). The displaced disc is indicated by the reduced joint space laterally, elongated medial discal ligament and localised area of low signal medially (white arrow).

Fig. 11j.

A coronal T2 weighted turbo spin echo MR image through the centre of the condyle of Joint 1. The remodelling and degenerative changes in the head of the condyle are indicate by the heterogeneous low signal of the articular surface. The displaced disc images as a localised low signal area medially (white arrow) and a reduction in joint space laterally.
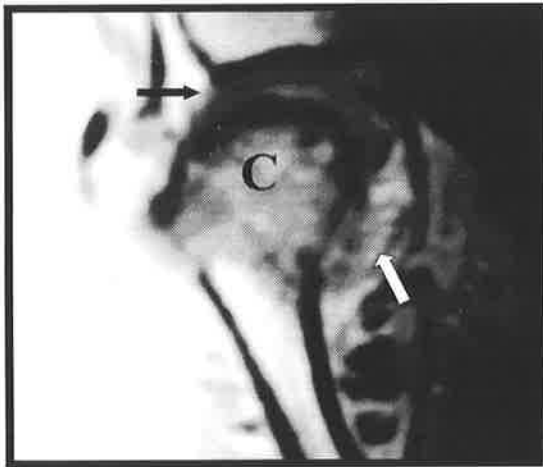
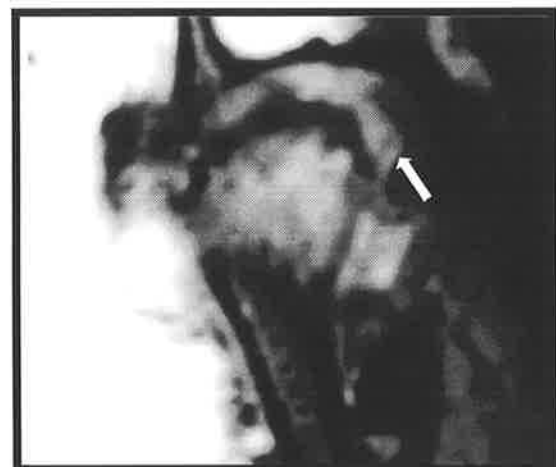Fig. 11a.

Fig. 11b.

Fig. 11g.
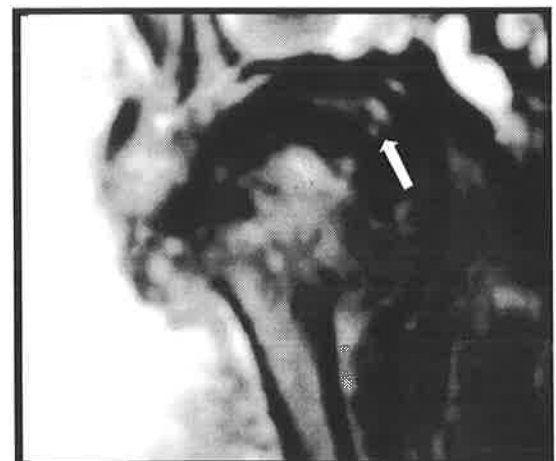

Fig. 11h.

Fig. 11i.

Fig. 11j.

4.4.1.3. Joint with lateral discal perforation, remodelling of the articular surface and medial disc displacement (Joint 3)

(i) Anatomic slice

This joint exhibited a diverse range of pathology from the lateral to medial pole (Fig. 12a). Laterally the disc was completely perforated with only remnants remaining of retrodiscal tissue posteriorly and discal tissue anteriorly. Laterally and centrally the condyle exhibited thickening of the articular surface. Central and medial sections showed the disc had a linear appearance with the perforation restricted to the retrodiscal tissues over the remodelled condyle. Medially the disc was intact but displaced and folded over the medial pole of the condyle with elongation of the medial discal ligament.

(ii) Histologic sections

Histological sections of this pathologic joint exhibited changes to the disc and articular surfaces of the condyle and temporal component (Fig. 12b). Lateral sections showed a remnant of discal tissue anteriorly and a remnant of retrodiscal tissue posteriorly. The anterior remnant of discal tissues contained blood vessels and was highly cellular with fibroblasts evident. In more medial sections the fibrous disc had a more linear arrangement, consisting of avascular collagen fibres. The retrodiscal tissues had assumed a "pseudodisc" like appearance and were elongated over the superior crest of the condyle. In all sections the articulating surfaces of the condyle and fossa were disintegrating with the development of deep vertical clefts, fibrillation and localised destruction of the fibrocartilage layer. The underlying cortical bone had undergone osteoclastic resorption and there was evidence of rapid attempt at repair with highly cellular fibrocartilagenous tissue being laid down.

(iii) T1 weighted spin echo sequence

The outline of the fossa and articular eminence were accurately imaged in all sagittal sections (Fig. 12c). Laterally, where there was a discal perforation, the head of the condyle imaged as medium signal due to the breakdown of cortical bone and hyperplastic cartilaginous changes. Medial joint sections imaged the shape of the condyle accurately. Laterally the discal and retrodiscal tissue remnants were not imaged and it was not possible to identify the discal perforation. Medio-central sections imaged the disc displaced anteriorly, however the junction with the retrodiscal tissues was not evident. Medial sections accurately imaged the discal remnant displaced and folded over the medial pole of the condyle confirming the anteromedial displacement.

A mid-condylar coronal T1SE image of the same joint accurately imaged the increased cartilage in the head of the condyle as an area of medium signal intensity (Fig. 12g). No indication of the lateral perforation was evident. The anteromedial disc displacement was indicated by the reduction in the joint space laterally, however the bulk of the disc positioned medially was not well imaged.

(iv) T1 weighted gradient echo sequence

The articular surface changes were well imaged (Fig. 12d). The increased fibrocartilagenous tissue and denudation of the cortical bone was accurately imaged. The lateral discal perforation could not be diagnosed from the MR image. The disc displacement was suggested by the low signal discal tissue in medial sections but difficulties in interpretation occured due to the lack of information in lateral and central sections.

A mid-condylar coronal section of the same joint accurately indicated that there were osteocartilagenous changes in the head of the condyle (Fig. 12h). However the disc displacement and lateral perforation failed to image.

(v) T2 weighted spin echo sequence

The sagittal sequence of images accurately imaged the osteocartilagenous changes in the articular surface of the condyle (Fig. 12e). The lateral and central increase in cartilage tissue and alteration in shape and the medial narrowing were all imaged. The discal perforation laterally was imaged by high signal from the increased fluid in the joint space. In medio-central sections where the discal-retrodiscal tissue complex was intact it was possible to delineate the low signal outline of discal tissue. Medially the displaced disc could be seen folded over the medial pole of the condyle.

The coronal sections accurately imaged the osteocartilagenous changes in the head of the condyle (Fig. 12i). The lateral perforation was easily identified by the localised area of high signal laterally. The medially displaced disc could be diagnosed by the herniated medial discal tissue and elongation of the medial discal ligament.

(vi) T2 weighted turbo spin echo sequence

The sagittal images were highly sensitive to the articular surface remodelling of the head of the condyle (Fig. 12f). The lateral perforation could be identified by the localised areas of high signal from fluid in the joint space on the superior aspect of the condyle that disappeared medially. The image was highly accurate in recording the linear shape and anterior position of the disc and the discal-retrodiscal junction in medial sections where the

perforation was no longer evident. The most medial section clearly imaged the displaced disc folded over the medial pole of the condyle.

The coronal sections provided a detailed image of the head of the condyle indicating that osteocartilagenous changes were occurring (Fig. 12j). The lateral perforation was indicated by the localised area of high signal and reduced joint space. The disc displacement imaged as a herniated, medial sac of medium signal and elongation of the medial discal ligament was evident.

151

Fig. 12a.

A sagittal anatomic section through a right TMJ (Joint 3-Flinders Medical Centre). The articular surface of the condyle is thickened (C). The disc (D) has a linear shape and is displaced anteromedially. The disc is perforated at the junction with the retrodiscal tissues (arrow).

Fig. 12b.

Photomicrograph of a sagittal histologic section of the same right TMJ (Joint 1-Flinders Medical Centre) as seen in Figure 12a. The retrodiscal tissues have assumed a fibrous pseudo-disc like appearance. The disc contains densely collagenous fibrous connective tissue. Resorption of the bony end plate and highly cellular fibrocartilage is present in the head of the condyle. The perforation is seen as a deep cleft on the superior surface of the retrodiscal tissues (white arrow). (Trichrome stain, Orig Mag X 8).

Fig. 12c.

A sagittal T1 weighted spin echo MR image of the same sagittal section of Joint 3 as seen in figure 12a. The outline of the articular surface of the condyle (C)and fossa can be seen, however remodelling in the head of the condyle is poorly imaged. The junction of the disc with the perforated retrodiscal tissues can not be seen and the displacement is indicated by the anterior linear low signal area (arrow).

Fig. 12d.

A sagittal T1 weighted gradient echo MR image of the same sagittal section of Joint 3 as seen in Figure 12a. The remodelling is indicated by the increased low signal area on the head of the condyle. The disc and retrodiscal tissues fail to image.

Fig. 12e.

A sagittal T2 weighted spin echo MR image of the same sagittal section of Joint 3 as seen in Figure 12a. The remodelling in the head of the condyle images as a heterogeneous low signal surface layer. The disc images as a linear low signal anteriorly (arrow) and the junction with the high signal retrodiscal tissues can be seen (white arrow). The perforation images as a localised high signal at the head of the condyle in the joint space.

Fig. 12f.

A sagittal T2 weighted spin echo MR image of the same sagittal section of Joint 3 as seen in Figure 12a. The remodelled head of condyle (C) images with heterogeneous low signal intensity (white arrow). The disc's linear low signal outline and position can be seen. The perforation posteriorly images as a localised high signal area in the superior joint space (arrow).
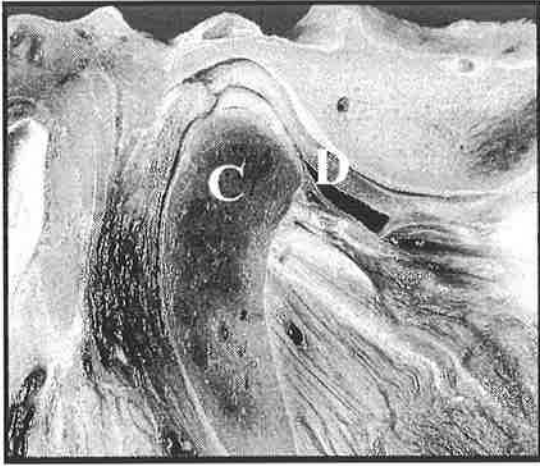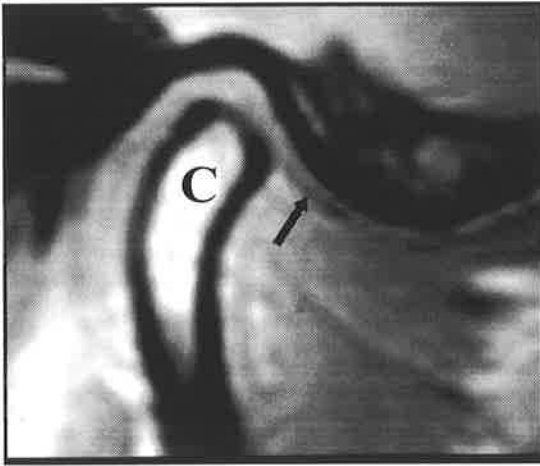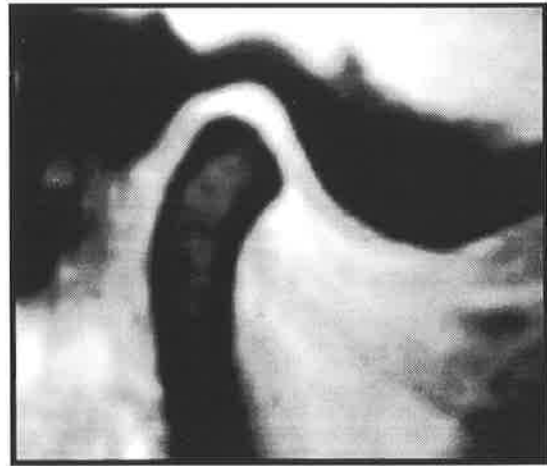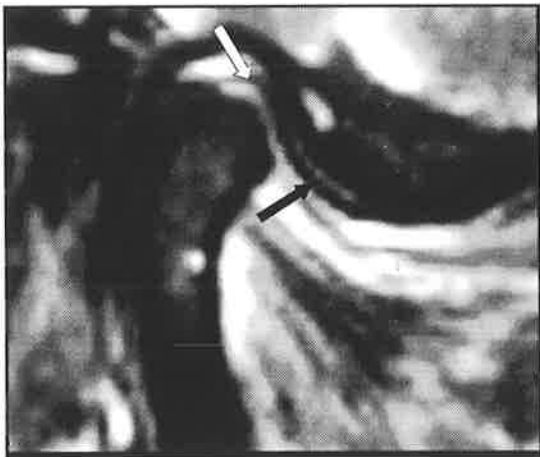
Fig. 12a.

Fig. 12b.

Fig. 12c.

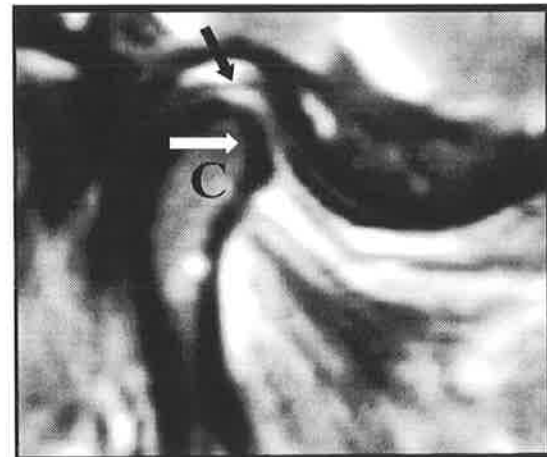

Fig. 12d.

Fig. 12e.

Fig. 12f.

Fig. 12a.

A sagittal anatomic section through a right TMJ (Joint 3-Flinders Medical Centre). The articular surface of the condyle is thickened (C). The disc (D) has a linear shape and is displaced anteromedially. The disc is perforated at the junction with the retrodiscal tissues (white arrow).

Fig. 12b.

Photomicrograph of a sagittal histologic section of the same right TMJ (Joint 1-Flinders Medical Centre) as seen in Figure 12a. The retrodiscal tissues have assumed a fibrous pseudo-disc like appearance. The disc contains densely collagenous fibrous connective tissue. Resorption of the bony end plate and highly cellular fibrocartilage is present in the head of the condyle. The perforation is seen as a deep cleft on the superior surface of the retrodiscal tissues (white arrow). (Trichrome stain, Orig Mag X 8).

Fig. 12g.

A coronal T1 weighted spin echo MR image through the centre of the condyle of Joint 3. Remodelling in the head of the condyle (C) images as medium to low signal in the surface layer. The displaced disc is indicated by the elongated and distorted medial discal ligament (white arrow). The perforation laterally and centrally cannot be seen

Fig. 12h.

A coronal T1 weighted gradient echo MR image through the centre of the condyle of Joint 3. Remodelling is indicated by the heterogeneous low signal in the head of the condyle (C). The perforation laterally and centrally cannot be seen. The displaced disc is indicated by the distorted medial discal ligament (white arrow).

Fig. 12i.

A coronal T2 weighted spin echo MR image through the centre of the condyle of Joint 3. The remodelling in the head of the condyle (C) images as patchy low signal in the head of the condyle. The perforation laterally and centrally images as high signal in the reduced joint space (arrow). The disc images as a herniated low signal medially (white arrow).

Fig. 12j.

A coronal T2 weighted turbo spin echo MR image through the centre of the condyle of Joint 3. The remodelling is well imaged as heterogeneous low signal on the superior aspect of the condyle (C). The perforation laterally and centrally images as a high signal in the reduced joint space (arrow). The disc displacement images as a herniated medial sac of low signal (white arrow).
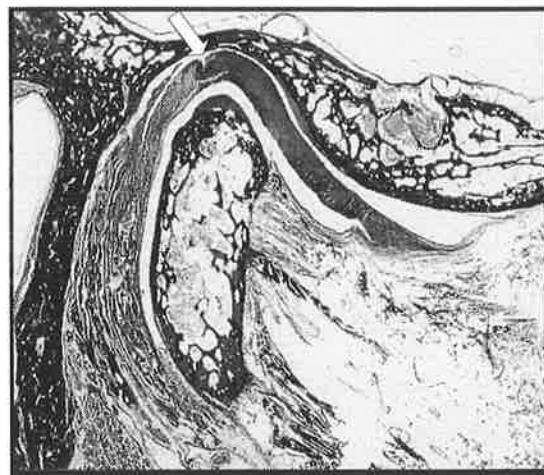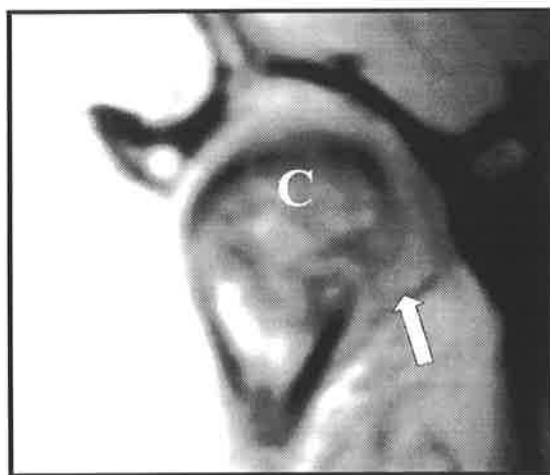
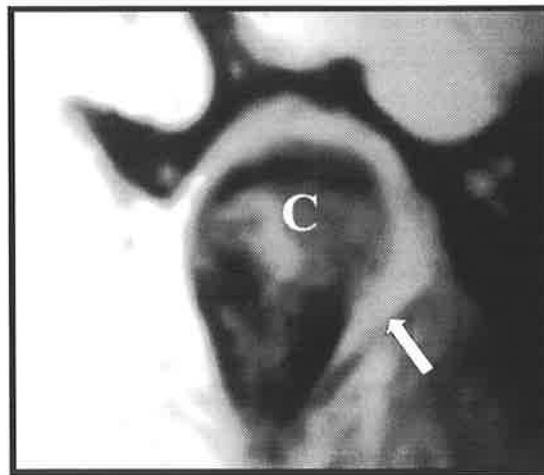**Fig. 12a.**

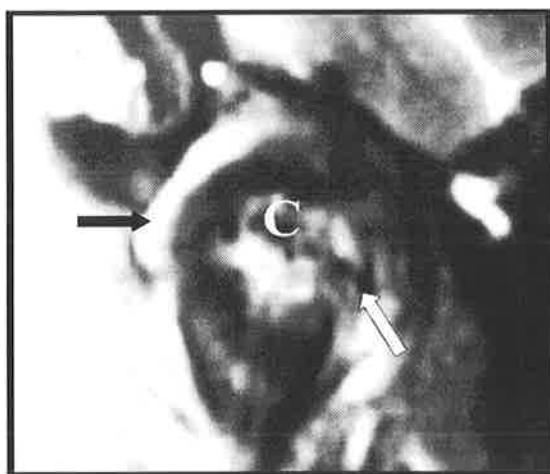**Fig. 12b.**

Fig. 12g.

Fig. 12h.

Fig. 12i.

Fig. 12j.

changes in the head of condyle were under-represented. The outline of the fossa and articular eminence were clearly imaged and appeared normal.

(iv) T1 weighted gradient echo sequence

The position and configuration of the discal-retrodiscal tissues could be interpreted in central coronal images by the normal joint space. However little information about the nature of the tissues could be obtained as these tissues imaged with uniform medium to high signal intensity (Fig. 13d). The outline of the fossa could be easily interpreted as intense low signal. Remodelling and degenerative changes in the head of the condyle were indicated by the heterogeneous low signal and flattening of the surface of the condyle.

Sagittal T1GE images of the same joint also provided little information about the disc position or configuration and it was not possible to identify the discal-retrodiscal junction (Fig. 13h). However the normal joint space and relative position of the condyle-fossa complex would indicate that the disc would be in place. The outline of the fossa and articular eminence was well imaged by low signal. The condyle appeared normal with the remodelling and degenerative changes under-represented.

(v) T2 weighted spin echo sequence

The position and status of the discal-retrodiscal tissues was difficult to interpret as they imaged with a heterogeneous medium signal intensity (Fig. 13e). The fossa outline could not be accurately identified. The remodelling and degenerative changes in the head of the condyle were well imaged as an irregular to low signal surface layer.

Sagittal T2SE images of the same joint accurately imaged the disc configuration and position (Fig. 13i). The junction with the retrodiscal tissues at the one o'clock position could be easily interpreted. Difficulties occured in discriminating the outline of the fossa from the disc which both imaged with low signal intensity. The shape of the condyle could be easily interpreted however the image was not sensitive to the remodelling and degenerative changes.

(vi) T2 weighted turbo spin echo sequence

Coronal images provided imaged the outline of the fossa and anterior articular eminence as low signal (Fig. 13f). It was possible to delineate the medium to low signal discal-retrodiscal tissues from the low signal fossa and condyle. The imaging of the uniform joint space and low signal capsule insertions indicated the disc was in place. Remodelling and degenerative changes in the surface of the head of condyle imaged as heterogeneous low signal.

Sagittal T2TSE images of the same joint provided additional diagnostic information (Fig. 13j). The junction of the low signal discal tissues with the medium to high signal retrodiscal tissues at the one o'clock position could be easily identified. The fossa and articular eminence imaged with lower signal than the discal tissues allowing identification of the two joint components. The remodelling and degeneration of the head of condyle was difficult to diagnose from the sagittal images.

Conclusion

Interpretation of the sagittal and coronal T2TSE images provided the most accurate three dimensional picture of this joint when the images were compared to anatomic slices and

histologic sections. Coronal images were valuable in imaging remodelling and degenerative changes in the head of condyle which were not imaged by sagittal MRI's. Sagittal T2SE and T2TSE images allowed identification of the disc configuration and junction with the retrodiscal tissues which was difficult to identify in coronal images.

Fig. 13a.

A coronal anatomic section through a left TMJ (Joint 2-Flinders Medical Centre). The bulk of the disc (D) can be seen over the head of the condyle (C). The elongated lateral capsule can be seen over the lateral pole of the condyle (arrow). The surface contour of the condyle appears irregular, but smooth.

Fig. 13b.

Photomicrograph of a coronal histologic section of the same left TMJ (Joint 2-Flinders Medical Centre) as seen in Figure 13a. Histologic sections of this joint showed a normal fibrous disc (D). However remodelling in the head of condyle was evident (C). Fibrillation and clefting of the surface layer of the condyle can be seen (arrow). Proliferation of cartilage and resorption of the subchondral bony end plate was evident. (Trichrome stain, Orig Mag X 7.5).

Fig. 13c.

A coronal T1 weighted spin echo MR image of the same coronal section of Joint 2 as seen in Figure 13a. Remodelling in the condyle (C) is indicated by the irregular low signal surface outline (arrow). The disc space appears uniform and the insertions of the lows signal discal ligament medially appears normal (white arrow). The fossa outline is ill defined.

Fig. 13d.

A coronal T1 weighted gradient echo MR image of the same coronal section of Joint 2 as seen in Figure 13a. The low signal outline of the fossa and remodelled condyle can be seen (white arrow). The joint space images with high to medium signal.

Fig. 13e.

A coronal T2 weighted spin echo MR image of the same coronal section of Joint 2 as seen in Figure 13a. The condyle images with heterogeneous low signal indicating remodelling is occurring (white arrow). The fossa is not well imaged. The medial discal ligament images as low signal (arrow). The disc images as low signal on the superior surface of the condyle (D).

Fig. 13f.

A coronal T2 weighted spin echo MR image of the same coronal section of Joint 2 as seen in Figure 13a. The disc images as low signal on the head of condyle (D). Remodelling in the head of condyle is indicated by the irregular contour (white arrow). The fossa outline is poor.
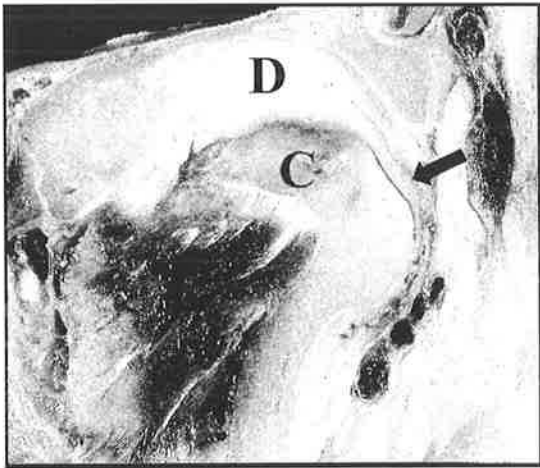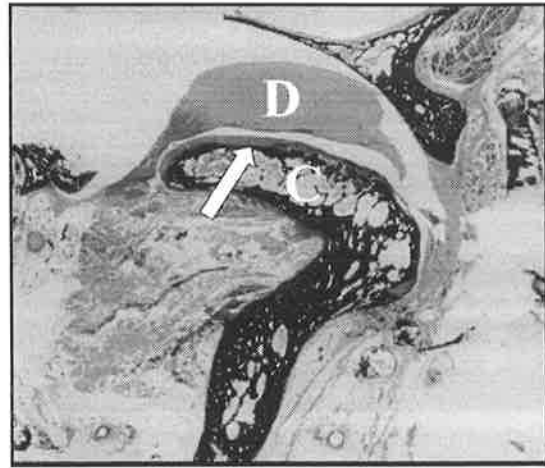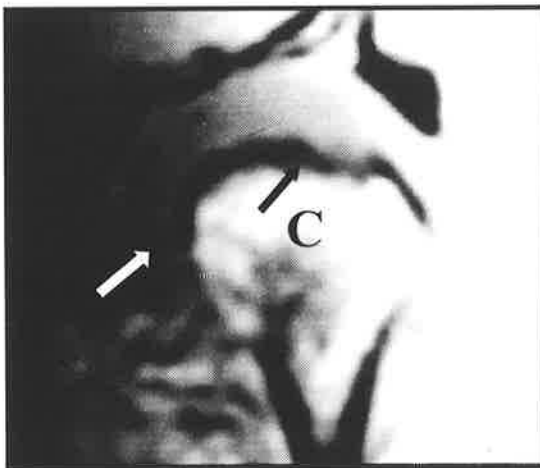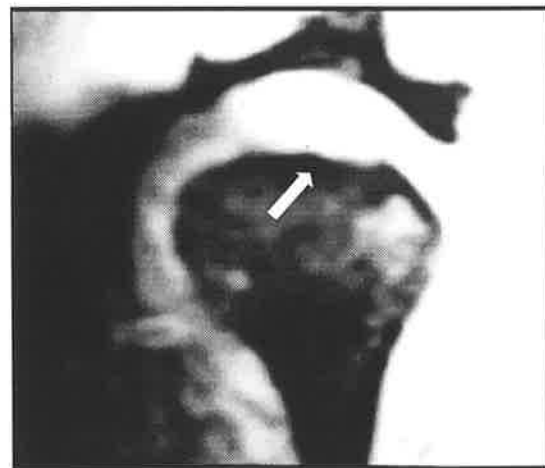
Fig. 13a.
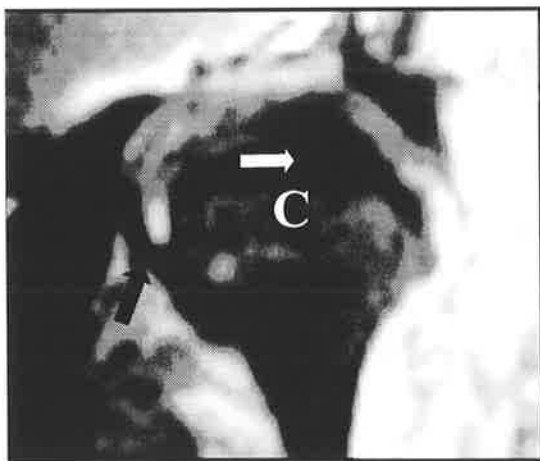

Fig. 13b.

Fig. 13c.

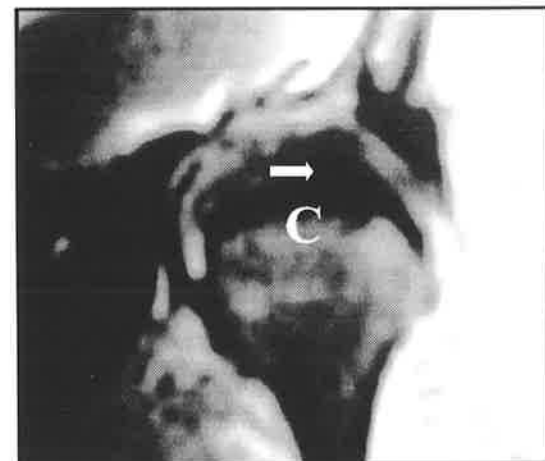

Fig. 13d.

Fig. 13e.

Fig. 13f.

Fig. 13a.

A coronal anatomic section through a left TMJ (Joint 2-Flinders Medical Centre). The bulk of the disc (D) can be seen over the head of the condyle (C). The elongated lateral capsule can be seen over the lateral pole of the condyle (arrow). The surface contour of the condyle appears irregular, but smooth.

Fig. 13b.

Photomicrograph of a coronal histologic section of the same left TMJ (Joint 2-Flinders Medical Centre) as seen in Figure 13a. Histologic sections of this joint showed a normal fibrous disc (D). However remodelling in the head of condyle was evident (C). Fibrillation and clefting of the surface layer of the condyle can be seen (arrow). Proliferation of cartilage and resorption of the subchondral bony end plate was evident. (Trichrome stain, Orig Mag X 7.5).

Fig. 13g.

A sagittal T1 weighted spin echo MR image through the centre of the condyle of Joint 2. The disc images as a low signal bow tie and the junction with the high signal retrodiscal tissues can be seen (white arrow). The low signal outline of the condyle (C) and fossa (F) is well imaged, however remodelling in the condyle is poorly imaged.

Fig. 13h.

A sagittal T1 weighted gradient echo MR image through the centre of the condyle of Joint 2. The condyle (C) and fossa (F) outline are well defined, however degenerative changes are under represented. The disc images as medium signal, but is poorly defined.

Fig. 13i.

A sagittal T2 weighted spin echo MR image through the centre of the condyle of Joint 2. The bow tie shape of the disc imaged as low signal and the junction with the high signal retrodiscal tissues can be seen (white arrow). Remodelling in the condyle (C) is indicated by the patchy low signal on the head of condyle.

Fig. 13j.

A sagittal T2 weighted turbo spin echo MR image through the centre of the condyle of Joint 2. The junction of the high signal retrodiscal tissues with the low signal bow tie shaped discal tissues can be seen (white arrow). The condyle and fossa are outlined as low signal.
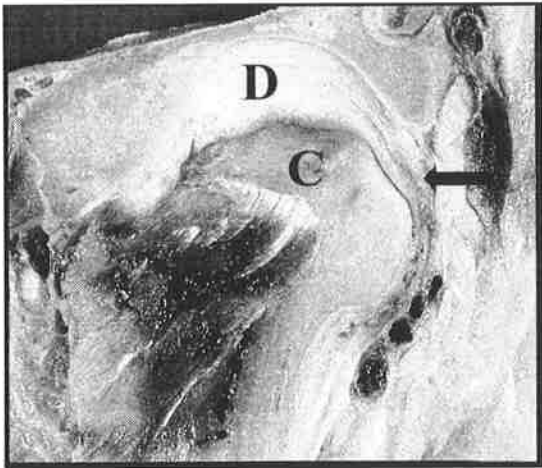
Fig. 13a.
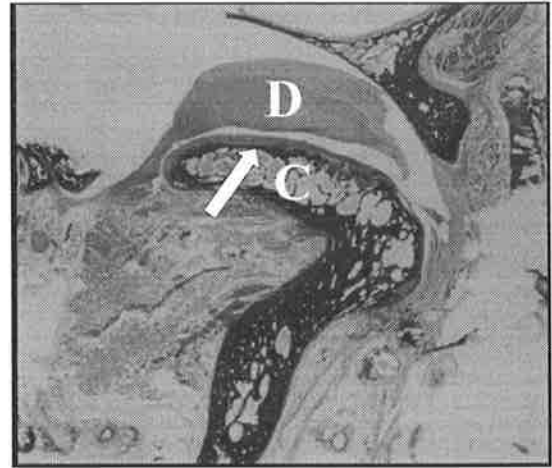
Fig. 13b.
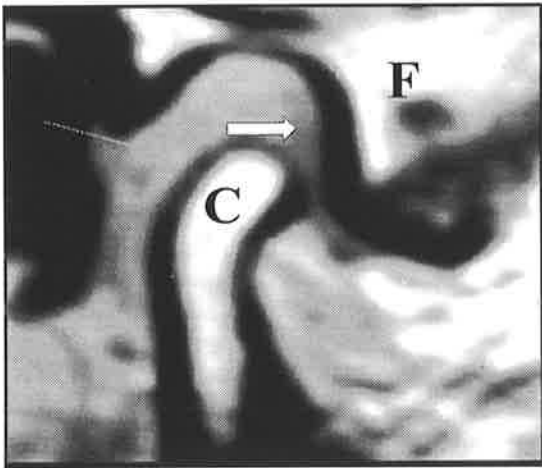
Fig. 13g.
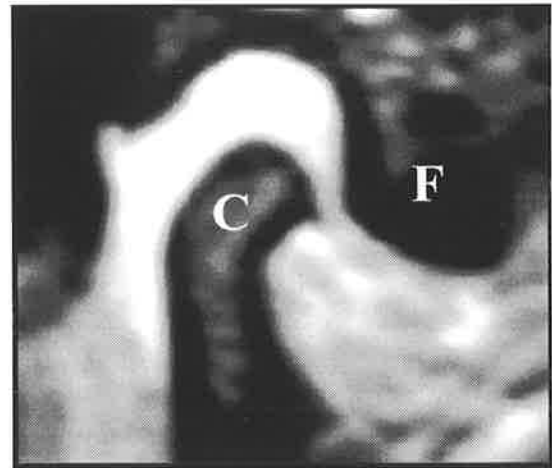
Fig. 13h.
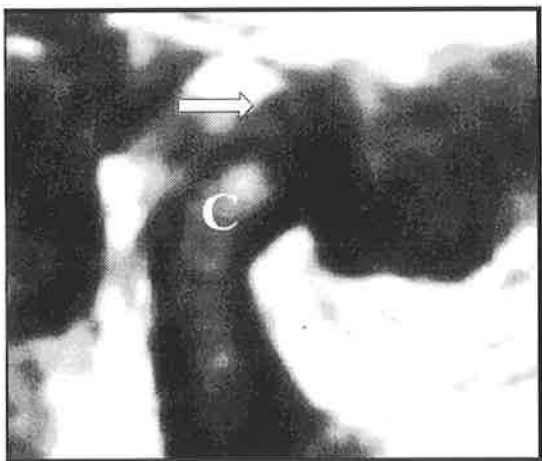
Fig. 13i.
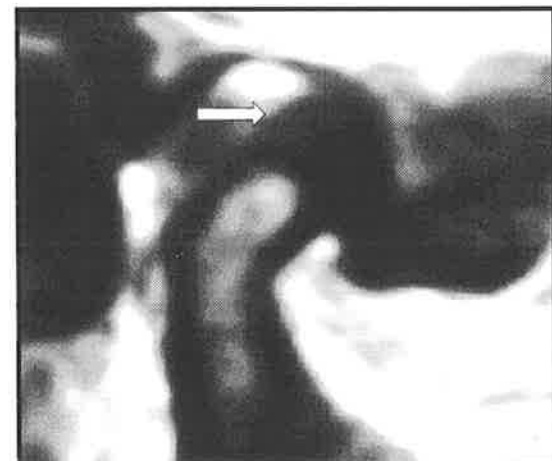
Fig. 13j.

a less intense localised area of low signal. The reduction of joint space and thinning of the disc-capsule complex laterally could not be identified.

Sagittal T1SE images of the same joint failed to clearly image either the configuration or position of the disc relative to the articulating surfaces (Fig. 14g). Remodelling was indicated by the irregular surface contour of the head of the condyle and the increased signal which represented the increased cartilage tissue present.

(iv) T1 weighted gradient echo sequence

The anteromedially displaced disc was imaged as a localised hypointense area of signal medially and the elongated medial discal ligament (Fig. 14d). Thinning of the joint space and elongation of the disc-capsule complex laterally could not be identified. The irregular surface contour of the remodelled head of condyle was well depicted. The remodelling and destruction of the head of condyle was indicated by the increased low signal area on the head of the condyle.

Sagittal T1GE images of the same joint showed the extensive remodelling and degenerative changes in the head of the condyle from lateral to medial (Fig. 14h). It was not possible to identify either the position or configuration of the disc or its junction with the retrodiscal tissues posteriorly. In medial sections it was difficult to distinguish the low signal of the antero-medially displaced disc from the low signal of the central tendon of the lateral pterygoid muscle.

(v) T2 weighted spin echo sequence

The surface contour of the remodelled and degenerative head of condyle was well imaged (Fig. 14e). The surface contour of the fossa was also well imaged and it was possible to identify the thinned joint space laterally. The insertion of the medial and lateral capsules into the condyle could be seen. The displaced disc could be seen as the bulk of the low signal discal tissues was positioned medially with the remainder thinned and elongated over the superior head of condyle.

Sagittal T2SE images of the same joint were difficult to interpret (Fig. 14i). The surface contour of the remodelled head of condyle was poorly imaged. The disc position, configuration and junction with the posterior retrodiscal tissues was not clear. A localised area of high signal on the superior aspect of the condyle may be represent a perforation.

(vi) T2 weighted turbo spin echo sequence

Coronal T2TSE images of this joint provided an accurate outline of the fossa and remodelled head of condyle (Fig. 14e). It was possible to identify the reduced joint space laterally. The disc could be seen thinned over the lateral pole and displaced over the medial aspect and the medial and lateral capsular insertions could be seen.

Sagittal T2TSE images of the same joint were difficult to interpret (Fig. 14j). The surface contour of the remodelled head of condyle imaged poorly. The surface of the fossa and articular eminence imaged as low signal and could be distinguished from the discal tissues. The bulk of disc medially and the junction with the higher signal retrodiscal tissues could be seen.

Conclusion

The T1GE images provided the most information in regard to bone contour and remodelling in the head of condyle, but failed to provide any information in relation to disc position and configuration. The T2TSE images although limited in providing an accurate 3D image of the remodelling of the condyle did provide an accurate representation of disc position and configuration.

Fig. 14a.

A coronal anatomic section through a left TMJ (Joint 1-Flinders Medical Centre). This joint demonstrates a anteromedially displaced disc (D) and elongation of the lateral discal ligament (arrow). The head of the condyle (C) has remodelled.

Fig. 14b.

Photomicrograph of a coronal histologic section of the same left TMJ (Joint 1-Flinders Medical Centre) as seen in Figure 14a. Blood vessels can be seen distributed through the collagenous disc (arrow). The synovial lined capsule (C) can be seen attaching the disc to the condyle and fossa. Resorption and cartilage proliferation in the condyle is evident (open arrow). (Trichrome stain, Orig Mag X 7.5).

Fig. 14c.

A coronal T1 weighted spin echo MR image of the same coronal section of Joint 1 as seen in Figure 14a. The disc images as a herniating low signal sac medially with the elongated and distended low signal medial discal ligament evident (white arrow). The irregular low signal outline of the remodelled condyle (C) can be seen.

Fig. 14d.

A coronal T1 weighted gradient echo MR image of the same coronal section of Joint 1 as seen in Figure 13a. The disc and discal ligament image as low signal medially (white arrow). The condyle and fossa outline can be seen, however the thinning of the joint space laterally is not evident.

Fig. 14e.

A coronal T2 weighted spin echo MR image of the same coronal section of Joint 1 as seen in Figure 14a.The irregular contour of the remodelled condyle (C) can be seen. The fossa shape is also clear as is the thinned joint space laterally. The disc and discal ligament image as low signal over the medial pole (white arrow).

Fig. 14f.

A coronal T2 weighted spin echo MR image of the same coronal section of Joint 1 as seen in Figure 14a. The fossa (F) and remodelled condyle (C) are well imaged. The low signal disc can be seen thinned over the lateral pole and displaced over the medial pole of the condyle (white arrow).

Fig. 14a.
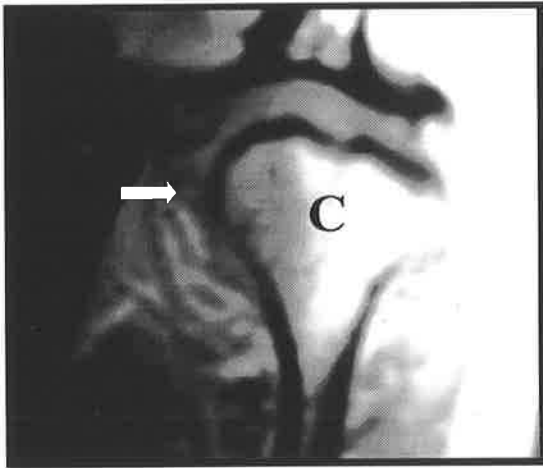
Fig. 14b.

Fig. 14c.
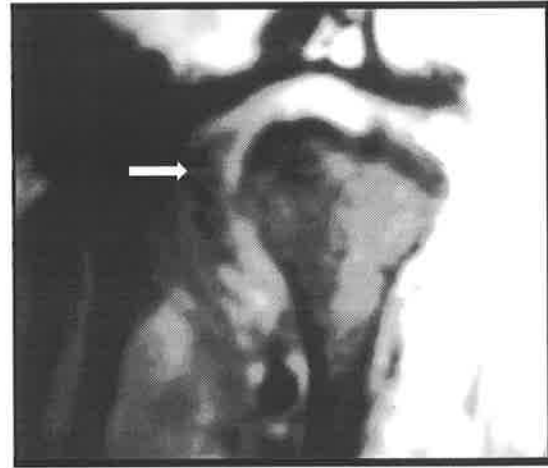
Fig. 14d.
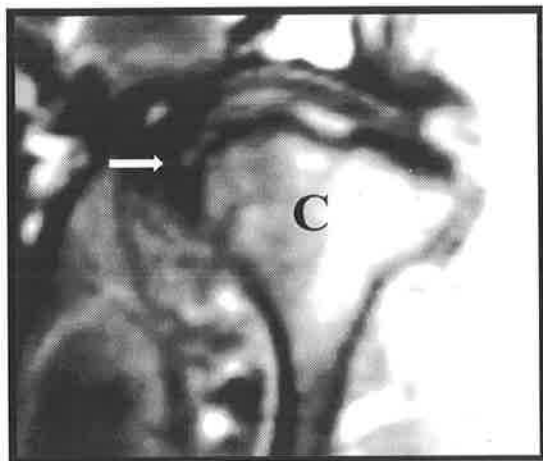
Fig. 14e.

Fig. 14f.

Fig. 14a.

A coronal anatomic section through a left TMJ (Joint 1-Flinders Medical Centre). This joint demonstrates a anteromedially displaced disc (D) and elongation of the lateral discal ligament (arrow). The head of the condyle (C) has remodelled.

Fig. 14b.

Photomicrograph of a coronal histologic section of the same left TMJ (Joint 1-Flinders Medical Centre) as seen in Figure 14a. Blood vessels can be seen distributed through the collagenous disc (arrow). The synovial lined capsule (C) can be seen attaching the disc to the condyle and fossa. Resorption and cartilage proliferation in the condyle is evident (open arrow). (Trichrome stain, Orig Mag X 7.5).

Fig. 14g.

A sagittal T1 weighted spin echo MR image through the centre of the condyle of Joint 1. The remodelled head of condyle (C) imaged as medium signal representing the increased cartilage layer and resorption of the bony end plate. The disc position and junction with the retrodiscal tissues could not be seen.

Fig. 14h.

A sagittal T1 weighted gradient echo MR image through the centre of the condyle of Joint 1. Remodelling in the head of condyle (C) can be seen as patchy low signal of the surface layer (white arrow). The disc position and configuration can not be seen.

Fig. 14i.

A sagittal T2 weighted spin echo MR image through the centre of the condyle of Joint 1. Remodelling in the head of condyle (C) is indicated by the irregular low signal outline of the surface. The disc images as low signal anteriorly. However it is difficult to interpret (white arrow).

Fig. 14j.

A sagittal T2 weighted turbo spin echo MR image through the centre of the condyle of Joint 1. The remodelling of the condyle (C) images as patchy low signal on the superior aspect. The disc images as a bow-tie like area of low signal (white arrow).
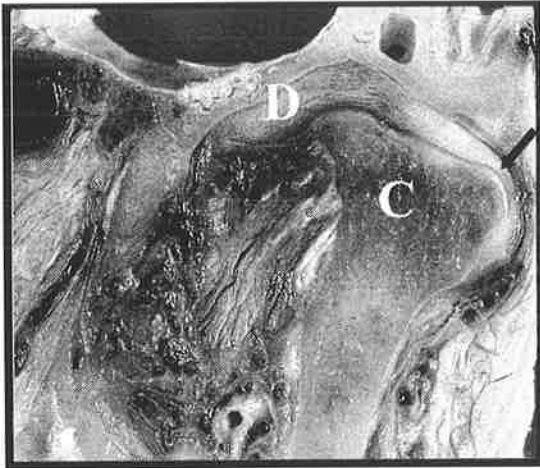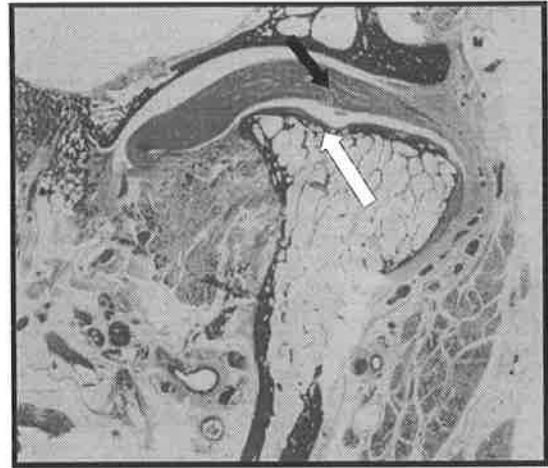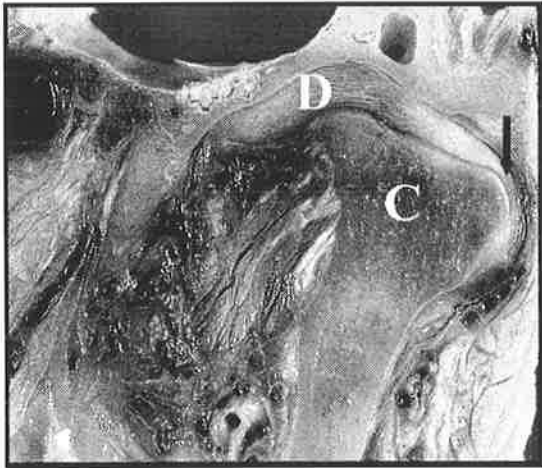
Fig. 14a.
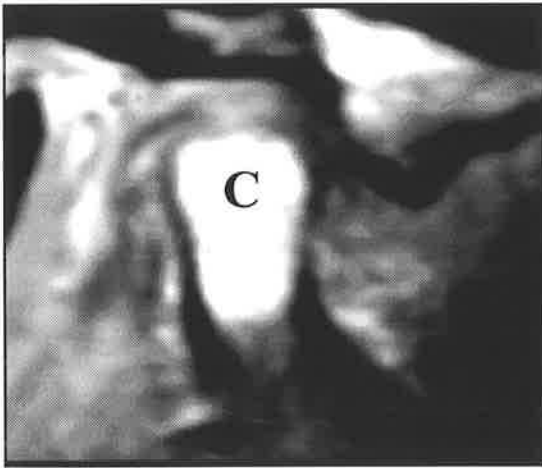
Fig. 14b.

Fig. 14g.
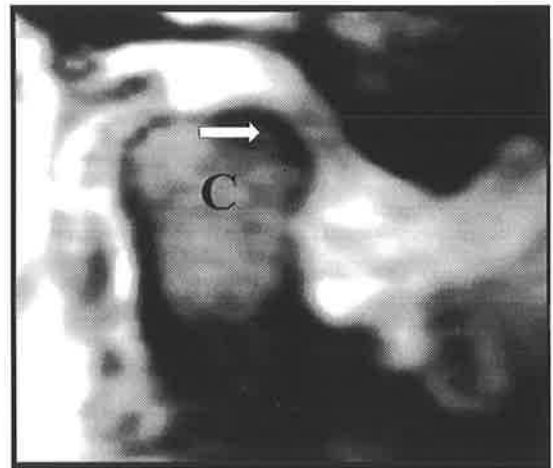
Fig. 14h.
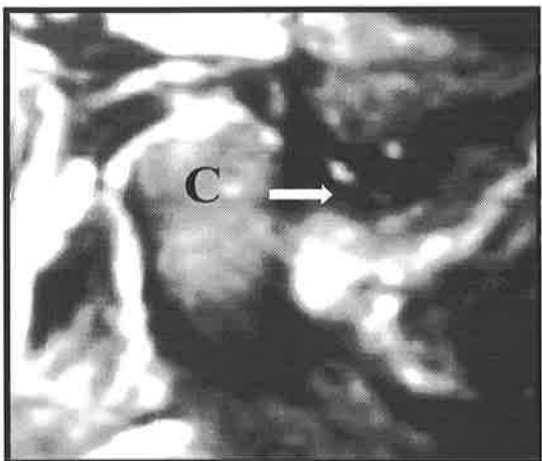
Fig. 14i.
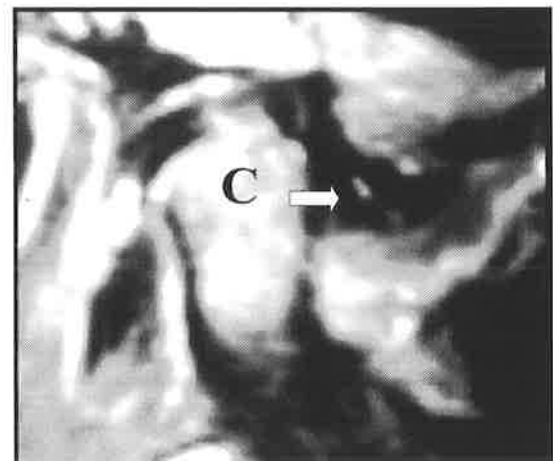
Fig. 14j.

4.4.2.3. Joint demonstrating remodelling, lateral discal perforation and antero-lateral disc displacement (Joint 3)

(i) Anatomic slices

Anterior coronal sections indicated the bulk of the disc positioned anteriorly indicating a disc displacement had occured. Posterior anatomic sections of this joint demonstrated a lateral discal perforation with the condyle and temporal surfaces articulating against each other (Fig. 15a). Flattening and erosion of the superior head of condyle indicated that remodelling had occured. A remnant of discal-retrodiscal tissue remained over the head of the condyle.

(ii) Histologic sections

Anterior histologic sections of this joint demonstrated a diverse range of pathology with articular surface degeneration and progressive remodelling occurring simultaneously (Fig. 15b). Centrally the surface layer of the superior head of the condyle consisted of dense collagen fibres organised in a swirling pattern in areas, whereas deeper layers consisted of high turnover, predominantly cellular fibrocartilage tissue. Laterally the disc was thinned and perforated and the condyle and temporal surface were articulating against each other. The fibrocartilagenous surface layer in this region consisted predominantly of collagen fibres and there were deep vertical clefts and splitting evident in this layer. Medially the condylar surface layer of fibrocartilage tissue was slightly thickened. Across the whole surface of the condyle, denudation of the cortical bone was evident with osteoclastic resorption and replacement by fibrocartilagenous tissue. The temporal surface of the fossa did not demonstrate changes in either the fibrous outer layer or in the cartilage zone. The sections show a remnant of fibrous discal tissue on the lateral-inferior surface of the condyle and vascular, fibroelastic retrodiscal tissue on the superior aspect of the condyle.

(iii) T1 Weighted Spin Echo Sequence

A mid condylar coronal image showed that degenerative changes were occurring, evident as a heterogeneous signal in the condyle (Fig. 15c). This was particularly prominent laterally where there was a loss of the low signal from the cortical bone and an increased signal from the repair tissue. The perforation laterally imaged as a loss of joint space and a relative blending of the low signal from the condyle and temporal surface. The retrodiscal tissues imaged as an area of intermediate signal over the head of the condyle. There was no indication of the anteromedial disc displacement.

Sequential sagittal images indicated by the increased signal intensity on the head of the condyle that remodelling or degeneration was occurring (Fig. 15g). The lateral discal perforation failed to image. The antero-lateral disc displacement imaged as a linear area of low signal anterior to the head of the condyle but it was ill defined as the junction with the retrodiscal tissues could not be identified.

(iv) T1 Weighted Gradient Echo Sequence

The mid-condylar coronal image indicated that pathologic changes were occurring in the head of the condyle evidenced by the heterogeneous signal of the cortical bone (Fig. 15d). The lateral perforation was under-represented and the only indication was the reduced joint space laterally. It was difficult to diagnose the insertions of the discal ligaments or disc position and shape.

Sagittal images suggested that remodelling of the articulating surface of the condyle had occured (Fig. 15h). An antero-lateral disc displacement was suggested by the localised area of low signal anteriorly to the head of the condyle in lateral sections. Central and medial

sections of the same joint did not confirm the displacement as the joint space maintained a normal bow-tie like shape.

(v) T2 Weighted Spin Echo Sequence

The coronal images showed the bulk of the disc displaced anteriorly and laterally over the head of the condyle as a defined area of low signal (Fig. 15e). The degenerative and remodelling changes in the condyle imaged as heterogeneous, low signal. The perforation laterally could be identified by the high signal from the fluid in the joint space separating the low signal of the cortical bone of the condyle and temporal surfaces articulating against each other.

Sagittal images showed the degenerative and remodelling changes in the head of the condyle as heterogeneous medium to low signal (Fig.15i). Lateral sagittal images showed the bulk of the disc displaced anteriorly to the lateral pole of the condyle. The lateral perforation could be identified by the homogeneous localised area of high signal filling the joint space laterally. Central and medial images indicated the discal-retrodiscal tissues were no longer perforated. The disc imaged as a thin, linear area of low signal and its junction with the intermediate signal of the retrodiscal tissues could be identified.

(vi) T2 Weighted Turbo Spin Echo

The osteocartilagenous changes in the head of the condyle were indicated by the irregular surface contour (Fig. 15f). The lateral perforation imaged as high signal fluid in the joint space and the articulation of the low signal condyle and temporal surfaces. The laterally displaced disc imaged as a lateral area of low signal in anterior coronal images.

The antero-lateral disc displacement imaged as a localised area of low signal in lateral sagittal sections (Fig. 15j). The perforated disc imaged as high signal from the fluid in the joint space laterally. Recapture of the discal-retrodiscal complex was indicated by the intermediate signal intensity in central and medial sections. Articular changes were indicated by the irregularity in signal intensity on the superior head of the condyle.

Conclusion

Interpretation of the sagittal and coronal T2TSE images provided the most accurate three dimensional picture of this joint when the images were compared to anatomic slices and histologic sections. Coronal images were valuable in imaging remodelling and degenerative changes in the head of condyle which were not imaged by sagittal MRI's. It was possible to identify from the T2SE and T2TSE MRI's the discal perforation. Sagittal T2SE and T2TSE images allowed identification of the disc displacement and perforation as well as remodelling in the articular surfaces.

Fig. 15a.

A coronal anatomic section through a left TMJ (Joint 3-Flinders Medical Centre). The lateral disc is perforated and the condyle (C) and fossa (F) are articulating against each other. A remnant of either discal or retrodiscal tissues remains superiorly and medially (arrow).

Fig. 15b.

Photomicrograph of a coronal histologic section of the same left TMJ (Joint 3-Flinders Medical Centre) as seen in Figure 15a. Extensive remodelling and destruction of the condyle is occurring. The articular surface of the condyle (C) consists of highly cellular fibrocartilage tissue and resorption of the bony end plate is occurring (arrow). The tissue superior to the head of condyle is vascular, fibroelastic retrodiscal tissue (R), while inferiorly, collagenous discal tissue is present (D). (Trichrome stain, Orig Mag X 8)

Fig. 15c.

A coronal T1 weighted spin echo MR image of the same coronal section of Joint 3 as seen in Figure 15a. The increased low signal of the surface of the condyle (C) indicates the remodelling occurring (white arrow). The perforation laterally is indicated by the loss of joint space laterally and blending of the articular surfaces (arrow). The intermediate signal superiorly is likely to be retrodiscal tissues (R).

Fig. 15d.

A coronal T1 weighted gradient echo MR image of the same coronal section of Joint 3 as seen in Figure 15a. The intense and increased low signal of the surface of the head of the condyle indicates remodelling is occurring (white arrow). The perforation laterally is indicated by the reduced joint space laterally (arrow).

Fig. 15e.

A coronal T2 weighted spin echo MR image of the same coronal section of Joint 3 as seen in Figure 15a. The bulk of the disc can be seen as a area of low signal anteromedially (white arrow). Degenerative changes are indicated by the heterogeneous low signal of the head of condyle (arrow). The perforation laterally is indicated by the high signal in the joint space laterally (P).

Fig. 15f.

A coronal T2 weighted spin echo MR image of the same coronal section of Joint 3 as seen in Figure 15a. Remodelling of the head of condyle is indicated by the patchy low signal of the surface layer. The perforation laterally images as a localised high signal area (P).
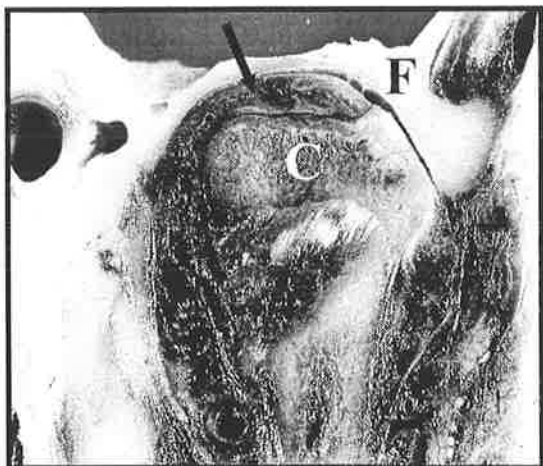
Fig. 15a.
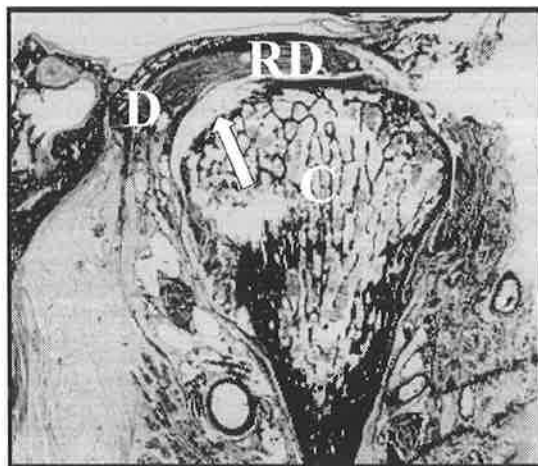
Fig. 15b.
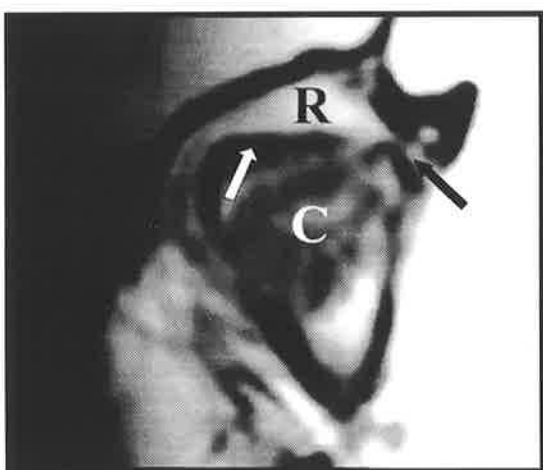
Fig. 15c.
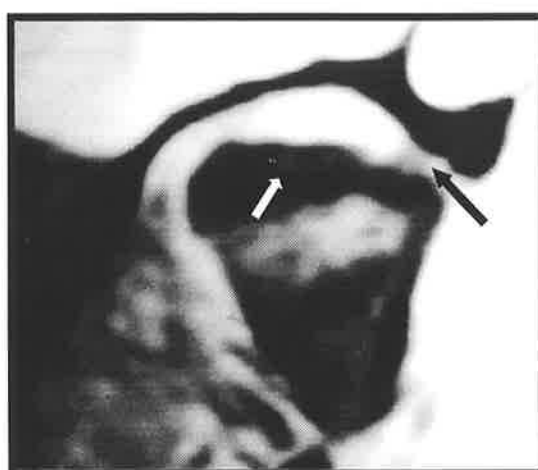
Fig. 15d.
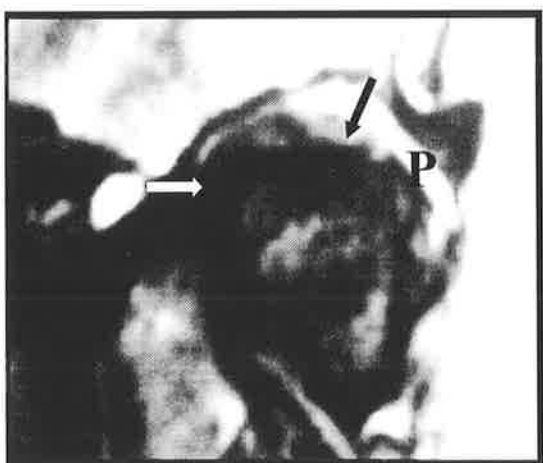
Fig. 15e.

Fig. 15f.

Fig. 15a.

A coronal anatomic section through a left TMJ (Joint 3-Flinders Medical Centre). The lateral disc is perforated and the condyle (C) and fossa (F) are articulating against each other. A remnant of either discal or retrodiscal tissues remains superiorly and medially (white arrow).

Fig. 15b.

Photomicrograph of a coronal histologic section of the same left TMJ (Joint 3-Flinders Medical Centre) as seen in Figure 15a. Extensive remodelling and destruction of the condyle is occurring. The articular surface of the condyle (C) consists of highly cellular fibrocartilage tissue and resorption of the bony end plate is occurring (arrow). The tissue superior to the head of condyle is vascular, fibroelastic retrodiscal tissue (R), while inferiorly, collagenous discal tissue is present (D). (Trichrome stain, Orig Mag x 8)

Fig. 15g.

A sagittal T1 weighted spin echo MR image through the centre of the condyle of Joint 3. The articular surface of the condyle (C) images with medium to low signal indicating remodelling is occurring (white arrow). The perforation laterally cannot be identified. The bulk of the low signal disc can be seen anteriorly (arrow).

Fig. 15h.

A sagittal T1 weighted gradient echo MR image through the centre of the condyle of Joint 3. Remodelling in the head of the condyle is indicated by the heterogeneous low signal of the articular surface (white arrow). The disc and anterior discal-retrodiscal junction fails to image.

Fig. 15i.

A sagittal T2 weighted spin echo MR image through the centre of the condyle of Joint 3. The heterogeneous medium-low signal in the head of condyle (C) indicate remodelling is occurring (white arrow). The perforation images as an intense localised high signal on the superior aspect of the head of condyle (P). The disc images as a linear low signal area positioned anteriorly (D).

Fig. 15j.

A sagittal T2 weighted turbo spin echo MR image through the centre of the condyle of Joint 3. The articular surface of the condyle has a irregular medium-low signal intensity indicating remodelling is occurring (white arrow). The perforation is indicated by the intense high signal superiorly (P). The displacement is indicated by the well defined low signal of the discal tissues anteriorly (D).
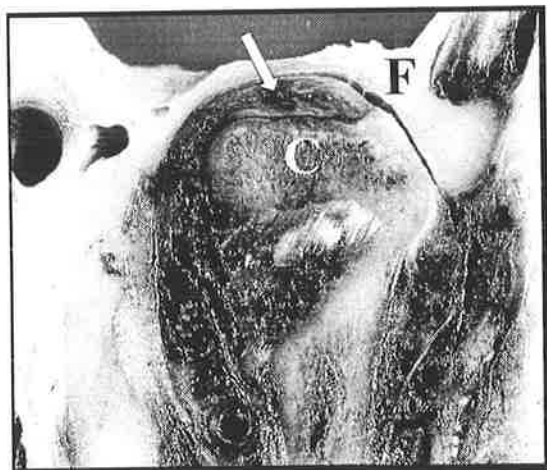
Fig. 15a.
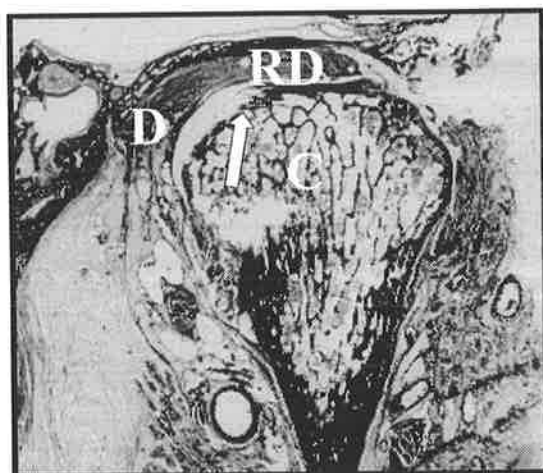
Fig. 15b.
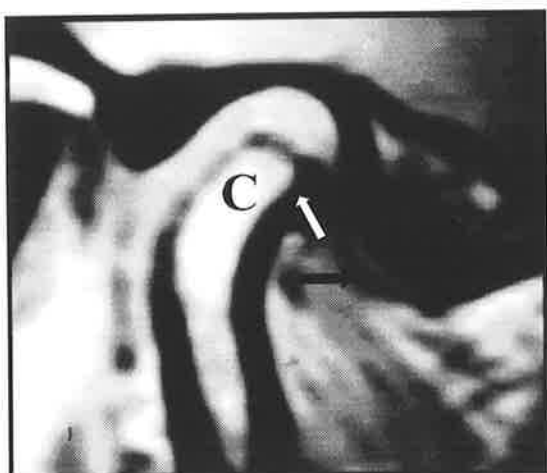
Fig. 15g.
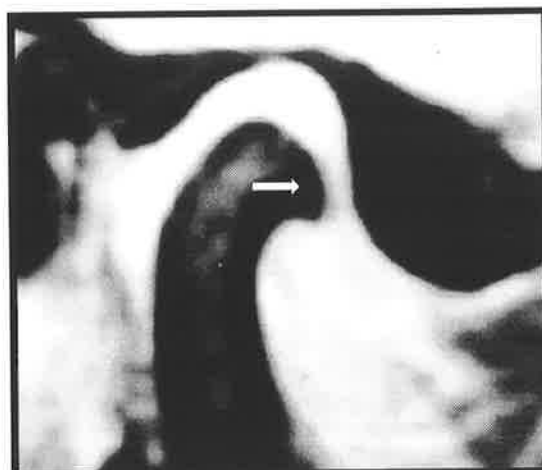
Fig. 15h.
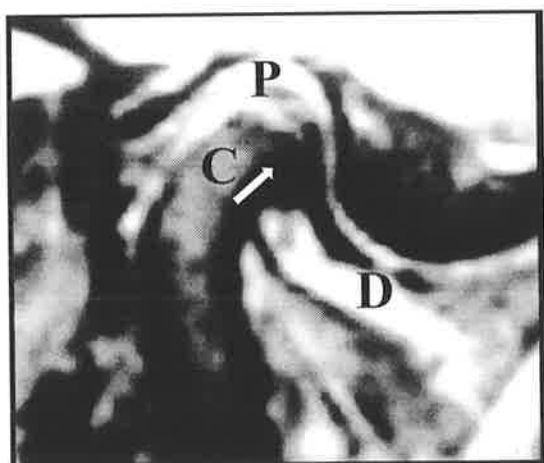
Fig. 15i.
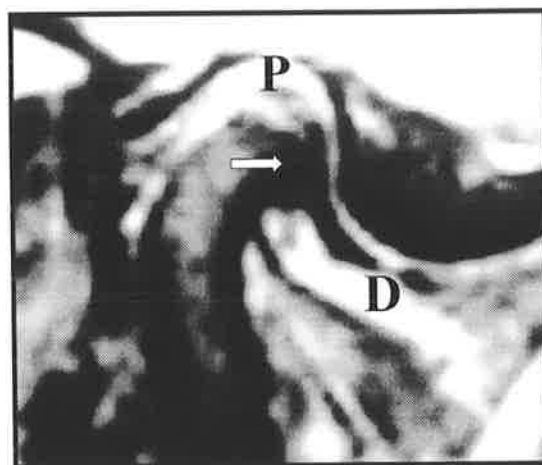
Fig. 15j.

CHAPTER FIVE

DISCUSSION

DISCUSSION

5.1. GENERAL ASPECTS OF ACCURACY OF MRI

5.2. USE OF CADAVER MATERIAL IN MR STUDIES

5.3. ACCURACY OF DIAGNOSING FROM T1 WEIGHTED IMAGES IN JOINTS DEMONSTRATING ANATOMICAL AND HISTOLOGICAL FEATURES OF NORMAL ANATOMY, INTERNAL DERANGEMENT, ARTICULAR SURFACE CHANGES AND DISC PERFORATIONS

(Wakefield Memorial Hospital, Flinders Medical Centre and Vienna MRI's)

5.4. COMPARISON OF DIAGNOSTIC ACCURACY OF SAGITTAL AND CORONAL T1SE, T1GE, T2SE AND T2TSE IMAGES OF THE TMJ

(Flinders Medical Centre MRI's)

DISCUSSION

Magnetic resonance imaging is a non-invasive, non-irradiating diagnostic procedure that has the potential to produce high quality tomographic images in any plane with excellent soft tissue resolution. Contrast between tissues in MR images is not dependent on tissue density but reflects variations in molecular structure and tissue characteristics allowing discrimination between osseous, muscular, fibrous, adipose and vascular tissue.

5.1. GENERAL ASPECTS OF ACCURACY OF MRI

The results of this study suggest a high diagnostic accuracy with MR imaging. The diagnostic accuracy reported is higher than in previous MR studies (Westesson et al 1987, Westesson et al 1987, Katzberg et al 1988, Hansson et al 1989, Schwaighofer et al 1990). This could be due to a number of factors including improved image quality as the result of improvements in hardware and software technology, improvements in imaging technique and greater accumulated experience in the interpretation of images.

MRI with its ability to image soft tissues is superior to plain radiography in the assessment of patients with TMJ dysfunction. Recently, Nilner and Petersson (1995) concluded that no single radiographic finding was found to be related to the treatment outcome in patients with TMJ disorders and that plain radiography had only a minor role in determining the management of these patients. Nethertheless radiographic examinations should be used to exclude other dental and jaw pathology that might be causing referred pain to the TMJ region.

Arthrography of the TMJ became popular in the 1960's as a means of investigating the position and state of the disc within the joint. The advantages of arthrography over MRI are that a true dynamic record of joint movement is obtained and that disc perforations may be revealed. However there are reports that perforations are over diagnosed with arthrography (Ryan et al 1990, Watt-Smith et al 1993). The disadvantages of arthrography are that ionising radiation is involved and it is an invasive procedure that is technically demanding. Consequently, magnetic resonance imaging is now the technique of choice for determining disc position and status.

Computerised tomography was a popular method of imaging the TMJ in the 1980's but has declined in popularity as a result of MR imaging. However, CT is still the method of choice for imaging complex craniofacial trauma involving the TMJ region and in this situation 3-D reconstruction is very valuable. It can also be a useful technique for imaging neoplastic and developmental disease. CT is inferior to MRI for imaging the soft tissues, particularly the disc, as the tendinous attachment of the lateral pterygoid muscle often has a similar appearance (Dixon 1991). MR imaging has been reported to be superior to tomography for assessment of osseous changes (Rohlin et al 1986, Bean et al 1977, Dixon 1991).

In this study bone marrow within the condyle, zygomatic process and articular eminence was easily identified in T1 images due its high signal. The lateral pterygoid muscle and vascular retrodiscal tissues produce an intermediate signal. The densely collagenous disc was characterised by a medium/low signal. Cortical bone had a very low signal image and bony abnormalities such as osteophytes were well highlighted when adjacent to tissues with a medium/high signal.

5.2. USE OF CADAVER MATERIAL IN MR STUDIES

This study used cadaver material which was sliced and sectioned to provide anatomic and histologic comparisons to the MR images. The use of cadaver material is advantageous, since it allows accurate determination of morphologic detail of joints (Westesson et al 1987, Schwaighofer et al 1990). An alternative method would be based on correlation of MRI to surgery. This is less optimal because the inaccessibility of the medial part of the joint make it difficult to evaluate morphologic characteristics accurately during surgery. Furthermore comparative surgical MRI models can only include joints with abnormalities, and the detection of false negative diagnoses would be prevented.

While correlative analysis of cadaver material and MR images has advantages there are disadvantages associated with this particular approach. Obviously one disadvantage of using cadaver material is the lack of knowledge about the clinical symptoms that these persons might have had during life. Another possible disadvantage of the cadaver material is differences in age and sex of the sample pool compared with patient material. Additionally patients presenting with TMJ dysfunction are frequently in the 20 to 40 year age group whereas cadaver material is often from an older age group. Analysis of cadaver material may therefore provide a sample pool showing pathological changes which are not necessarily reflected in the "real life" pool of patients who are normally seen in TMJ practise.

However experience from clinical work with TMJ patients suggests that the morphologic alterations occurring with displacement and deformation of the disc and the osseous changes are similar, if not identical, to those seen in cadavers (Cirbus et al 1987; Donlon

and Moon 1987; Payne and Nakielny 1996). A further disadvantage of the cadaver model is that evidence of inflammatory changes in the form of joint effusion's could not be evaluated. Recent studies have suggested that inflammatory changes are associated with joint pain (Schellhas 1987, Westesson et al 1992).

It has been reported by Tasaki and Westesson (1993) that MR imaging of cadaver material results in a slightly different grey scale than is observed in patients. These authors reported that MRI contrast between the disc and surrounding soft tissues is less prominent than that in patients because of postmortem proteoglycan enzyme effects on the tissues. This decrease in contrast in comparison with the clinical situation is a possible disadvantage of using cadaver material in studies such as the present one.

The MR images in this study were free of motion artefact. Motion artefact may occasionally be a problem in patients, especially for the open mouth images obtained in patients with pain. However, with recent upgrades in imaging technology such as bilateral TMJ head coils and reduced imaging times, patient motion which leads to image artefact is less of a problem than in the past.

5.3. ACCURACY OF DIAGNOSING FROM T1 WEIGHTED IMAGES IN JOINTS DEMONSTRATING ANATOMICAL AND HISTOLOGICAL FEATURES OF NORMAL ANATOMY, INTERNAL DERANGEMENT, ARTICULAR SURFACE CHANGES AND DISC PERFORATIONS

(Wakefield Memorial Hospital, Flinders Medical Centre and Vienna MRI's)

5.3.1. MR image of joints demonstrating normal anatomy

Interpreting the MR image of joints which are structurally normal is difficult as there is often an expectation that each separate component of the TMJ should image in a homogeneous manner. Scapino (1991) has described individual structural entities such as the disc or the retrodiscal tissues as being composed of many cellular and extracellular matrix components with varying orientations and densities. The MR image of such a structural entity may lack homogeneity but accurately reflects the histologic diversity of that joint component.

T1 weighted images of normal joints show that cortical bone with a characteristic low signal provides an accurate outline of the glenoid fossa, articular eminence and mandibular condyle. The signal of the cortical bone is highlighted between the high signal image of the bone marrow and the intermediate signal of the intracapsular soft tissues. In coronal views the lateral pterygoid muscle insertion to the pterygoid fovea can be identified by a discontinuity in the low signal cortical plate of the condyle (Figs 2a, 2b and 2c).

Disc position and shape is well imaged because the densely collagenous fibrous connective tissue of the disc has an intermediate MR signal which provides good contrast between

osseous and soft tissue components of the TMJ. In sagittal MR images the disc has a biconcave appearance. The differences in discal thickness and collagen fibre orientation between the cental part of the disc and the thicker anterior and posterior bands of the disc gave a characteristic bow tie like appearance to the disc in MR images.

In the literature there is controversy regarding the extent to which the disc and its attachments can be accurately imaged. Roberts (1985) stated that the boundary between the intermediate zone and the posterior band can be mistaken for the boundary between the posterior band and the posterior attachment. This would lead to the conclusion that the disc is in a more anterior position than it actually is. Scapino (1991) reported that variations in signal intensity in the posterior band of the disc may occur due to regional variations in the vascularity and content of polyanionic glycosaminoglycans in this area, resulting in difficulties in identification of the junction of the posterior band of the disc and the retrodiscal tissues. In this study, line drawings of sagittal anatomic sections demonstrated that the discal/retrodiscal junction could be accurately identified by sagittal MR images.

In this study in sagittal images, the vascular retrodiscal tissues presented as an area of high signal bounded by the low signal of the condyle and fossa. Anteriorly the contrast between this high signal area and the intermediate signal of the posterior band of the disc assisted in identifying the discal/retrodiscal junction. The dense fibrous posterior capsule of the joint formed the posterior and inferior boundary of the retrodiscal tissues and was frequently seen in sagittal images as a low signal band running from the condyle to the squamotympanic fissure. In coronal views the medial and lateral capsule were well imaged against the low signal of the cortical bone of the fossa and the high signal of the tissues lateral to the joint.

Sagittal images in this study showed that the superior and inferior heads of lateral pterygoid were seen in the medial half of the joint with the higher signal bands of the central tendon and fatty tissue imaged between the two heads (Fig. 1c). However it can be difficult to distinguish discal tissues from the central tendon of lateral pterygoid in sagittal MR images. Studies using arthrography, CT and MRI have often described severely displaced discs as being folded on themselves. There is a potential for the central tendon of displaced discs to be confused with discal tissues giving a false impression of a displaced and folded disc (Dixon 1991, Watt-Smith et al 1993).

5.3.2. MR images of joints demonstrating internal derangement

T1 weighted MR images accurately indicate disc position and the more common anteromedial displacements are characterised in sagittal views by the posterior band imaged forward of the crest of the condyle and by a low signal area medial to the medial pole in the mid condyle coronal view. The medial hernia sac seen in anatomic sections as the disc is displaced medially was not imaged in either sagittal or coronal MR views. This may be better imaged in T2 weighted images which would highlight this fluid filled space. A full MR examination of the TMJ for positional disc abnormalities would include imaging in both the sagittal and coronal planes.

In a direct medial disc displacement, sagittal images are of limited value because the posterior band of the disc may still be over the crest of the condyle. In central coronal MRI's, the combination of an area of low signal medially and the absence of disc space laterally enhanced the representation of a medially displaced disc.

Interpretation of disc position over the lateral pole is difficult as this is the area where the joint space is narrowest and the disc is often thinned and has lost its "bow-tie" appearance. In an early derangement, where the disc is displaced only over the lateral pole, it is difficult for MR to determine whether the disc is thinned and displaced or just thinned.

Tasaki and Westesson (1993) and Westesson et al (1987) reported that errors in diagnosis of lateral disc displacements occured when only lateral sagittal image were used and that additional coronal images were required to visualise this type of displacement. The present study found that lateral disc displacements can be identified from coronal MR views as a band of low signal adjacent to the lateral pole. Sagittal MR images may not be contributory as the expected "bow-tie" is absent as there may be no disc tissue present over the head of the condyle.

5.3.3. MR images of joints showing articular surface changes

Results from this study indicate that subtle changes in the contour of the cortical bone were accurately imaged by central coronal MRI's. This finding is in agreement with those of Schwaighofer (1990) and Tasaki (1993). Frequently sagittal MRI's failed to identify articular surface remodelling. In contrast, the coronal view of the same joint gave a more accurate representation of the changes in contour of the cortical bone of the articular surface from lateral to medial clearly depicting erosion's and flattening of the condyle. This strengthens the recommendation that a central coronal view should be included in the TMJ screening sequence. MR has an accuracy rate in identifying osseous abnormalities, such as those found in degenerative joint disease, comparable with that of CT (Westesson et al 1987), although these alterations may be less clearly visualised by MR (Katzberg et al

1988). Other reports suggest that CT remains superior in delineating osseous abnormalities (Harms et al 1985, Westesson et al 1987).

Frequently severe internal derangement's are not clearly visualised in coronal MRI's in joints with severe degenerative changes involving a significantly thinned disc (Tasaki and Westesson 1993, Schwaighofer et al 1990). The present study showed that difficulties occured in distinguishing the disc from the joint spaces and the surrounding tissues where degenerative changes were occurring as the pathologic tissues imaged with an equal signal intensity. Consequently, a distinct delineation of the thinned disc from surrounding tissues was not possible by MRI.

5.3.4. MR images of joints with perforated discs

An important potential limitation of MR is its inability to reveal TMJ disc perforations, which are shown readily by arthrography (Donlon and Moon 1987, Westesson and Rohlin 1984). Whereas an early study showed that it was possible to diagnose disc perforations by sagittal T1 weighted images (Harms et al 1985), more recent reports suggest that disc or retrodiscal perforations may be missed by either sagittal or coronal MR imaging (Westesson et al 1987, Donlon and Moon 1987). The present study found that it was possible to identify perforations in the disc when the fragments were widely separated. Difficulties in diagnosing perforations occured in joints demonstrating degenerative joint disease when the joint space was "thinned" laterally.

Summary

MR imaging of the TMJ has been shown to have a high diagnostic accuracy and should be considered as the prime imaging modality for soft and hard tissue changes of the TMJ. However MR imaging is dependent on technical factors such as magnetic field strength, gradient coil strength, software and surface coils to achieve a high quality image.

The small number of false diagnoses in this study were consistently related to underestimation of the pathologic conditions (Tables 3 and 4). All of the false diagnoses were false negative's and included an underestimation of disc displacements, disc deformations or osseous changes. The underestimations were usually due to the inability of MR imaging to depict the most lateral or most medial part of the joint. The most lateral and most medial parts of the joint were not depicted with the same high quality images as the central zone.

Although the diagnostic accuracy in this study was high, it may be possible to further improve the MR images. One possibility would be to use MR imaging sections that are thinner than 3mm. In this way volume averaging of oblique structures would be reduced, and the image quality of the most lateral and most medial parts of the joint would be improved. Another way to improve MR imaging would be to use a smaller field of view, resulting in higher spatial resolution.

5.4. COMPARISON OF DIAGNOSTIC ACCURACY OF SAGITTAL AND CORONAL T1SE, T1GE, T2SE AND T2TSE IMAGES OF THE TMJ

(Flinders Medical Centre MRI's)

5.4.1. Normal anatomy

Previous studies report a high success rate in imaging joints with normal anatomy by sagittal and coronal MRI and have prompted the suggestion that MR imaging should be the prime imaging modality for assessment of both soft and hard tissues of the TMJ (Katzberg 1986; Katzberg et al et al 1989; Westesson et al 1987; Schwaighofer et al 1990; Tasaki and Westesson 1993). The current study indicated a high success rate in interpretation of T1 and T2 weighted MR images of joints demonstrating normal anatomy.

In this study a joint was classified as anatomically normal when the articular surfaces were smooth, the discal-retrodiscal junction was at the one o'clock position, the disc was biconcave and there was no fissuring, fraying or perforation of the disc. Interestingly histologic examination of the same joints demonstrated that variations occured. When the anatomically normal joint components were assessed microscopically these changes included thinning of the cortical bony end plate, cartilage hyperplasia and fibrous thickening of the articular surface. Nethertheless and importantly in both joints which showed normal joint anatomic topography the disc consisted of densely collagenous, fibrous connective tissue and the junction with the vascular retrodiscal tissues was evident.

Sagittal and coronal T1 and T2 weighted images of the two normal joints in this study showed variations in sensitivity and accuracy. Sagittal T1 weighted spin echo, T2 weighted

spin echo and T2 weighted turbo spin echo images were highly accurate in imaging the disc shape and position, junction with the retrodiscal tissues and the articular surface changes. Sagittal T2 spin echo and T2 turbo spin echo images provided addition information relating to disc position and shape due to the high signal from joint fluid outlining the disc and the insertion of the anterior joint capsule. Sagittal T1 weighted gradient echo images failed to show the sensitivity in imaging the articular surface changes and the disc failed to image. Findings from this study are in agreement with Jahn and Schellhas (1991) who reported that multiecho long TR/short-long TE evaluation of the TMJ with MRI was found to be the most accurate pulse sequence for multipurpose joint analysis, as this technique satisfactorily defines disc T2 morphology and position in relation to the mandibular condyle and temporal bone, glenoid fossa, as well as demonstrating signal changes in the bone marrow and masticatory muscles.

T1 Weighted spin echo, T2 weighted spin echo and T2 weighted turbo spin echo coronal images in this study could be easily interpreted as showing normal osseous anatomy. The smooth articular surfaces of the fossa and condyle from lateral to medial and the uniform joint space from lateral to medial could be interpreted from all MR images. The T1 weighted spin echo, T2 weighted spin echo and T2 weighted turbo spin echo images provided additional information as the insertions of the medial and lateral joint capsules could be seen strengthening the argument put forward by Tasaki and Westesson (1993) for a coronal image to be included in a MRI sequence of the TMJ.

5.4.2. Internal derangement with disc displacement

The junction of the posterior band of the disc with the retrodiscal tissues is normally at the one o'clock position in relation to the condyle in the mouth closed position (Drace et al 1990). The two main types of positional disc abnormalities are anterior displacement which reduces during mouth opening and fixed anterior displacement which does not reduce. The former occurs in 40 to 80% of symptomatic joints and the latter in 30% (Rao et al 1993; Helms et al 1989). The authors reported that the disc will be normal in position in symptomatic joints in 19 to 60% of cases and an anteriorly displaced disc is found in up to 15% of asymptomatic volunteers. Medial and lateral disc displacements may also occur, most commonly associated in conjunction with anterior displacement, and rarely in isolation (Brooks 1993). The reported accuracy of MR in depicting disc position and reducibility ranges from 88 to 100% (Watt-Smith et al 1994; Tasaki and Westesson 1993; Rao et al 1990).

The normal disc is biconcave in shape with the posterior body being slightly larger than the anterior body (Rees 1954). In joints with chronic disc displacements the disc may become flattened, thickened or thinned in appearance. Abnormally shaped non reducible, anteriorly displaced discs are associated with a much higher incidence of osteoarthritic changes in the joint (Watt-Smith et al 1993; Helms et al 1989; DeBont 1994).

Results from this study showed that joints demonstrating a disc displacement displayed histological evidence of fibrosis of the anterior retrodiscal tissues and that the disc had lost its band like pattern having adopted a more linear profile in cases. These changes are in agreement with the studies by Scapino (1991) and Wilkinson and Crowley (1994).

Steinhardt (1933) and Blackwood (1968) have reported that folding of the disc occurs in joints with a displacement, however, the disc retains a normal histologic appearance. Scapino (1983) has described the histologic appearance of the disc as being abnormal in joints with a displaced disc, with the forward location of the transverse fibres of the posterior band and the neomorphic addition of transverse fibres that disrupts the normal fibre pattern of the central part of the disc due to remodelling caused by abnormal loading of the disc by the condyle Similar findings have been reported by Besette et al 1985, Katzberg 1986 and Westesson 1987. This current study did not show such changes in the internal fibre arrangement of the disc. In the literature other changes described in discs demonstrating disc displacement include calcification (Scapino 1983; Besette et al 1985; Katzberg 1986; Westesson 1987). These changes have been reported to be imaged by MR and to be diagnostic of a displaced disc (Katzberg 1986; Kaplan and Helms 1989). Histologic evidence of disc calcification was not found in the material examined in the present study. Whether such a feature, when present, images in MRI's when there is a displaced disc thus could not be confirmed.

Results from this study indicated that the most accurate sagittal image of anteromedial disc displacements was the T2 weighted spin echo or T2 weighted turbo spin echo sequence. Displacements could be diagnosed from T2 weighted sagittal images by the forward position of the anterior capsule and the anteriorly positioned junction of the disc with the fibrosed retrodiscal tissues. The coronal T2 weighted images demonstrated the thinning of the joint space laterally, herniation of the medial discal ligament and the low signal of the bulk of the disc displaced medially over the head of condyle. Standard protocols that would use only sagittal MR images would thus not be accurate in the evaluation of disc

displacements. Consequently a full MR examination of the TMJ for positional disc abnormalities would include imaging in both coronal and sagittal planes.

T1 weighted sagittal images of the same joints failed to image the anteromedial disc displacement as the disc position and junction with the retrodiscal tissues posteriorly was poorly imaged. The clearest indication of the displacement was the thinning of the joint space laterally in coronal images.

The results of this study indicate that inaccurate assessment of disc position by T1 and T2 weighted MR images occured primarily in joints with severe degenerative changes of the articular surfaces involving a severely thinned and displaced disc. For these cases, the joint spaces and surrounding tissues also had degenerative changes with an MR signal intensity similar to that of the disc. Consequently, a distinct delineation of the thinned TMJ disc was not possible by MRI. Further in joints with disc displacements and degenerative changes, difficulties occur in differentiating the disc from the joint capsule.

5.4.3. Articular surface changes

Degenerative changes and remodelling of the articular surfaces are frequently seen in cases of non reducible anteriorly displaced discs (Watt-Smith et al 1993; Helms et al 1989). The anatomical signs are condylar flattening, osteophyte beaking on the anterior aspect of the condyle, cortical thickening and erosion's. A cadaver study by Tasaki and Westesson (1993) using long imaging times gave a 93% accuracy in detecting these signs. However, *in vivo* studies with surgical correlation show a significantly poorer detection ranging down to 13% sensitivity (Watt-Smith et al 1993; Raustia et al 1994).

In this study it was found that the susceptibility artefact and the poorer spatial resolution of the coronal and sagittal T1 weighted gradient echo sequence method made it less sensitive in detecting bony changes compared to the T1 weighted spin echo sequence. The most accurate imaging modality was the sagittal and coronal T2 weighted sequences which were highly sensitive to articular surface changes. When the images were compared to the histologic sections of the same joint this accuracy was highlighted. For example in joints examined histologically where thinning of the bony end plate was evident, the T2 weighted images accurately recorded this as a thinned low signal area on the head of the condyle. In addition where joints showed histologically an increased fibrocartilage surface area, T2 images showed this as an increased low signal area.

The combination of the sagittal and coronal images provided a highly accurate and sensitive image of remodelled and degenerative joints which could be easily interpreted. Coronal images were more accurate in depicting erosion's and flattening of the condyles, sagittal images showed osteophytes better.

Schellhas et al (1989) have reported on the incidence of avascular necrosis and osteochondritis dissecans as separate pathologic entities that may affect the condyle. Avascular necrosis has been reported as a large area of cortical and medullary infarction, often resulting in structural weakening which predisposes the joint to collapse and osseous degeneration. Osteochondritis dissecans has been reported to occur as a consequence of transchondral fracture, where the depressed cortical bone fails to heal or reunite to adjacent normal bone. Schellhas et al (1989) demonstrated a high correlation between internal derangement, joint inflammation, disc perforation and avascular necrosis. It was also reported by these authors that avascular necrosis and osteochondritis dissecans was imaged

by T1 and T2 weighted MRI's as a localised area of hypo-intense signal surrounded by a well defined high signal area. Anatomic and histologic evaluations in this present study failed to reveal lesions which could be diagnosed as either of these pathologic entities. The question must be asked as to whether other conditions may present similar low signal areas in the condyle to avoid making false positive diagnosis of these conditions. Bone marrow may contain enlarged marrow spaces that could be described as subcortical cyst like spaces, and these may also present as a low signal subcortical MR image. Caution is suggested in interpreting these normal variations as pathologic entities.

5.4.4. Perforations

Perforations may occur in the disc or at its posterior attachment to the retrodiscal tissues. Tasaki and Westesson (1993) reported that perforations could be detected by MRI and Watt-Smith et al (1993) showed a 78% sensitivity and 98% specificity for the detection of perforations. However other studies show an extremely poor detection rate for disc perforations (Moses et al 1989; Katzberg 1989).

The results of this study confirm that perforation's can be detected by MRI. T2 weighted sagittal images were more sensitive than other sequences as the low signal of the two discal fragments separated by the high signal of the joint fluid could be detected. The results also indicate that perforations frequently occur in joints which demonstrate articular surface changes. Difficulties in interpretation of MR images occured in these joints as the cortical bone and disc both image with a heterogeneous low signal making it difficult to accurately delineate the two tissues. T1 weighted sagittal spin echo and gradient echo images did not image disc perforation well.

Coronal images were frequently difficult to interpret as the perforations were always lateral and the only indication of a perforation was the laterally reduced joint space. The T2 weighted coronal images were more sensitive in imaging the perforations than the T1 weighted images. Overall the results of this study indicate that the combination of the sagittal and coronal images give a three dimensional interpretation of the joint thus aiding the detection of disc perforations.

CHAPTER SIX

CONCLUSIONS

CONCLUSIONS

1. MR imaging of the TMJ has a high diagnostic accuracy and should be considered as the prime imaging modality for soft and hard tissue changes of the TMJ. However MR imaging is dependent on technical factors such as magnetic field strength, gradient coil strength, software and surface coils to achieve a high quality image.

The small number of false diagnoses in this study were consistently related to underestimation of the pathologic conditions. All of the false diagnoses were false negative's and included an underestimation of disc displacements, disc deformations or osseous changes. The underestimations were usually due to the inability of MR imaging to depict the most lateral or most medial part of the joint. The most lateral and most medial parts of the joint were not depicted with the same high quality images as the central zone.

Although the diagnostic accuracy in this study was high, it may be possible to further improve the MR images. One possibility would be to use MR imaging sections that are thinner than 3mm. In this way volume averaging of oblique structures would be reduced, and the image quality of the most lateral and most medial parts of the joint would be improved. Another way to improve MR imaging would be to use a smaller field of view, resulting in higher spatial resolution.

2. The most accurate imaging modality for normal and pathologic joints was the sagittal and coronal T2 weighted sequences which were highly sensitive to articular surface changes, disc displacements and perforations. When the images were compared to the histologic sections of the same joint this accuracy was highlighted.

The results also showed that the use of sagittal MR images alone does not provide sufficient accuracy in the evaluation of disc position and articular surface changes. Consequently a full MR examination of the TMJ for positional disc abnormalities and osseous changes should include imaging in both coronal and sagittal planes.

APPENDICES

APPENDICES

APPENDIX ONE: Decalcification

APPENDIX TWO: Dehydration, Infiltration and Embedding

APPENDIX THREE: Subbing Slides

APPENDIX FOUR: Haematoxylin and Eosin Staining Method

APPENDIX FIVE: Trichrome Staining Method

APPENDIX SIX: Standard Processing Procedure

APPENDIX SEVEN: Printing onto Multigrade 3 Paper

APPENDIX EIGHT: Proforma of analysis of sagittal anatomic slices of joints

from Adelaide (Wakefield St. Hospital and Flinders

Medical Centre and Vienna).

APPENDIX NINE: Proforma of analysis of coronal anatomic slices of joints

from Adelaide (Flinders Medical Centre) and Vienna.

APPENDIX TEN: Proforma of accuracy of diagnosis of disc position, disc

perforation and osseous abnormalities in sagittally sliced

TM joints by sagittal and complementary coronal MR

images.

APPENDIX ELEVEN: Accuracy of diagnosis of disc position, disc perforation

and osseous abnormalities in coronally sliced

temporomandibular joints by coronal and

complementary sagittal magnetic resonance images.

APPENDIX TWELVE: Histologic assessment of joints scanned at Flinders

Medical Centre.

Appendix One

Decalcification

Ingredients

950 mls HCL (technical grade 36% concentration)

100 gms sodium acetate MW 82.04 dissolved within 1 litre of water tap water

100 gms EDTA dissolved within 1 litre of warm tap water

7050 mls of cold tap water

Method

Weigh sodium acetate and dissolve within 1 litre of warm tap water and place in a 10 litre container.

Weigh 100gms EDTA and dissolve within 1 litre of water and add to the 10 litre container.

Add 7050 mls of cold tap water to the container.

Add with care 950 mls of HCL. Always add the acid to the water taking care as acid is both exothermic and explosive when mixed with small quantities of water.

The pH of the 10 litre solution is less than 0.1 depending on the pH of the tap water used to mix the solutions.

Decalcification is monitored using X-Ray end point determination.

The specimens were then washed for up to one day in running tap water both to neutralise the acid and to remove EDTA or other salt precipitation on, or within, the tissue. Washing

was also necessary to neutralise the acid effects within the tissue itself so that staining with basophilic dyes such as haematoxylin were not effected.

Tissue was then transferred to formalin or 70% alcohol for processing or preservation and photographic recording prior to processing.

Appendix 2

Dehydration

All specimens were processed in the following reagents.

Dehydration was achieved under vacuum (25 inches of mercury) at room temperature.

1. 70% ethanol- Overnight to several days depending on the time taken for photographs. Seventy percent ethanol restores the colour to formalin fixed tissues.

2. 80% ethanol- Half a day.

3. 90% ethanol- Half a day.

4. 100% ethanol- Half a day.

5. 100% ethanol- Half a day.

6. 100% ethanol- Overnight.

7. Chloroform- One hour (to reduce the fat content).

8. Histoclear[R] - One day.

9. Histoclear[R]- Overnight.

Infiltration

The blocks were infiltrated under vacuum (25 inches of mercury) at 60 degrees Celsius.

1. Wax- half a day to one day depending on the size of the tissue block. Blue coloured Surgipath infiltrating medium or Paraplast plus were the preferred waxes.

2. Wax- half a day to one day.

3. Wax- half a day to one day. Joint specimens retaining the orange smell of Histoclear required another change of wax.

Embeding

Tissue blocks were embeded in Surgipath (Blue Ribbon[TM]) embedding media in a rubber mould large enough to seat the joint section. Blue Ribbon[TM] is a universal paraffin containing synthetic polymers that is intended for use as both an embedding and infiltrating medium.

Surgipath Embedding Material was used at a working temperature of 58 degrees Celsius. When sectioning the joints a water bath set at 35-40 degrees Celsius was used to collect sections.

Appendix 3

Subbing Slides

1. Rinse precleaned glass slides in distilled water.

2. Allow slides to drain for 2-3 seconds.

3. Dip into subbing solution.

4. After the dipping allow to dry vertically in a dust free environment.

Subbing Solution

1. Dissolve completely in 1 litre of warm distilled water 5 grams of unflavoured gelatin.

2. Add 0.5 grams of chrome alum.

3. Cool and filter through a No. 1 filter paper.

4. Store for 48 hours at 5 degrees Celsius and then discard.

Appendix 4

Haematoxylin and Eosin Staining Method

1. Xylol for 5 minutes.

2. Xylol for 5 minutes.

3. Absolute alcohol for 2 minutes.

4. Absolute alcohol for 2 minutes.

5. Rinse in tap water for 5 minutes.

6. Haematoxylin 5 minutes

7. Rinse in running tap water for 5 minutes.

8. Differentiate in 0.5 to 1.0% hydrochloric acid in 70% alcohol for 30 seconds.

9. Rinse in running tap water for 10 minutes.

10. Eosin 45 seconds.

11. Absolute alcohol for 1 minute.

12. Absolute alcohol for 1 minute.

13. Absolute alcohol and xylol mix for 2 minutes.

14. Xylol for 2 minutes.

15. Xylol for 2 minutes.

16. Mount in xylene.

Results

Nuclei	: Blue to blue black
Karyosomes	: Dark blue
Cartilage	: Pink or light blue
Cement lines of bone	: Blue
Calcium and calcified bone	: Purplish blue
Basophil cytoplasm	: Purplish
Red blood cells, eosinophil granules, zymogen granules	: Bright orange red

Appendix 5

Trichrome Staining Method

1. Bring sections to water.

2. Stain nuclei with Cole's, Harris's or Mayer's Haemalum for 10 minutes.

3. Wash well in tap water, rinse in distilled water.

4. Stain for 5 to 20 minutes in:

Chromotrope 2R	0.6 grams
Fast green FCF	0.3 grams
Phosphotungstic acid	0.6 grams
Glacial acetic acid	1 ml
Distilled water	100 ml

5. Rinse in 0.2 per cent acetic acid.

6. Dehydrate and clear in alcohol and xylene.

7. Mount in xylene.

Results

Connective tissue	: Green
Muscle	: Red
Cytoplasm	: Red
Nuclei	: Grey blue

Appendix 6

Standard Processing Procedure

The film was processed using Ilford Multigrade Paper Developer mixed with distilled water at 1:1 dilution for 7 minutes at 20 degrees Celsius. The film was then washed for 3 minutes and fixed for 10 minutes and then dried.

Appendix 7

Printing onto Multigrade 3 Paper

Printed through a Leitz 35mm enlarger and then printed onto Ilford Multigrade 3 paper. The procedure involved using Multigrade Developer with a processing time of 1 minute, washing for 30 seconds, fixed for 3 minutes using Hypam Rapid Fix and a postfixation wash for 10 minutes before being dried.

Appendix 8

Proforma of analysis of sagittal anatomic slices of joints from Adelaide (Wakefield St. Hospital and Flinders Medical Centre) and Vienna.

	Vienna joints										Wakefield				Flinders			Total
Joint	1	2	3	4	5	6	7	8	9	10	1	2	3	4	1	2	3	
Normal Anatomy																		
Anterior Disc Displacement																		
Medial Disc Displacement																		
Lateral Disc Displacement																		
Perforated Disc																		
Articular Changes																		

Appendix 9

Proforma of analysis of coronal anatomic slices of joints from Adelaide (Flinders Medical Centre) and Vienna.

Coronally Dissected Joints														
	Vienna Joints										Flinders			Total
Joint	1	2	3	4	5	6	7	8	9	10	1	2	3	
Normal Anatomy														
Anterior Disc Displacement														
Medial Disc Displacement														
Lateral Disc Displacement														
Perforated Disc														
Articular Changes														

Appendix 10-Proforma

Accuracy of diagnosis of disc position, disc perforation and osseous abnormalities in sagittally sliced TM joints by sagittal and complementary coronal MR images.

Joint Condition	Anatomical Diagnosis	Diagnosis by Sagittal MRI	Diagnosis by Complementary Coronal MRI
Normal Anatomy			
Disc Position			
Disc Displacement			
ADD			
MDD			
LDD			
Perforation			
Articular Changes			

Appendix 11-Proforma

Accuracy of diagnosis of disc position, disc perforation and osseous abnormalities in coronally sliced TM joints by coronal and complementary sagittal MR images.

Joint Condition	Anatomical Diagnosis	Diagnosis by Coronal MRI	Diagnosis by Complementary Sagittal MRI
Normal Anatomy			
Disc Position			
Disc Displacement			
ADD			
MDD			
LDD			
Perforation			
Articular Changes			

Appendix 12-Proforma

Histologic assessment of joints scanned at Flinders Hospital.

Histologic Signs	Grading Total
Disc Displacement-Reduction in vascularity, splitting, fibrosis and hyaline degeneration of the retrodiscal tissues	Y/N
Perforation-Perforation of the discal-retrodiscal tissues	Y/N
Articular Tissue Disintegration	
<u>Fibrocartilage</u>	
-Normal Appearance	Y/N
-Superficial fibrillation associated with intact articular surface	Y/N
-Fibrillation involving the articular surface	Y/N
-Deep vertical clefts and/or splitting in the depth of the cartilage	Y/N
-Complete destruction of fibrocartilage	Y/N
<u>Disc</u>	
-Normal appearance	Y/N
-Loosening of collagen fibre arrangement	Y/N
-Superficial splits	Y/N
-Deep clefts	Y/N
Deviation in form	
-Normal, smooth articular surface	Y/N
-Microscopically irregular articular surface	Y/N
-Grossly deformed articular surface	Y/N

Progressive remodelling

<u>Fibrocartilage</u>

-Diffusely increasing cellularity or clusters of chondrocytes   Y/N

and/or increased metachromatic staining

<u>Subchondral bone</u>

-Vascular invasion of cartilage and endochondreal ossification   Y/N

<u>Disc</u>

-Increased collagen fibre density or adhesions   Y/N

Regressive remodelling

<u>Fibrocartilage</u>

-Decreased cellularity   Y/N

<u>Subchondral bone</u>

-Osteoclastic resorption and replacement by soft tissue   Y/N

<u>Disc</u>

-Atrophy and/or decreased collagen fibre density   Y/N

Circumferential remodelling

-Metaplastic conversion to fibrocartilage and/or ossification   Y/N

 of the anterior capsules insertions

-Osteophytic lipping

Appendix 12-Proforma

Histologic assessment of joints scanned at Flinders Hospital.

Joint 1 sagittally sectioned

Histologic Signs	Grading
Disc Displacement-Reduction in vascularity, splitting, fibrosis and hyaline degeneration of the retrodiscal tissues	Y/N
Perforation-Perforation of the discal-retrodiscal tissues	Y/N
Articular Tissue Disintegration	
Fibrocartilage	
-Normal Appearance	Y/N
-Superficial fibrillation associated with intact articular surface	Y/N
-Fibrillation involving the articular surface	Y/N
-Deep vertical clefts and/or splitting in the depth of the cartilage	Y/N
-Complete destruction of fibrocartilage	Y/N
Disc	
-Normal appearance	Y/N
-Loosening of collagen fibre arrangement	Y/N
-Superficial splits	Y/N
-Deep clefts	Y/N
Deviation in form	
-Normal, smooth articular surface	Y/N
-Microscopically irregular articular surface	Y/N
-Grossly deformed articular surface	Y/N

Progressive remodelling

Fibrocartilage

-Diffusely increasing cellularity or clusters of chondrocytes   Y/N

and/or increased metachromatic staining

Subchondral bone

-Vascular invasion of cartilage and endochondreal ossification   Y/N

Disc

-Increased collagen fibre density or adhesions   Y/N

Regressive remodelling

Fibrocartilage

-Decreased cellularity   Y/N

Subchondral bone

-Osteoclastic resorption and replacement by soft tissue   Y/N

Disc

-Atrophy and/or decreased collagen fibre density   Y/N

Circumferential remodelling

-Metaplastic conversion to fibrocartilage and/or ossification   Y/N

 of the anterior capsules insertions

-Osteophytic lipping   Y/N

Appendix 12-Proforma

Joint 1 coronally sectioned

Histologic assessment of joints scanned at Flinders Hospital.

Histologic Signs	Grading
Disc Displacement-Reduction in vascularity, splitting, fibrosis and hyaline degeneration of the retrodiscal tissues	Y/N
Perforation-Perforation of the discal-retrodiscal tissues	Y/N
Articular Tissue Disintegration	
Fibrocartilage	
-Normal Appearance	Y/N
-Superficial fibrillation associated with intact articular surface	Y/N
-Fibrillation involving the articular surface	Y/N
-Deep vertical clefts and/or splitting in the depth of the cartilage	Y/N
-Complete destruction of fibrocartilage	Y/N
Disc	
-Normal appearance	Y/N
-Loosening of collagen fibre arrangement	Y/N
-Superficial splits	Y/N
-Deep clefts	Y/N
Deviation in form	
-Normal, smooth articular surface	Y/N
-Microscopically irregular articular surface	Y/N
-Grossly deformed articular surface	Y/N

Progressive remodelling

Fibrocartilage

-Diffusely increasing cellularity or clusters of chondrocytes   **Y/N**

and/or increased metachromatic staining

Subchondral bone

-Vascular invasion of cartilage and endochondreal ossification   **Y/N**

Disc

-Increased collagen fibre density or adhesions   **Y/N**

Regressive remodelling

Fibrocartilage

-Decreased cellularity   **Y/N**

Subchondral bone

-Osteoclastic resorption and replacement by soft tissue   **Y/N**

Disc

-Atrophy and/or decreased collagen fibre density   **Y/N**

Circumferential remodelling

-Metaplastic conversion to fibrocartilage and/or ossification   **Y/N**

of the anterior capsules insertions

-Osteophytic lipping   **Y/N**

Appendix 12-Proforma

Joint 2 sagittally sectioned

Histologic assessment of joints scanned at Flinders Hospital.

Histologic Signs	Grading
Disc Displacement-Reduction in vascularity, splitting, fibrosis and hyaline degeneration of the retrodiscal tissues	Y/N
Perforation-Perforation of the discal-retrodiscal tissues	Y/N
Articular Tissue Disintegration	
Fibrocartilage	
-Normal Appearance	Y/N
-Superficial fibrillation associated with intact articular surface	Y/N
-Fibrillation involving the articular surface	Y/N
-Deep vertical clefts and/or splitting in the depth of the cartilage	Y/N
-Complete destruction of fibrocartilage	Y/N
Disc	
-Normal appearance	Y/N
-Loosening of collagen fibre arrangement	Y/N
-Superficial splits	Y/N
-Deep clefts	Y/N
Deviation in form	
-Normal, smooth articular surface	Y/N
-Microscopically irregular articular surface	Y/N
-Grossly deformed articular surface	Y/N

Progressive remodelling

Fibrocartilage

-Diffusely increasing cellularity or clusters of chondrocytes   **Y/N**

and/or increased metachromatic staining

Subchondral bone

-Vascular invasion of cartilage and endochondreal ossification   **Y/N**

Disc

-Increased collagen fibre density or adhesions   **Y/N**

Regressive remodelling

Fibrocartilage

-Decreased cellularity   **Y/N**

Subchondral bone

-Osteoclastic resorption and replacement by soft tissue   **Y/N**

Disc

-Atrophy and/or decreased collagen fibre density   **Y/N**

Circumferential remodelling

-Metaplastic conversion to fibrocartilage and/or ossification   **Y/N**

 of the anterior capsules insertions

-Osteophytic lipping   **Y/N**

Appendix 12-Proforma

Joint 2 coronally sectioned

Histologic assessment of joints scanned at Flinders Hospital.

Histologic Signs	Grading
Disc Displacement-Reduction in vascularity, splitting, fibrosis and hyaline degeneration of the retrodiscal tissues	Y/N
Perforation-Perforation of the discal-retrodiscal tissues	Y/N
Articular Tissue Disintegration	
Fibrocartilage	
-Normal Appearance	Y/N
-Superficial fibrillation associated with intact articular surface	Y/N
-Fibrillation involving the articular surface	Y/N
-Deep vertical clefts and/or splitting in the depth of the cartilage	Y/N
-Complete destruction of fibrocartilage	Y/N
Disc	
-Normal appearance	Y/N
-Loosening of collagen fibre arrangement	Y/N
-Superficial splits	Y/N
-Deep clefts	Y/N
Deviation in form	
-Normal, smooth articular surface	Y/N
-Microscopically irregular articular surface	Y/N
-Grossly deformed articular surface	Y/N

Progressive remodelling

Fibrocartilage

-Diffusely increasing cellularity or clusters of chondrocytes   Y/N

and/or increased metachromatic staining

Subchondral bone

-Vascular invasion of cartilage and endochondreal ossification   Y/N

Disc

-Increased collagen fibre density or adhesions   Y/N

Regressive remodelling

Fibrocartilage

-Decreased cellularity   Y/N

Subchondral bone

-Osteoclastic resorption and replacement by soft tissue   Y/N

Disc

-Atrophy and/or decreased collagen fibre density   Y/N

Circumferential remodelling

-Metaplastic conversion to fibrocartilage and/or ossification   Y/N

 of the anterior capsules insertions

-Osteophytic lipping   Y/N

Appendix 12-Proforma

Joint 3 sagittally sectioned

Histologic assessment of joints scanned at Flinders Hospital.

Histologic Signs	Grading
Disc Displacement-Reduction in vascularity, splitting, fibrosis and hyaline degeneration of the retrodiscal tissues	Y/N
Perforation-Perforation of the discal-retrodiscal tissues	Y/N
Articular Tissue Disintegration	
Fibrocartilage	
-Normal Appearance	Y/N
-Superficial fibrillation associated with intact articular surface	Y/N
-Fibrillation involving the articular surface	Y/N
-Deep vertical clefts and/or splitting in the depth of the cartilage	Y/N
-Complete destruction of fibrocartilage	Y/N
Disc	
-Normal appearance	Y/N
-Loosening of collagen fibre arrangement	Y/N
-Superficial splits	Y/N
-Deep clefts	Y/N
Deviation in form	
-Normal, smooth articular surface	Y/N
-Microscopically irregular articular surface	Y/N
-Grossly deformed articular surface	Y/N

Progressive remodelling

Fibrocartilage

-Diffusely increasing cellularity or clusters of chondrocytes   Y/N

and/or increased metachromatic staining

Subchondral bone

-Vascular invasion of cartilage and endochondreal ossification   Y/N

Disc

-Increased collagen fibre density or adhesions   Y/N

Regressive remodelling

Fibrocartilage

-Decreased cellularity   Y/N

Subchondral bone

-Osteoclastic resorption and replacement by soft tissue   Y/N

Disc

-Atrophy and/or decreased collagen fibre density   Y/N

Circumferential remodelling

-Metaplastic conversion to fibrocartilage and/or ossification   Y/N

 of the anterior capsules insertions

-Osteophytic lipping   Y/N

Appendix 12-Proforma

Joint 3 coronally sectioned

Histologic assessment of joints scanned at Flinders Hospital.

Histologic Signs	Grading
Disc Displacement-Reduction in vascularity, splitting, fibrosis and hyaline degeneration of the retrodiscal tissues	Y/N
Perforation-Perforation of the discal-retrodiscal tissues	Y/N
Articular Tissue Disintegration	
Fibrocartilage	
-Normal Appearance	Y/N
-Superficial fibrillation associated with intact articular surface	Y/N
-Fibrillation involving the articular surface	Y/N
-Deep vertical clefts and/or splitting in the depth of the cartilage	Y/N
-Complete destruction of fibrocartilage	Y/N
Disc	
-Normal appearance	Y/N
-Loosening of collagen fibre arrangement	Y/N
-Superficial splits	Y/N
-Deep clefts	Y/N
Deviation in form	
-Normal, smooth articular surface	Y/N
-Microscopically irregular articular surface	Y/N
-Grossly deformed articular surface	Y/N

Progressive remodelling

Fibrocartilage

-Diffusely increasing cellularity or clusters of chondrocytes   **Y/N**

and/or increased metachromatic staining

Subchondral bone

-Vascular invasion of cartilage and endochondreal ossification   **Y/N**

Disc

-Increased collagen fibre density or adhesions   **Y/N**

Regressive remodelling

Fibrocartilage

-Decreased cellularity   **Y/N**

Subchondral bone

-Osteoclastic resorption and replacement by soft tissue   **Y/N**

Disc

-Atrophy and/or decreased collagen fibre density   **Y/N**

Circumferential remodelling

-Metaplastic conversion to fibrocartilage and/or ossification   **Y/N**

 of the anterior capsules insertions

-Osteophytic lipping   **Y/N**

REFERENCES

REFERENCES

ALI S.Y., EVANS I. 1973.
>   Enzymatic degradation of cartilage in osteoarthritis.
>   Fed. Proc. 32:1494.

ATHANSOU N.A., QUINN J., HERYET A., PUDDLE B., WOODS C.G., McGEE J. 1988.
>   The immunohistology of synovial lining cells in normal and inflamed synovium.
>   J. of Path. 155:133-142.

BEAN L.R., OMNELL K.A. and OBERG T. 1977.
>   Comparison between radiological observations and macroscopic tissue changes in temporomandibular joints.
>   Dentomaxillofacial Radiology. 6;90.

BELL 1983.
>   In Clinical Management of Temporomandibular Disorders, Year Book, Medical Publishers Inc.

BJORK A. 1966.
>   Sutural growth of the upper face studied by the implant method.
>   Acta Odontol Scand. 24:109.

BLACKWOOD H.J.J. 1966.
>   Cellular remodelling in articular tissue.
>   Journal Dental Research. 45;480.

BLACKWOOD H.J.J. 1966.
>   Adaptive changes in the mandibular joints with function.
>   Dental Clinics of North America. 10:559.

BLACKWOOD H.J.J. 1969.
>   Pathology of the temporomandibular joint.
>   Journal of the American Dental Association. 79:118-24.

BLASCHKE D.D.
>   Arthrography of the temporomandibular joint: review

BLAUSTEIN D.I., SCAPINO RP. 1986.
>   Remodelling of the temporomandibular joint disc and posterior attachment in disc displacement specimens in relation to glycosaminoglycans content.
>   Plast Reconstr Surg. 78:756-764.

BLOCH F., HANSEN W.W., PACKARD M.E. 1946.
>   Nuclear induction.
>   Phys Rev. 69:127.

BOERING G. 1966.
      Arthrosis deformans van het Kaakgewricht.
      Diss. Groningen, Drukkerij Van Denderen.

BROOKS S.L., WESTESSON P.L. 1993.
      Temporomandibular joint: value of coronal images.
      Radiology. 188:317-321.

BURNETT K.R., DAVIS C.L., Read J. 1987.
      Dynamic display of the temporomandibular joint meniscus by using "fast-scan"
      MR imaging.
      AJR. 149:959-962.

CARLSSON G.E., OBERG T., BERGMAN F., et al. 1967.
      Morphologic changes in the mandibular joint disc in temporomandibular joint
      pain dysfunction syndrome.
      Acta Odontol Scand. 25:163-181.

CARLSSON G.E., OBERG T. 1974.
      Remodelling of the temporomandibular joint.
      In: Melcher A.H. Oral Science Review 1V, Copenhagen: Munksgaard.

CIRBUS M.T., SMILACK M.S., BELTRAN J., SIMON D.C. 1987.
      Magnetic resonance imaging in confirming internal derangement of the
      temporomandibular joint.
      J Prosthet Dent. 57:488-494.

CONWAT W.F., HAYES C.W., CAMPBELL R.L. et al. 1989.
      Temporomandibular joint motion: Efficacy of fast low angle shot MR
      imaging.
      Radiology. 172:821-826.

CROWLEY C.M., WILKINSON T.M., PIEHSLINGHER E., WILSON D.,
      CZERNY C. 1996.
      Correlations between anatomic and MRI sections of human cadaver
      temporomandibular joints in the coronal and sagittal planes.
      J Orofacial Pain. 10;199-216.

CZERVIONKE L.F., CZERVIONKE J.M., DANIELS D.L., HAUGHTON V.M.
      1988
      Characteristic features of MR truncation artefacts.
      AJNR. 9:815-824.

DAMADIAN R.1971
      Tumor detection by nuclear magnetic resonance.
      Science. 171:1151.

DeBONT L.G.M., STEGEGNA B. 1993.
    Pathology of Temporomandibular Joint Internal Derangement and
    Osteoarthrosis.
    Int. J. Oral Maxillofacial Surg. 22:71-74.

DIXON D.C. 1991
    Diagnostic imaging of the temporomandibular joint.
    Dental Clinics of North America. 35:53-72.

DONLON W.C., MOON K.L. 1987.
    Comparison of magnetic resonance imaging, arthrotomography and clinical
    and surgical findings in temporomandibular joint internal derangement's.
    Oral Surg, Oral Med, Oral Path. 64:2-5.

DuBRUL E.L.1980
    Sicher's oral anatomy. 7th ed.
    St Louis: The CV Mosby Co, 153-4.

ERIKSSON L., WESTESSON P.L. 1983
    Clinical and radiological study of patients with anterior disc displacement of
    the temporomandibular joint.
    Swed Dent J. 7(2):55-64.

FULLERTON G.D. 1988
    Physiological basis of magnetic relaxation.
    In Stark DD, Bradley WG, editors: Magnetic resonance imaging, St Louis,
    The CV Mosby Co.

FOSTER M.A., HUTCHINSON J.M. 1987
    Practical NMR Imaging. Oxford, IRL Press Ltd.

FREEMAN M.A.R. 1972.
    The pathogenesis of osteoarthrosis: an hypothesis.
    In: Appley A.G. (ed) Modern trends in orthopaedics.
    Butterworths, London. Vol. 6:40.

FREEMAN M.A.R., KEMPSON G.E. 1973.
    Load carriage.
    In: Freeman M.A.R. Adult articular cartilage.
    Pitman Medical, Alden Press, Oxford. 287-329.

GAGE J.P., FRANCIS M.J.O. and TRIFFIT J.T. 1989
    Collagen and Dental Matrices, Butterworths, London.

GAGE J.P., VIRDI A.S., TRIFFIT J.T., HOWLETT C.R., FRANCIS M.J.O. 1990
    Presence of Type III Collagen in Disc Attachments of Human in internal
    derangement of the temporomandibular joint.
    Oral Surg, Oral Med, Oral Path. 58:375-381.

GEDIKOGHER O., BOGLISS M.T., ALI S.Y., TUNCER I. 1986.
Biochemical and histological changes in osteoarthritis synovial membrane.
Annuals of the Rheumatic Diseases. 45:289-293.

HALL B.K. 1984.
Matrices control the differentiation of cartilage and bone.
Prog Clin Biol Res. 151:147-169.

HANSSON T., NORDSTROM B. 1977
Thickness of the soft tissue layers and the articular disc in the
temporomandibular joint with deviations in form.
Acta Odontol Scand. 35:281.

HANSSON T., OBERG T., CARLSSON G.E., KOPP J. 1977.
Thickness of the soft tissue layers and the articular disc in the
temporomandibular joint.
Acta Odontol Scand. 35:77.

HARMS S.E., WILK R.M., WOLFORD L.M., CHILES D.G., MILAM S.B. 1985
The Temporomandibular Joint: Magnetic Resonance Imaging Using Surface
Coils.
Radiology. 157:133-136.

HARMS S.E., WILK R.M. 1987.
Magnetic resonance imaging of the temporomandibular joint.
Radiographics. 7:521-542.

HASSO A.N., ALDER M.E., KNEPEL KA.
Magnetic Resonance Imaging. In Temporomandibular Joint Imaging by
Christiansen EL and Thompson JR, Mosby Year Book.

HELLSING G., HOLMLUND A. 1985.
Development of anterior disc displacement in the temporomandibular joint: an
autopsy study.
J Pros Dent. 53: 397-401.

HELMS C.A., GILLESPY T., SIMS R.E., RICHARDSON M.L. 1986.
Magnetic resonance imaging of internal derangement of the
temporomandibular joint.
Radio Clinics North America. 24:189-192.

HYLANDER W.L. 1979.
The functional significance of primate mandibular form.
J Morphol. 160(2):223-240.

INEROTH S., HEINEGARD D., ANDELL L., PISSON S.E. 1978.
Articular cartilage proteoglycans in ageing and osteoarthritis.
Biochem J.

ISBERG A, ISACSSON G. 1986.
Tissue reactions associated with internal derangement of the temporomandibular joint. A radiographic, cryomorphologic and histologic study.
Acta Odontol Scand. 44:159-164.

JAHN J.A., SCHELLHAS K.P. 1991.
Magnetic Resonance Imaging of the Temporomandibular Joint: Preliminary Evaluation of Partial Flip Angle Three-Dimensional Volume Acquisitions Against Conventional Single and Multiecho Pulse Sequences.
Journal of Craniomandibular Practice. 9:145-151.

JEFFERY A.K. 1973.
Osteogenesis in the osteoarthritic femoral head. A study using radioactive p and tetracycline bone markers.
J Bone Joint Surg.

JOHNSON J.E. 1962.
Cephalometric assessment of effective mandibular ramus height.
Am J Orthodont. 48:471-472.

KAPLAN P.A. 1987.
Current status of Temporomandibular Joint Imaging for the Diagnosis of Internal Derangement.
American Journal of Radiology. 152:687-705.

KATZBERG R.W., BESSETTE R.W., TALLENTS R.H., PLEWES D.B., MANZIONE J.V., SCHENCK J.F., FOSTER T.H. 1986.
Normal and Abnormal Temporomandibular Joint: MR Imaging with Surface Coil. Radiology. 158:183-189.

KATZBERG R.W., DOLWICK M.F., HELMS C.A, HOPENS B., BALES D.E., COGGS G.C. 1980.
Arthrotomography of the temporomandibular joint .
AJR. 134:995-1005

KATZBERG R., KEITH D.A., GURALNICK W.C., MANZIONE J.V., TEN EICK W.R. 1983.
Internal derangement's of the temporomandibular joint: an assessment of condylar position in centric occlusion.
J. Pros Dent. 49:250.

KATZBERG RW. 1989
Temporomandibular joint imaging.
Radiology. 170:297-307.

KATZBERG R.W., WESTESSON P.L., TALLENTS R.H., ANDERSON R., KURITA K., MANZIONE J.V., TOTTERMAN S. 1988.
Temporomandibular Joint: MR Assessment of Rotational and Sideways Disc Displacement.
Radiology. 169:741-748.

KATZBERG R.W., BESSETTE R.W., TALLENTS R.H., PLEWES D.B.,
    MANZIONE J.V., SCHENCK J.F., FOSTER T.H. 1986.
    Normal and Abnormal Temporomandibular Joint: MR Imaging with Surface
    Coil.
    Radiology. 158:183-189.

KOPP S., CARLSSON G.E., HANSSON T.. OBERG T. 1978.
    Degenerative disease in the temporomandibular, metatarsophalangeal and
    sternoclavicular joints. An autopsy study.
    Acta Odontol Scand. 34:23.

KURITA K., WESTESSON P.L., STERNBY N.H., ERIKSSON L, CARLSSON L.E.,
    LUNDH H. 1989.
    Histologic features of the temporomandibular joint disc and posterior
    attachment: Comparison of symptom free persons with normally positioned
    discs and patients with internal derangement.
    Oral Surg, Oral Med, Oral Path. 67:635-643.

LAUTERBUR P.C. 1973.
    Image formation by induced local interactions: examples employing unclear
    magnetic resonance.
    Nature. 242:190-191.

LEREIM P., GOLDIE I. 1975.
    Relationship between morphologic features and hardness of the subchondral
    bone of the medial tibial condyle in the normal state and in osteoarthritis and
    rheumatoid arthritis.
    Arch. Orthop. Unfallchir. 81:1.

LINDBLOM G. 1960.
    On the anatomy and function of the temporomandibular joint.
    Acta Odontol Scand (Suppl 28) 17.

LUDEKE K.M., ROSCHMANN P., TISCHLER R. 1985.
    Susceptibility artefacts in NMR imaging.
    Mag Res Imag. 3:329-343.

MAHAN P.E., WILKINSON T.M., GIBBS C.H., MAUDERLI A., BRANNON L.S.
    1983.
    Superior and inferior bellies of the lateral pterygoid EMG activity at basic jaw
    positions.
    J Pros Dent. 50:710-8.

MANZIONE J.V., KATZBERG R.W. and MANZIONE T.J. 1984.
    Internal derangement of the temporomandibular joint: normal anatomy,
    physiology and pathophysiology.
    Int. J. Periodont. Rest. Dent. 4:9-15.

MARAVILLA KR. 1988.
    Rapid imaging pulse sequences for CNS evaluation.
    MRI Decisions. 6:3-14.

McCARTHY P. 1974.
  Dermatology.
  Dent Clinics North America. 18: 97-110.

McCOY J.M., GOTCHER J.E., CHASE D.C. 1986.
  Histologic grading of TMJ tissues in internal derangement.
  Cranio. 4:213-218.

MOFFETT B.C. 1962.
  The temporomandibular joint.
  In: Completed Denture Prosthodontics (Ed. Sharry J.J.) McGraw-Hill, New
  York, Toronto, London: 56-99.

MOFFETT B.C., JOHNSON L.C., McCABE I.B., ASKEW H. 1964.
  Articular remodelling in the adult human temporomandibular joint.
  Am. J. Anat. 115:119.

MOFFETT B.C., JOHNSON L.C., McCABE J.B., ASILWHEW H.C. 1974.
  Articular remodelling in the adult human temporomandibular joint.
  American Journal of Anatomy. 115;119-41.

MONGINI F. 1972.
  Remodelling of the mandibular condyle in the adult and its relationship to the
  condition of the dental arches.
  Acta Anat. 82:437.

MONGINI F. 1975.
  Dental abrasion as a factor in remodelling of the mandibular condyle.
  Acta Anat. 92(2):292-300.

MORIMOTO K., HASHIMOTO N., SUETSUGO T.1987.
  Prenatal developmental process of human temporomandibular joint.
  J Pros Dent. 57:723-729.

MOSES J.J., SARATORIS D., GLAS R et al. 1989.
  The effect of arthroscopic surgical lysis and lavage of the superior joint space
  on TMJ disc position and mobility.
  Journal of Oral and Maxillofacial Surgery. 47:674-678.

MOSS M., KRUGER G.O., REYNOLDS D.C. 1965.
  The effect of chondroitin sulphate on bone healing.
  Oral Surg. 20:795-801.

MURNANE T.W., DOKU H.C. 1971.
  Light and electron microscopic appearance of synovial lining tissues in a
  patient with temporomandibular joint dysfunction.
  Oral Surg. 31:452-459.

MURPHY W. A. 1981.
  Arthrography of the temporomandibular joint.
  Radiol Clinics North America. 19:365-378.

NILNER M, PETERSSON A. 1995.
Clinical and radiological findings related to treatment outcome in patients with temporomandibular disorders.
Dentomaxillofacial Radiology. 24:128-131.

OBERG T. 1964.
Morphology, growth and matrix formation of the mandibular joint of the guinea pig.
Diss Trans Royal Schools of Dent Stockholm/Umea. 2:10.

OBERG T., FAJERS C.M. 1971.
The temporomandibular joint. A morphologic study on human autopsy material.
Acta Odontol. Scand. 29:349.

OBERG T. 1971.
Morphology, growth and matrix formation of the mandibular joint of the guinea pig.
Diss. Trans Royal Schools of Dent Stockholm/Umea 2,10

OBERG T. CARLSSON G.E., FAJERS C.M. 1971.
The temporomandibular joint. A morphological study on human autopsy material.
Acta Odontol Scand. 29:349-84.

OBERG T., CARLSSON G.E., FAJERS C.M., BERGMAN F. 1966.
Ageing of the human disc with special reference to the occurrence of cartilaginous cells.
Odontol Tidskr. 74,122.

OKESON J.P. 1993.
In Management of Temporomandibular Joint Disorders and Occlusion 3rd edition.
Mosby Year Book, St. Louis, pp:310.

OSBORNE J.W. 1985.
The disc of the human temporomandibular joint: Design, function and failure.
J Oral Rehabilitation. 16:279-292.

PAYNE M., NAKIELNY R.A. 1996.
Review: Temporomandibular Joint Imaging.
Clinical Radiology. 51:1-10.

PURCELL E.M., TORREY H.C., POUND R.V. 1946.
Resonance absorption by nuclear magnetic moments in a solid.
Phys Rec. 69:127.

RABI I.I., MILLMAN S., KUSCH P. et al. 1939.
Molecular beam resonance method for measuring of nuclear magnetic moments of Li^6, Li^7, $9P^{10}$.
Phys Rev. 55:526.

RADIN E.L., PARKER G.H., PUGH J.W., STEINBERG R.S., PAUL I.L., ROSE R.M. 1973.
Response of joints to impact loading. III. Relationship between trabecular microfracture and cartilage degeneration.
J. Biomechanics. 6:51.

RAMFORD S.P., ASH M.M. 1971.
Occlusion.
Ed 2. Philadelphia WB Saunders Co. 248-250.

RAO V.M., FAROLE A., KARASICK D. 1990.
Temporomandibular joint dysfunction: Correlation of MR imaging, arthrography and arthroscopy.
Radiology. 174:663-667.

RAUSTIA A.M., PYHTINEN J., PERNU H. 1994.
Clinical, magnetic resonance imaging and surgical findings in patients with temporomandibular joint disorders- a survey of 47 patients.
Fortschr Rontgenstr. 47:406-411.

REES L.A. 1954.
The structure and function of the temporomandibular joint.
British Dental Journal. 96:125-133.

RICHARDS L.C., LAU E., WILSON D.F. 1984.
Histopathology of the mandibular condyle.
Journal of Oral Pathology. 14;624-630.

RICKETTS R.M. 1950.
Variations of the temporomandibular joint as revealed by cephalometric laminography.
American Journal of Orthodontics. 36;877-898.

ROBERTS D., SCAPINO R.A., EL-MONEIM ZAKI A.B.D., DANIEL J., LENKINSKI R.E., COHEN S.G. 1990.
Relationship between magnetic resonance signal and TMJ tissue.
In: Christiansen EL, Thompson JR (eds). Temporomandibular Joint Imaging.
St. Louis: Mosby. 129-146.

ROHLIN M., AKERMAN S., KOPP S. 1986.
Tomography as an aid to detect microscopic changes of the temporomandibular joint.
Acta Odontol Scand. 44:131-140.

RYAN D., AHMED S., HARRIS M. 1990.
Arthrotomography and the surgical correction of temporomandibular disorders.
British Journal of Oral and Maxillofacial Surgery. 28:228-233.

SAUSER D.D., THOMPSON J.R. 1990.
In Temporomandibular Joint Imaging, Mosby Year Book. 76.

SCAPINO R.P. 1983.
Histopathology associated with malposition of the human temporomandibular
joint disc.
Oral surgery, Oral Medicine, Oral Pathology. 55:382-397.

SCAPINO R.P. 1991.
The posterior attachment: Its structure, function and appearance in TMJ
imaging studies. Part 1
Journal of Craniomandibular Disorders Facial Oral Pain. 5:83-95.

SCAPINO R.P. 1991.
The posterior attachment: Its structure, function and appearance in TMJ
imaging studies. Part 2.
Journal of Craniomandibular Disorders Facial Oral Pain. 5:155-166.

SCHELLHAS K.P., WILKES C.H., FRITTS H.M., OMLIE M.R., HEITHOFF K.B.,
JAHN J.A. 1987. 1988.
Temporomandibular joint: MR imaging of internal derangements and
postoperative changes.
AJNR 1987;8:1093-1101, AJR 1988;150:381-389.

SCHELLHAS K.P., WILKES C.H., FRITTS H.M., OMLIE M.R.,
LANGROTTERIA L.B. 1989.
MR of Osteochondritis Dissecans and Avascular Necrosis of the Mandibular
Condyle.
American Journal of Radiology. 152:551-560.

SCHMID F.R., OGATA R.I. 1967.
The composition and examination of synovial fluid.
Journal of Prosthetic Dentistry. 18:449-65.

SCHWAIGHOFER B.W., TANAKA T.T., KLEIN M.V., SARTORIS D.J.,
RESNICK D. 1990.
MR Imaging of the Temporomandibular Joint: A Cadaver Study of the Value
of Coronal Images.
AJR. 154:1245-1249.

SICHER H. 1950.
Functional anatomy of the temporomandibular joint.
In: Sarnat B.G. The Temporomandibular Joint.
Thomas Illinois USA. 3-38.

SOKOLOFF L. 1982.
The remodelling of the articular cartilage.
Rheumatology. 7:11-18.

SOLBERG W.K., HANSSONN T.L., NORDSTROM B. 1985.
> The temporomandibular joint in young adults at autopsy: A morphologic classification and evaluation.
> J Oral Rehabil. 12:303-321.

STEGEGNA B., DeBONT L.G.M., BOERING G. 1989.
> Osteoarthrosis as the cause of craniomandibular pain and dysfunction: A unifying concept.
> J Oral Maxillofac Surg. 47:249-256.

STEIHARDT G. 1933.
> Zur pathologischen anatomie und pathogenesese einiger akuter und chronischer kiefergelenkerkraukungen.
> Deutsche Zahn. 86:66-72.

SWETS J.A. 1988.
> Measuring the accuracy of diagnostic systems.
> Science. 240:1285-1293.

TASAKI M.M., WESTESSON PL. 1993.
> Temporomandibular joint: diagnostic accuracy with sagittal and coronal MR imaging.
> Radiology. 186:723-729.

TELHAG H. 1973.
> Effect of tranexamic acid on the synthesis of chondroitin sulphate and the content of hexosamine in the same fraction on normal and degenerated joint cartilage in the rabbit.
> Acta Orthop. Scand. 44:249.

THILANDER B., CARLSSON G.E., INGERVALL B. 1976.
> Post natal development of the human temporomandibular joint. A histological study.
> Acta Odontol Scand. 34(2): 117-126.

TOLLER P.A. 1961.
> The synovial membrane apparatus and temporomandibular joint function.
> British Dental Journal. 111:355-362.

WALTER E. 1988.
> CT and MR imaging of the temporomandibular joint.
> Radiology. 8:327-348.

WATT-SMITH S., SADLER A., BADDLERY A. 1993.
> Comparison of arthrotomography and magnetic resonance images of 50 temporomandibular joints with operative findings.
> British Journal of Oral and Maxillofacial Surgery. 31:139-143.

WARD P.C.J. 1980.
Interpretation of synovial fluid data.
Post Grad Med. 3:175.

WEINBERG L.A. 1979.
Role of condylar position in TMJ dysfunction-pain syndrome.
Journal of Prosthetic Dentistry. 41(6):636-43.

WESTESSON P.L., ROHLIN. 1984.
Internal derangement related to osteoarthrosis in temporomandibular joint
autopsy specimens.
Oral Surg, Oral Med, Oral Path. 57:17-22.

WESTESSON P.L. 1985.
Structural hard tissue changes in temporomandibular joints with internal
derangement's.
Oral Med, Oral Path. 59:220-224.

WESTESSON P.L., BRONSTEIN S.L., LIEBERG J. 1986.
Temporomandibular joint: correlation between single contrast
videoarthrography and post mortem morphology.
Radiology. 160:767-771.

WESTESSON P.L., KATZBERG R.W., TALLENTS R.H., SANCHEZ-
WOODWORTH R.E., SVENSSON S.A. 1987.
Temporomandibular joint: comparison with autopsy specimens.
AJR. 148:1165-1171.

WESTESSON P.L., KATZBERG R.W., TALLENTS R.H.,
SANCHEZ-WOODWORTH R.E., SVENSSON S.A.,
ESPELAND M.A. 1987.
Temporomandibular joint: comparison of MR images with cryosectional
anatomy.
Radiology. 164:59-64.

WESTESSON P.L., KATZBERG R.W., TALLENTS R.H.,
SANCHEZ-WOODWORTH R.E., SVENSSON S.A. 1987.
CT and MR of the temporomandibular joint: Comparison with autopsy
specimens.
AJR. 148:1165-1171.

WESTESSON P.L. 1992.
Magnetic resonance imaging of the temporomandibular joint.
Oral Maxillofacial Surgical Clinics of North America. 4:183-205.

WESTESSON P.L., BROOKS S.L. 1992.
Temporomandibular Joint: Relationship Between MR Evidence of Effusion
and the Presence of Pain and Disc Displacement.
American Journal of Radiology. 159:59-563.

WILK R.M., HARMS S.E. 1988.
>   Temporomandibular joint: multislab, three dimensional Fourier
>   transformation magnetic resonance imaging.
>   Radiology. 167:861-863.

WILK R.M., HARMS, WOLFORD L.M. 1988.
>   Sensitivity and selectivity of magnetic resonance images of the
>   temporomandibular joint.
>   J Dent res. 67: Abstract.

WILKES C.H. 1978.
>   Arthrography of the temporomandibular joint in patients with the TMJ pain
>   dysfunction syndrome.
>   Minn Med. 61:645-52.

WILKINSON T., MARYNIUK G. 1983.
>   The correlation between sagittal anatomic sections and comuterised
>   tomography of the TMJ.
>   The Journal of Craniomandibular Practice. 1:38-45.

WILKINSON T.M. 1988.
>   The relationship between the disk and the lateral pterygoid muscle in the
>   human temporomandibular joint.
>   J. Pros Dentistry. 60:715-724

WILKINSON T.M., CROWLEY C.M. 1994.
>   A Histologic Study of Retrodiscal Tissues of the Human Temporomandibular
>   Joint in the Open and Closed Position.
>   Journal of Orofacial Pain. 8:7-17.

YALE S., ALLISON B.D., HAUPTFUEHRER J.D. 1966.
>   An epidemiological assessment of mandibular condyle morphology.
>   Oral Surgery. 21, 169-177.

YALE S. 1969.
>   Radiologic evaluation of the temporomandibular joint.
>   J. Am. Dent. Assoc. 79:102.